

Global Safety Assessment of Concrete Structures using Nonlinear Finite Element Analysis

Master of Science Thesis in the Master's Programme Structural Engineering and Building Technology

MATTIAS BLOMFORS

Department of Civil and Environmental Engineering
Division of Structural Engineering
Concrete Structures
CHALMERS UNIVERSITY OF TECHNOLOGY
Göteborg, Sweden 2014
Master's Thesis 2014:163

Global Safety Assessment of Concrete Structures using Nonlinear Finite Element Analysis

*Master of Science Thesis in the Master's Programme Structural Engineering and
Building Technology*

MATTIAS BLOMFORS

Department of Civil and Environmental Engineering
Division of Structural Engineering
Concrete Structures

CHALMERS UNIVERSITY OF TECHNOLOGY

Göteborg, Sweden 2014

Global Safety Assessment of Concrete Structures using Nonlinear Finite Element Analysis

Master of Science Thesis in the Master's Programme Structural Engineering and Building Technology

MATTIAS BLOMFORS

© MATTIAS BLOMFORS, 2014

Examensarbete / Institutionen för bygg- och miljöteknik,
Chalmers tekniska högskola 2014:163

Department of Civil and Environmental Engineering
Division of Structural Engineering
Concrete Structures
Chalmers University of Technology
SE-412 96 Göteborg
Sweden
Telephone: + 46 (0)31-772 1000

Cover:

Crack pattern of reinforced concrete frame subjected to vertical and horizontal load.
Plot obtained in case study using DIANA, TNO DIANA (2014)

Chalmers Reproservice
Göteborg, Sweden 2014

Global Safety Assessment of Concrete Structures using Nonlinear Finite Element Analysis

Master of Science Thesis in the Master's Programme Structural Engineering and Building Technology

MATTIAS BLOMFORS

Department of Civil and Environmental Engineering

Division of Structural Engineering

Concrete Structures

Chalmers University of Technology

ABSTRACT

To increase the efficiency of new structures and to perform safety evaluations of existing structures the nonlinear behavior of reinforced concrete should be modelled and analyzed. It is unclear if the safety formats for nonlinear analysis in present design codes correctly assess the probability of failure for indeterminate structures subjected to loading in several directions. In this thesis the safety formats for nonlinear analysis in Model Code 2010 have been evaluated for a reinforced concrete portal frame subjected to vertical and horizontal loading. The frame was designed according to Eurocode 2 based on linear elastic analysis. The design load carrying capacity was determined for the safety format *Estimation of COefficient of Variance of resistance* (ECOV), the *Global Resistance Factor method* (GRFm) and *Partial Safety Factor method* (PSF). Two load histories were studied, differing by which of the loads that were applied first. The results were compared in terms of the probability of failure assessed by applying the first order reliability method to a response surface fitted to results from nonlinear FE analyses. The ECOV safety format was found not to satisfy the intended probability of failure of 0.1% when the vertical load was applied first. The other safety formats all met the intended safety level and yielded design resistances 6-8% below the linear elastic design load for both load histories. The results indicate that the load history of the structure is important when it comes to safety evaluation. It was concluded that more research is required regarding the loading of complex structures and how it affects the safety level.

Key words: reinforced concrete, nonlinear finite element analysis, safety formats, first order reliability method, response surface.

Contents

ABSTRACT	I
CONTENTS	III
PREFACE	V
NOTATIONS	VI
1 INTRODUCTION	1
1.1 Background	1
1.2 Problem description	1
1.3 Aim	1
1.4 Limitations	2
1.5 Method	2
2 SAFETY ASSESSMENT USING NONLINEAR FEA	3
2.1 The finite element method for reinforced concrete	3
2.1.1 Linear finite element analysis	3
2.1.2 Nonlinear finite element analysis	4
2.1.3 Strategy for structural Finite Element modelling	4
2.2 Background for structural reliability	7
2.2.1 Principles of limit state design	7
2.2.2 Basic variables	8
2.2.3 Deterministic measures of structural reliability	8
2.2.4 Probabilistic measures of structural reliability	10
2.2.5 Uncertainties	12
2.2.6 Reliability level	13
2.3 Safety formats for nonlinear analysis	13
2.3.1 Probabilistic method	14
2.3.2 Global resistance method	14
2.3.3 Partial factor method	16
2.3.4 Discussion regarding safety formats	16
2.4 Reliability analysis of structures	16
2.4.1 Monte Carlo simulations	17
2.4.2 First and second order reliability method (FORM/SORM)	19
2.4.3 Response surface	21
2.4.4 Procedure suggested in Model Code 2010	23
3 CASE STUDY – COMPARISON OF SAFETY FORMATS	24
3.1 Solution strategy for NLFEA	24
3.1.1 Portal frame experiment	24
3.1.2 Collapse analysis of frame	26
3.1.3 Setup of the NLFE-model	27
3.1.4 Benchmarking results	29
3.1.5 Chosen solution strategy	35

3.2	Design using LFEA ANSYS/MultiCon	38
3.2.1	Frame properties and loading	38
3.2.2	Modelling in ANSYS	39
3.2.3	Design using in-house postprocessor MultiCon	39
3.3	Safety assessment of designed frame using different safety formats	44
3.3.1	Modelling consideration in DIANA	44
3.3.2	Checking the DIANA model	45
3.3.3	Loading and behavior of frame	46
3.3.4	Comparison between safety formats	63
3.4	Response surface and reliability assessment	64
3.4.1	Construction of the response surface	64
3.4.2	Results from response surface analysis	65
4	DISCUSSION	70
5	CONCLUSIONS AND SUGGESTIONS FOR FURTHER WORK	73
6	REFERENCES	74
7	APPENDICES	76

Preface

The Master's Thesis project resulting in this report has been conducted at Multiconsult AS office in Oslo, Norway, during the fall of 2014.

The thesis' examiner was Mario Plos; Associate Professor/Head of Division at the division of Structural Engineering within the department of Civil and Environmental Engineering at Chalmers University of Technology in Gothenburg, Sweden. The supervisor of the project has been Morten Engen, Research Fellow at Multiconsult AS. Further, Johan Karlsson has provided useful feedback on the project in his role as opponent.

I thank the employees at Multiconsult AS for sharing their knowledge and great work environment with me, especially my supervisor Morten Engen who has been a great source of inspiration and provided much useful feedback.

Oslo, December 2014

Mattias Blomfors

Notations

Roman upper case letters

A	Regression coefficient on scalar form
B	Regression coefficient on vector form
C	Regression coefficient on matrix form
D	Matrix containing constants and linear, quadratic and cross combinations of x_j
E_{cd}	Design Young's modulus for concrete
E_{ck}	Characteristic Young's modulus for concrete
E_{cm}	Mean Young's modulus for concrete
E_{sd}	Design Young's modulus for steel
E_{sk}	Characteristic Young's modulus for steel
E_{sm}	Mean Young's modulus for steel
F	Factor of safety
F_d	Design value of actions
F_H	Horizontal load
F_{ud}	Design ultimate strength of reinforcement steel
F_V	Vertical load
F_X	Cumulative distribution function (cdf) of the stochastic variable X
F_{yd}	Design yield strength of reinforcement steel
G	Limit state function
$\bar{G}(X)$	Response surface for vector of stochastic variables
G_{cd}	Design compressive fracture energy of concrete
G_{ck}	Characteristic compressive fracture energy of concrete
G_{cm}	Mean compressive fracture energy of concrete
G_{fd}	Design tensile fracture energy of concrete
G_{fk}	Characteristic tensile fracture energy of concrete
G_{fm}	Mean tensile fracture energy of concrete
P	Probability
Q	Vector containing loads
R	Structural resistance
R_d	Design value of structural resistance
R_i	Resistance of the i -th component
R_k	Structural resistance for analysis using characteristic material strengths
R_m	Structural resistance for analysis using mean material strengths
R_P	Vector containing plastic resistances
S	Load effect
S	Sampling plan for Latin hypercube sampling
V_R	Coefficient of variation of resistance
W	Weight factor for importance sampling
W_Q	External work
W_R	Internal work
X	Stochastic variable
X	Vector of stochastic variables

Roman lower case letters

d	Matrix containing regression coefficients
e	Vector containing regression errors
f_c	Compressive strength of concrete
f_{cd}	Design compressive strength of concrete
f_{cf}	Concrete strength parameter
f_{cfk}	Characteristic strength property of concrete
f_{ck}	Characteristic compressive strength of concrete
f_{cm}	Mean compressive strength of concrete
f_{ctd}	Design tensile strength of concrete
f_{ctk}	Characteristic tensile strength of concrete
f_{ctm}	Mean tensile strength of concrete
f_{uk}	Characteristic ultimate strength of reinforcement steel
f_{um}	Mean ultimate strength of reinforcement steel
f_y	Yield strength of reinforcement steel
f_{yd}	Design yield strength of reinforcement steel
f_{yk}	Characteristic yield strength of reinforcement steel
f_{ym}	Mean yield strength of reinforcement steel
f_X	Probability density function (pdf) of the stochastic variable X
f_X	Multivariate probability density function (pdf) of the vector X
h_v	Importance sampling probability density function
m	Vector from origin to design point in u-space
p_f	Probability of failure
p_{fN}	Nominal probability of failure
$r()$	Resistance as function of basic variable properties
s_{Di}	Load effect from dead load for the i-th component
s_{Li}	Load effect from live load for the i-th component
\hat{u}_i	Latin hypercube sample centered at the origin
\tilde{u}_i	Latin hypercube sample centered at the design point
x	Realization of the set of stochastic variables X
x_M	Design point for response surface fitting

Greek upper case letters

Φ	Normal (Gaussian) cumulative distribution function
--------	--

Greek lower case letters

α_{cf}	Factor accounting for sustained load and unfavorable load application effects
α_r	Weight factor for the reliability index
β	Reliability (safety) index
β_{HL}	Hasofer-Lind safety index, obtained by FORM
β_{SORM}	Safety index obtained by SORM
γ_C	Safety factor for concrete
γ_{Di}	Dead load partial factor for the i-th component
γ_{Li}	Live load partial factor for the i-th component

γ_R^*	Global safety factor
γ_R	Safety factor for resistance
γ_{Rd}	Model uncertainty safety factor
γ_S	Safety factor for reinforcement steel
ε_{ud}	Design ultimate strain of reinforcement steel
ε_{uk}	Characteristic ultimate strain of reinforcement steel
ε_{um}	Mean ultimate strain of reinforcement steel
λ	Load factor
μ_X	Mean value of random variable X
σ_i	Stress component
σ_{pi}	Permissible stress of the i-th component
σ_{ui}	Material strength of the i-th component
σ_X	Standard deviation of random variable X
ϕ	Normal (Gaussian) probability density function
ϕ_i	Partial factor for resistance for the i-th component
ϕ_u	Joint probability density function for importance sampling

1 Introduction

Large concrete structures exposed to a variety of loads acting in different directions, e.g. dams and offshore concrete structures, must be designed to meet requirements regarding structural capacity and reliability for a certain design life time. The design must also be feasible with respect to constructability.

1.1 Background

In engineering practice today the designs of large concrete structures are often verified using global linear finite element analyses (LFEA), Brekke *et. al.* (1994). Large solid elements are used in the analyses to reduce the number of elements, i.e. computational time. These analyses can therefore be described as large scale analyses.

Due to the nature of the linear analysis, load effects caused by various loads can be superimposed. Load combination is typically done after the LFEA using a post-processing program which also designs the structure.

1.2 Problem description

In reality reinforced concrete structures show nonlinear material behavior when subjected to increasing load. This is mainly due to cracking of concrete and yielding of reinforcement steel. The concrete can crack even for small loads, which changes the stiffness properties of the material and stresses are redistributed to sections with higher stiffness. This behavior is not represented by a LFEA.

An analysis that recognizes the nonlinear behavior of reinforced concrete is required to accurately represent the stress distribution, i.e. a Nonlinear Finite Element Analysis (NLFEA). Efforts are put towards finding a general, robust and stable solution strategy for conducting NLFEA, focusing on material behavior and reliability, Engen *et. al.* (2014).

The traditional design process using LFEA involves control of the utilization ratio (UR) locally in each design section to ensure safety. The material strength is scaled down and the load effect is scaled up using pertinent partial factors to obtain design values which are used for UR calculations. However, a global NLFEA reveals the capacity of the structure to which all sections contribute. Since a NLFEA yields the global response of a structure, the safety should be checked globally. Further research is needed to validate the safety formats in the design and model codes for structures with complex failure modes, Cervenka (2013).

1.3 Aim

One aim of this thesis is to provide an overview of the safety formats used today for global safety assessments using NLFEA. Another aim is to examine and compare the applicability of the different safety formats on more complex structures through case studies. The studied safety formats will be those in fib Model Code 2010 fib (2013).

1.4 Limitations

The thesis does not set out to develop a new safety format, but rather compare existing safety formats. Developing a new safety format requires substantial experience and time; therefore it is beyond the scope of the thesis. Furthermore, no practical experiments will be performed during this project.

1.5 Method

First a literature review is conducted to gain knowledge in the topic. Efforts will be put towards finding data from a relevant practical experiment that can be used for verification of computer models.

The next step is to establish a nonlinear finite element model (NLFEM) of a fairly complex structure which is verified or "benchmarked" using the experimental data.

Following the design approach suggested by Engen *et. al.* (2014) a structure, similar to the one verified but larger, is to be designed using LFEM software and an in-house post-processor. A large scale NLFEM of the design is established and then used for comparing the different safety formats' impact on the global safety assessment.

An assessment of the structural capacity is made by means of fitting a response surface to the implicit limit state function and applying second moment methods. This serves as a base for comparison of the different safety formats.

2 Safety assessment using nonlinear FEA

This chapter will present a theoretical basis for global safety assessment using nonlinear finite element analyses. The element method itself is presented briefly, followed by a background of structural reliability. Furthermore, the safety formats for NLFEA in the Model Code 2010 fib (2013) will be described. Different ways of evaluating the reliability of a structure is also accounted for.

2.1 The finite element method for reinforced concrete

The finite element method (FEM) is widely used in many fields of engineering and is a method to numerically solve field problems, Cook *et. al.* (2001). In civil engineering the stresses and displacements in a structure is often of interest. These can be described mathematically by differential equations. A model of the structure is divided into finite elements, in contrast to the infinitesimal elements used in calculus. The points that connect the finite elements to each other are called nodes and the arrangement of nodes and elements is called a mesh. The displacements are found at the nodes (i.e. node quantities) while the stress distribution varies over the elements (i.e. field quantities). In the FEM the stress variation over each element is approximated, often as a polynomial distribution, and the weak solutions to the differential equations are found. Therefore the element method does not provide an exact solution, however the mesh structure can be arranged in such a way that sufficient accuracy in the calculations is achieved.

Reinforced concrete is a composite material made of concrete and steel, and the material model for particularly concrete is complex. This causes the finite element analysis of reinforced concrete to sometimes be more involved than for example structural steel, which is easier to model material wise. For example, for a reinforced concrete structure a more detailed finite element model might yield less accurate results if the material model is unable to describe the concrete material in sufficient detail. The following sections will give an overview of linear and nonlinear finite element analysis. A computational model will also be accounted for.

2.1.1 Linear finite element analysis

In a linear finite element analysis (LFEA) the materials are assumed to show linear elastic behavior and the assumption of small deflections is implemented, Hinton *et.al.* (1992). The solution in a LFEA is obtained in a one-step calculation since material properties, geometry and boundary conditions are not varying with the load level. Moreover, the load effects from several loads can be combined according to the principle of superposition. This methodology has proven efficient in traditional design of reinforced concrete.

A well performed linear finite element analysis often yields a reasonable idealized stress field, which can be used in design. However, if an accurate response of a structure is sought the model needs to be more realistic.

2.1.2 Nonlinear finite element analysis

In order to represent the true behavior of a structure, nonlinearities need to be included in the analysis, Hinton *et.al.* (1992). Three important sources of nonlinearity are material, geometry and boundary conditions. The nonlinear behavior of the material is perhaps the most intuitive, e.g. concrete cracking and/or reinforcement steel yielding. Geometrical nonlinearity is when a structure deforms under loading and the change in geometry alters the structural resistance. Geometrical nonlinearity is pronounced in slender columns where deflections greatly influence the capacity. Boundary nonlinearities are present when the reactions from the boundary change nonlinearly due to increased loading. Reaction forces employed by means of friction can be an example of nonlinear boundary conditions.

2.1.3 Strategy for structural Finite Element modelling

This section will briefly present the elements of a computational model used for finite element analysis. The presentation is found in Hinton *et.al.* (1992) where it describes NLFEA. Here it is modified to also apply for LFEA and to treat the solution strategy in more detail. An overview of a typical computational model can be seen in Figure 2.1 below.

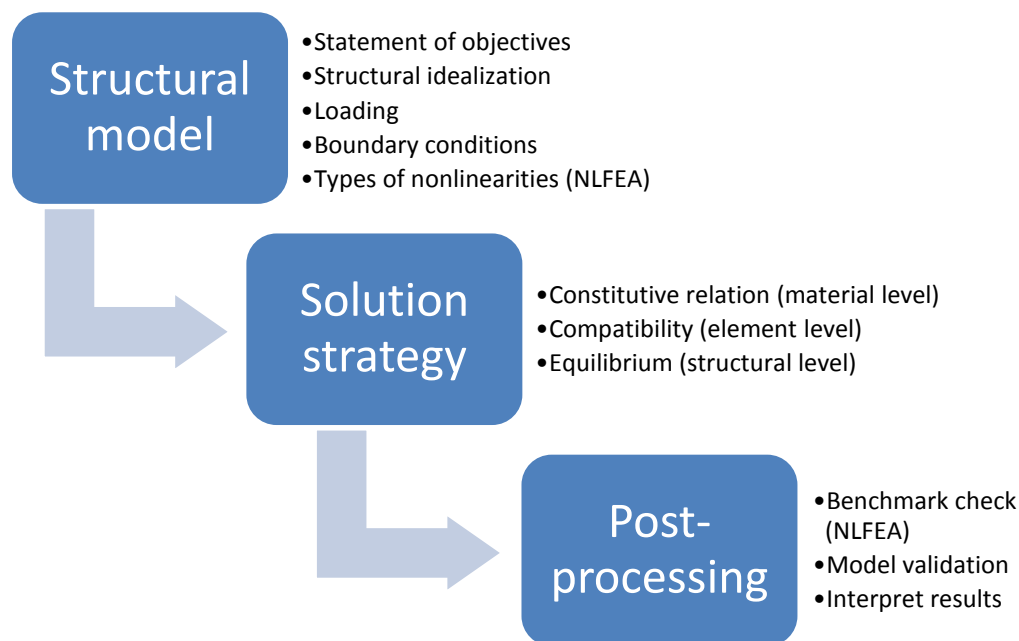


Figure 2.1 FEA computational model

2.1.3.1 Structural model

The first step when setting up a FE-model is to form a clear idea of the sought outcome. This will be of help when choosing how to idealize the structure. Depending on the goal with the analysis it might be best to use 1-D elements (beams, columns, cables etc.), 2-D (e.g. shells, walls) or 3-D elements. A combination of these types should also be considered. Further, clear goals with the analysis also help to decide how much structural detail that should be included in the model. It is also important to consider what the key features of the loading and boundary conditions are and how to

include these in the computational model. It can be advisable to exploit symmetries in the structural system in order to simplify the FE-model. However, one should be aware of such simplifications influence on the global response. In case of a nonlinear analysis, there are more considerations to be made. These include identification of the type(s) of nonlinearity, e.g. concerning boundary, geometry and material.

2.1.3.2 Solution strategy

The solution strategy for FEA includes the constitutive relation on material level, compatibility between strain and displacement on element level and equilibrium between internal and external forces on structural level. See Figure 2.2 below for an illustration.

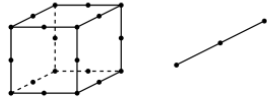
	LFEA	NLFEA
CONSTITUTIVE RELATION (material) <div style="text-align: center;"> \uparrow ε \downarrow σ, C </div>	Linear elastic material following Hooke's law for stress and strain: $\sigma = S\varepsilon$	Non-linear material model for concrete and reinforcement, and representation of cracking. Material stiffness matrix based on current tangent material stiffness. $\sigma = \sigma(\sigma, \varepsilon)$ $C = C_T(\sigma, \varepsilon)$
COMPATIBILITY (element) <div style="text-align: center;"> \uparrow d \downarrow r_e, k_e </div>	Finite element types and numerical integration scheme. <div style="text-align: center;">  </div> $u = Nd$ $\varepsilon = Bd$	$k_e = \int B^T C B dV$ $r_e = \int B^T \sigma dV$
EQUILIBRIUM (structure)	Assemble global matrices. $R_{int} = \sum (a_i)^T r_{e,i}, K = \sum (a_i)^T k_{e,i} a_i$	Calculate residual and iterative increment of nodal displacement: $R_{res} = R_{ext} - R_{int}$ $\delta d = (K_T)^{-1} R_{res}$
	Calculate nodal displacement: $d = K^{-1} R_{ext}$	

Figure 2.2 Depiction of FEM solution strategy by Engen (2014)

The linear elastic material model follows Hooke's law, i.e. the stiffness is independent of the stress level. In contrast, a nonlinear material model must be able to represent the real material with sufficient accuracy and in reality the stiffness is very much dependent of the stress state. Note that the solution strategy for NLFEA depicted in

Figure 2.2 is for small deformation only, i.e. geometrical nonlinearities are disregarded.

The continuous structural model principally described in Section 2.1.3.1 is to be discretized in order to obtain a finite number of degrees of freedom (D.O.F.). The type of unknowns should also be chosen, often displacements but other formulations are also used. The type of elements to be used should be decided, e.g. beam, shell or volumetric. The next step is to divide the structural model into elements, i.e. construct a mesh. The size of the elements can be varied in order to ensure adequate resolution of the results. For example, complex geometries can require smaller elements, i.e. denser mesh, in certain regions in order for the numerical approximation over the elements to be reasonable. The element stiffness matrices are constructed using the pertinent material stiffness matrices.

From the element stiffness matrices global stiffness matrices are assembled. In the case of LFEA, where the stiffness is independent of the stress, the equilibrium equations can be solved in one step and the nodal solution is obtained directly. For nonlinear analysis, however, the stiffness is dependent on the stress state in the material. Thus the equilibrium equations need to be solved in an iterative process. Nonlinear analyses are often performed using a scheme that gradually increases the load or node displacement. For each increment, equilibrium equations are obtained and solved. The Newton-Raphson method, or methods based in it, is commonly used to iteratively solve the system of equations. For each iteration the system of equations is updated with respect to the nonlinearities, e.g. changed element stiffness properties or large deformations. The iterations continue until a convergence criterion is fulfilled. It can for example be a tolerance put on the out of balance forces or incremental displacements. When the solution has converged for one load (or node displacement) step, an incremental increase of the load is applied and the iterative process continues. There must also be a criterion identifying divergence. Such a criterion can consist of comparing the magnitude of a reference displacement with the load increase. If the displacement is too large compared to the displacement caused by the prior load steps, the divergence criterion is fulfilled and the analysis is ended. The output data to be saved for post-processing needs to be selected. This is necessary since large amount of data is generated in the iterative process, much of which is not interesting for further use. What data to save is closely related to the objectives of the analysis described in Section 2.1.3.1.

2.1.3.3 Post-processing

The computational model needs to be validated in order to ensure meaningful results. This can be performed with different levels of depth depending on the user's experience from similar analyses. One way to validate the model is by benchmarking. That is, comparing the response of the computer model to known results from tables or practical experiments. Once sufficient confidence has been gained of the model yielding reasonable results, the analysis can be run for the loading conditions and material parameters of interest. The results from the analysis should be examined and engineering judgment should be employed. The typical output from a FEA are plots of deformed mesh, principal stresses and load-displacements plots. This output is common for both LFEA and NLFEA. In case of NLFEA, plots of plasticity zones and crack patterns is often also of interest. Previously defined components of the computer

model, e.g. element type, mesh, convergence criteria etc. might need to be changed in order to improve the analysis.

2.2 Background for structural reliability

This section serves to provide a background for reliability assessment of structures. The principles of limit state design will first be presented and then the concept of basic variables will be explained. Deterministic and probabilistic measures of limit state violation are presented and the concept of uncertainties and how they are accounted for will be described. Lastly considerations regarding the reliability levels of structures are accounted for.

2.2.1 Principles of limit state design

When a structure is subjected to a certain applied load it will respond in terms of internal stresses. The response is governed by the nature and magnitude of the load and the strength, stiffness and shape of the structure. The requirements put on the structure define if the response is acceptable or not, these are called limit states. There are two main types of limit states, considering the ultimate capacity and serviceability respectively. They are presented in more detail below.

2.2.1.1 Ultimate limit states

The ultimate limit state (ULS) relates to the maximum load carrying capacity of a structure but also the maximum deformability. Excess of an ultimate limit state is generally irreversible, meaning that failure occurs at the first violation. Below are some examples of ultimate limit states, JCSS (2001) and CEN (2008):

- maximum resistance capacity reached in sections, members or connections followed by excessive deformation or rupture
- loss of equilibrium in a part of the structure or the entire structure, leading to rigid body movement
- time dependent rupture of connections or members, e.g. fatigue induced rupture
- abrupt change of structural system, e.g. snap through failure

2.2.1.2 Serviceability limit state

The serviceability limit states (SLS) correspond, as the name implies, to the requirements put on the structure in service. Some examples are presented below, JCSS (2001):

- local damage that may reduce the durability or affect the appearance of an element in the structure, load carrying or not, e.g. excessive cracks in concrete
- deflections
- fatigue induced damage or damage due to other time dependent effects
- inadmissible deformations affecting the functionality or appearance to an unacceptable extent
- excessive vibrations which can disturb people and equipment

The violation of the serviceability limit state might be reversible. For example deflections might be non-permanent and retract to admissible levels once the situation causing the deflection is over. The conditions of failure with respect to the serviceability limit state should be specified. For example the number of times, or the duration, for which a certain deformation limit is allowed to be exceeded, JCSS (2001).

Structural reliability assessment aims to determine, using calculations and predictions, the probability of limit state violation at any stage of a structure's life time. Moreover, structural safety assessment is connected to the ultimate limit state of the structure. The probability of a limit state violation is the numerical value of the chance of it occurring. This value can be determined through long-term measurements of the event occurring on similar structures, but this is rarely used in practice. This is due to the long time span required for such measurements and the difficulty to find representative structures. The common procedure in practice is to use frequency observations of more general character, e.g. regarding structural properties, elements or materials, together with subjective estimates together in order to calculate the reliability using probabilistic calculations, Melchers (1999).

2.2.2 Basic variables

The behavior and safety of a structure can be described in terms of physical properties such as material strengths, dimensions, loads and weight etc. These are random in nature and pertain to the so called basic variables.

A wide definition of the basic variables also includes the parameters which characterize the model itself and sometimes also parameters describing the requirements on the structure. The basic variables are assumed to carry all the input data required for the analysis model, JCSS (2001).

The basic variables can be described as random variables with suitable probability distributions. What particular distribution to assign to a basic variable is often chosen based on observed data and experience. The central limit theorem is also used to justify the use of a normal distribution. That is, when several different components, regardless of the distributions, together form a basic variable it can be assumed to be normally distributed, Melchers (1999).

Furthermore, the basic variables are not limited to random variables, they can also be random processes, i.e. the evolution of the random variables over time, or random fields, e.g. material properties varies within a sample. There are standardizations in the JCSS Probabilistic Model Code, JCSS (2001) for the probability distributions of the basic variables depending on the class of the structural design problem.

2.2.3 Deterministic measures of structural reliability

A simplified way to check the reliability of a structure is to consider a special case where the basic variables are treated as deterministic. The values are derived from their probabilistic properties and are used directly in the calculations. Three measures for conducting such controls are presented below.

2.2.3.1 Factor of safety

A factor of safety is used to reduce the capacity of the material on the sectional level of a structure. It is typically used with linear elastic stress analysis and the limit state criterion is presented below:

$$\sigma_i(x) \leq \sigma_{pi} \text{ and } \sigma_{pi} = \frac{\sigma_{ui}}{F} \quad (2.1)$$

where $\sigma_i(x)$ is the i -th stress component in the point x of the structure and σ_{pi} is the maximum permissible stress or design stress. The value of σ_{ui} is based on the material strength, and the safety factor F reduces σ_{ui} to obtain the design stress. The safety factor value differs between construction materials and is regulated in the building codes. Typically a code committee decides the safety factor value based on experiments, experience and economy but sometimes also politics influence the decision, Melchers (1999).

The linear elastic stresses, obtained from e.g. LFEA, do not accurately describe the actual stress distribution in the structure, which has been stated previously. The stress field is changed due to stress concentration and redistribution along with boundary and physical size effects. Also the permissible stresses are obtained by linear scaling down the ultimate capacity, even though it is typically reached in the nonlinear region. The calculation can therefore be described as a conservative estimate rather than a precise calculation of the utilization of the section, Melchers (1999).

2.2.3.2 Load factor

The load factor approach was originally developed to be used in the plastic theory of structures. The loads are increased using a factor λ , which corresponds to how many times the set of loads must be multiplied in order to cause collapse of the structure. Here the strength of the structure is determined by using the plastic resistances. The structure is considered to have failed or collapsed when the external work exceeds the internal work, see equation (2.2) below:

$$W_R(\mathbf{R}_P) \leq W_Q(\lambda \mathbf{Q}) \quad (2.2)$$

where \mathbf{R}_P contains the plastic resistances, λ is the load factor and \mathbf{Q} contains all the applied loads. W_R and W_Q are the internal and external work respectively. The principal difference between the “factor of safety” and the “load factor” reliability measures is in which reference level they are applied. The prior is applied on the sectional level while the latter is applied on the structural level, Melchers (1999).

2.2.3.3 Partial factor

The “partial factor” measure of safety is developed from the two previously mentioned measures. It yields a limit state on member design level as presented in equation (2.3) below:

$$\phi_i R_i \leq \gamma_{Di} S_{Di} + \gamma_{Li} S_{Li} + \dots \quad (2.3)$$

where the index i represent the limit state, R is the member resistance and ϕ is the partial factor pertinent to R . Further, S_D and S_L are the load effects from the dead and live load and γ_D and γ_S are the partial factors. This safety format is an improvement

of the previously treated since it separates the uncertainty corresponding to dead and live loads as well as including a factor for modelling and construction uncertainty of the resistance.

The same safety format applied to plastic collapse on the structural level is presented in equation (2.4) below:

$$W_R(\phi \mathbf{R}) \leq W_Q(\gamma_D \mathbf{Q}_D + \gamma_L \mathbf{Q}_L + \dots) \quad (2.4)$$

where \mathbf{R} and \mathbf{Q} are vectors containing the resistances and loads and ϕ and γ are the partial factors. Note that the partial factors differs between member and structural level, i.e. between equations (2.3) and (2.4). This since for example load redistribution is included in the latter expression and should be reflected in the partial factors.

2.2.4 Probabilistic measures of structural reliability

The probability of failure is a central part of reliability assessment. It is not possible to obtain using the deterministic measures of failure presented above. A probabilistic measure of limit state violation is more complex and enables assessment of the probability of failure.

In order to describe the limit state function a simple case will first be presented and then a general approach will be introduced. Consider the case of a structure with a certain resistance (R) subjected to a certain load effect (S), which are both independent random variables. The probability of failure can for the simple case be written as:

$$p_f = P(R \leq S) = P(R - S \leq 0) \quad (2.5)$$

where p_f is the probability of failure, R is the resistance and S is the load effect. Or more generally as:

$$p_f = P[G(R, S) \leq 0] \quad (2.6)$$

where G is generally known as the limit state function. The bivariate (joint) probability density function of the resistance and load effect, $f_{RS}(r, s)$, can be used to calculate the failure probability. If the resistance and load effect are assumed independent the following is true, Melchers (1999):

$$p_f = P(R - S \leq 0) = \iint_D f_{RS}(r, s) dr ds \quad (2.7)$$

$$p_f = \int_{-\infty}^{\infty} \int_{-\infty}^{s \geq r} f_R(r) f_S(s) dr ds \quad (2.8)$$

where D represents the failure domain. Knowing that the cumulative distribution function is:

$$F_X(x) = P(X \leq x) = \int_{-\infty}^x f_X(y) dy \quad (2.9)$$

provided that $x \geq y$ the probability of failure can be written as:

$$p_f = \int_{-\infty}^{\infty} F_R(x) f_S(x) dx \quad (2.10)$$

where $F_R(x)$ is the cumulative distribution function (*cdf*) of the resistance and $f_S(x)$ is the probability density function (*pdf*) of the load effect. equation (2.10) is an intuitively attracting way to describe failure since $F_R(x)$ is the probability of a resistance lower than x and $f_S(x)$ corresponds to $x \leq S \leq x + \Delta x$ when $\Delta x \rightarrow 0$. In other words, the probability of the event where the load effect exceeds the resistance is integrated over the entire domain to obtain the probability of failure.

An illustration of the probability functions for load effect and resistance are depicted in Figure 2.3 below. The failure density, i.e. the integrand of equation (2.10), is also shown. The area under the failure density curve represents the probability of failure.

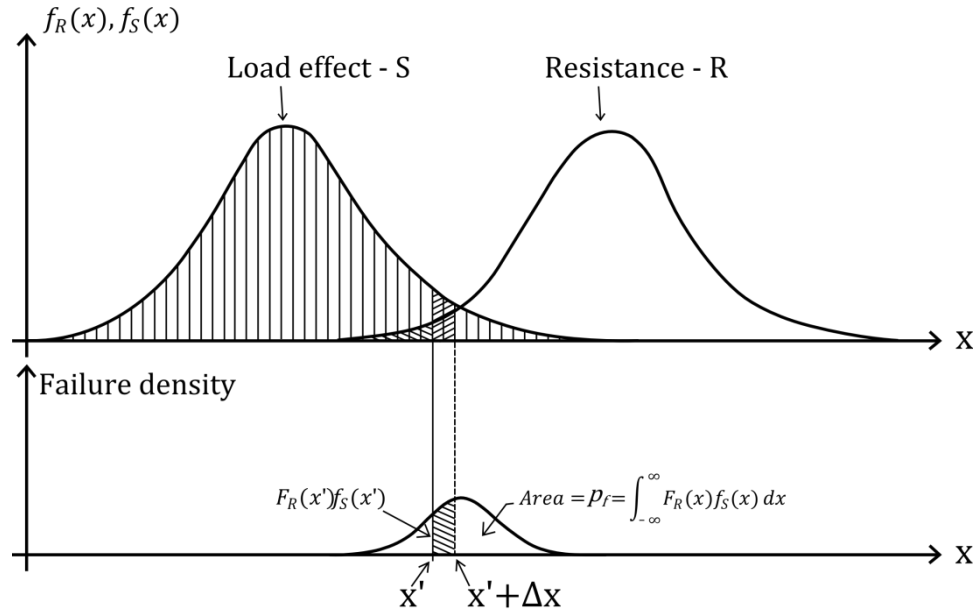


Figure 2.3 Depiction of a probability of failure calculation, adopted from Melchers (1999)

The basic case presented above needs to be generalized in order to be adequate for practical considerations. Both the load effect and the resistance will most probably be functions of several variables, each of which can be random. It is also possible that the resistance and the load effect are dependent, i.e. influence each other. This is the case when one or several loads contradict failure, e.g. in an overturning situation. A generalized approach is needed and the convolution integral in equation (2.10) is primarily for illustration.

The generalized limit state function can be described as a function of all the basic variables related to it. In analogy with the simple example treated earlier, the resistance can be written as $R = G_R(\mathbf{X})$ where \mathbf{X} is the vector containing the basic variables. The load effect can be written analogously. The model uncertainty should also be included. The probability density functions of these expressions can be integrated over the pertinent basic variables and be used to construct the convolution integral. But this is typically not done. Instead of having R and S separated, they are incorporated in equation (2.6) and the generalized limit state function (or performance function) can be written as:

$$G(\mathbf{X}) = G(G_R(\mathbf{X}), G_S(\mathbf{X}), G_\theta(\mathbf{X})) \quad (2.11)$$

and thus the limit $G > 0$ represent the safe domain while $G \leq 0$ represent failure. G_θ represents the model uncertainty. It should be noted that the generalized limit state function typically only contains R and S implicitly.

This probability of failure is evaluated in the same manner as described earlier, but the mathematics are now more complex:

$$p_f = P[G(\mathbf{X}) \leq 0] = \int_{G(\mathbf{X}) \leq 0} f_{\mathbf{X}}(\mathbf{x}) d\mathbf{x} \quad (2.12)$$

where $f_{\mathbf{X}}(\mathbf{x})$ is the bivariate probability density function of the n -dimensional vector \mathbf{X} containing the basic variables. Numerical integration is used in practical cases to calculate the probability of failure, Melchers (1999).

2.2.5 Uncertainties

Uncertainties originating from all important sources must be evaluated and included in the model of basic variables. The uncertainties can be characterized as, JCSS (2001):

- inherent physical or mechanical uncertainty, e.g. material and geometry uncertainties
- statistical uncertainty, e.g. when few observations form the base for design decisions
- model uncertainties

The material uncertainties are taken into account by modelling the material as random variables following some distribution. Also geometry is treated in a similar manner. All types of uncertainties where statistical estimators (e.g. sample mean and standard deviation) are used to find a suitable probability density functions are subjected to statistical uncertainty. This since the observations does not perfectly represent the actual variable. Several types of uncertainties can be present for the same basic variable. For example load modelling is based on statistical data and thus stained with statistical uncertainty. But it is also regarded as a simplification of reality and pertinent to the model uncertainties.

The modelling uncertainty is a very important part describing that a predicted solution obtained via a computational model will generally differ from the true solution. This might be due to lack of knowledge or simplifying assumptions. Some common simplifying assumptions are for example idealizations of the structure and selections of what loads to use in the analyses. In order to calibrate the model, model uncertainty parameters with certain statistical properties are included. The parameters describing the model uncertainty can be derived from experiments or observations. However, it was found by Schlune (2011) that the model uncertainty is hard to assess for difficult to model failure modes. Ideally, when the model uncertainty parameters are implemented in the computational model, it should on average predict the solutions correctly. It can be noted that many models in the design codes are intended to yield conservative results, i.e. they have an intentional bias which should be considered when comparing results gained using different methods.

2.2.6 Reliability level

The generalized reliability index is typically used as a reliability measure. The definition is corresponding to a certain probability of failure, based on a standardized normal distribution (standard Gaussian distribution). It can be described as the number of standard deviations (equal to unity in a standardized Gaussian distribution) away from the mean value (i.e. zero for said distribution) corresponding to the probability of failure. It is written as, JCSS (2001):

$$\beta = -\Phi^{-1}(P_f) \quad (2.13)$$

where P_f is the probability of failure and Φ^{-1} is the inverse Gaussian distribution. The probability of failure should be calculated from the standardized joint distribution of the basic variables including modelling uncertainty as well as statistical uncertainty.

A differentiation is made between component reliability and system reliability. As the names imply the component reliability is related to failure of a single component while the latter is associated with system failure. Systems can also be divided into redundant and non-redundant systems. Failure occurring in one component of a redundant system does not mean failure of the entire system, but it does in a non-redundant system. Probabilistic structural design is conducted primarily with respect to component failure, but the consequences of system failure are often more severe, JCSS (2001).

2.2.6.1 Target reliability

The consequences of a possible failure are central when determining the target reliability. More specifically, risk of personal injury and death together with economic and societal losses should be included in the assessment. Also the cost and effort to decrease the probability of failure should be considered when determining the target reliability level fib (2013). This is not uncontroversial since the probability of casualties and injuries are compared with the cost of reducing the risk. Recommendations for target reliability levels for different limit states and reference periods are available in the for example the Model Code 2010, fib (2013) and Eurocode 1990, CEN (2008).

2.3 Safety formats for nonlinear analysis

In order to verify the adequacy of a structure, it must be checked that the limit state function is satisfied. Traditionally checks on sectional level are conducted using partial coefficients, derived from the probability density functions of the basic variables. These checks have limited applicability to nonlinear analysis since the real behavior of the structure is sought, and it is not reflected by altering the sectional capacities and load effects. Another approach should be taken for NLFEA. The most probable, i.e. mean, resistance of the structure should be used as a reference for the safety evaluation. Since the basic variables contributing to the resistance are uncertain and vary randomly, the resistance is also random with a certain variation. There are also uncertainties related to the modelling which need to be addressed. The purpose of the safety formats is to account for these uncertainties and yield a design according to the chosen safety level, fib (2013).

The design condition used is as follows:

$$F_d \leq R_d, \quad R_d = \frac{R_m}{\gamma_R^* \gamma_{Rd}} \quad (2.14)$$

where F_d is the design value of actions, R_d is the design resistance, R_m is the mean resistance, γ_R^* is the global safety factor and γ_{Rd} is the model uncertainty factor.

There are several safety formats described in the Model Code that can be used to evaluate R_d . They are presented in the following sections.

2.3.1 Probabilistic method

When the probabilistic method is used, the design resistance is evaluated explicitly according to a specified safety index or probability of failure.

$$R_d = \frac{1}{\gamma_{Rd}} R(\alpha\beta), \quad \gamma_{Rd} > 1 \quad (2.15)$$

where γ_{Rd} is the modelling uncertainty factor and $R(\alpha\beta)$ is the resistance obtained from nonlinear analyses when all uncertainties are included. The uncertainties are those connected to the resistance side of the design equation, namely the geometry and materials properties and conceivably others depending on the situation. The resistance corresponding to the safety index β , directly transferable to a probability of failure, is used in the above equation. The safety index is reduced by a sensitivity factor α since only the resistance side of the design condition is treated.

A short description of how to perform a probabilistic analysis following the Model Code 2010 provisions is found in Section 2.4.4.

2.3.2 Global resistance method

For the global resistance method the design resistance is estimated with a simplified probabilistic approach. There are two methods included in the Model Code 2010, of which the second is more involved. Both methods are presented in the two following subsections.

2.3.2.1 Global resistance factor method (GRFm)

In the GRFm the mean resistances are used for the material properties. The difference in uncertainty between reinforcement steel and concrete is accounted for to achieve a common global safety factor for the mean strength of both steel and concrete. The design resistance is formulated as:

$$R_d = \frac{r(f_m, \dots)}{\gamma_R \gamma_{Rd}} \quad (2.16)$$

where the function r represents the resistance obtained from nonlinear analysis with mean input material parameters. The safety factors for resistance and model uncertainty, γ_R and γ_{Rd} , are here given as 1.2 and 1.06 respectively. The mean reinforcement steel properties can be approximated from the characteristic values as:

$$f_{ym} = 1.1 f_{yk} \quad (2.17)$$

The concrete properties to be used in the analysis can be calculated as:

$$f_{cf} = 1.1\alpha_{cf}f_{cfk}\frac{\gamma_s}{\gamma_c} \quad (2.18)$$

where f_{cf} is the concrete strength parameter. The reduction originates from the common global safety factor, here used for the both steel and concrete. Since the steel and concrete partial factors are formulated for the same failure probability but concrete have larger variability, concrete requires a larger safety margin. This is adjusted for in the expression above. Furthermore, $0.85 \leq \alpha_{cf} \leq 1.0$ is a factor accounting for sustained load and unfavorable load application effects and f_{cfk} is the characteristic concrete property.

2.3.2.2 Method of estimation of a coefficient of variance of resistance (ECOV)

This safety format is based on research suggesting that the randomness of the resistance can be described as a lognormal distribution with two parameters. The two parameters are the mean resistance and the variance of the resistance. These two parameters are sufficient to describe the lognormal distribution. Other parameters such as the quantiles of the resistance distribution, typically the 5% quantile that correspond to the resistance using characteristic material input, can be derived from this distribution. Since the variance of the resistance is typically unknown, two NLFEA are conducted. One performed with mean input parameters for the material data and one with characteristic values. From these resistances it is possible to estimate the coefficient of variance of resistance. This can be put in mathematical terms as:

$$R_m = r(f_m, \dots), R_k = r(f_k, \dots) \quad (2.19)$$

where r is the resistance from nonlinear analyses with mean and characteristic values as material input parameters respectively. As stated above, describing the resistance as a two parameter lognormal distribution enables determining the coefficient of variation of resistance as:

$$V_R = \frac{1}{1.65} \ln\left(\frac{R_m}{R_k}\right) \quad (2.20)$$

where V_R is the coefficient of variation of resistance for a characteristic value with 5% probability. The factor for global resistance γ_R can be calculated as follows:

$$\gamma_R = \exp(\alpha_R \beta V_R) \quad (2.21)$$

where α_R is a weight factor for the reliability index, β . The design value for the resistance can be calculated as:

$$R_d = \frac{R_m}{\gamma_{Rd}\gamma_R} \quad (2.22)$$

where the model uncertainty γ_{Rd} is suggested as 1.06 for numerical models with well documented validity. A higher value should be used for the model uncertainty if the prior requirement is not fulfilled.

2.3.3 Partial factor method

According to the partial factor method, the nonlinear analysis is performed using the deterministic design values derived from the random material parameters. Using so highly reduced material parameters, this approach does not capture the global safety and does not well describe the structural response of the structure. It can also cause the structure to fail in a distorted mode, not reflecting the actual behavior according to Cervenka (2013). Nevertheless, case studies suggest that the partial factor method can be used as a blunt but safe estimate. In mathematical terms, the design resistance is obtained as:

$$R_d = r(f_d, \dots) \quad (2.23)$$

where r represents the nonlinear analysis for the design value f_d of the input parameters. It should be noted that the model uncertainty factor γ_{Rd} is not included in the expression above. This since it is typically included in the partial safety factor γ_M for the materials and thus also in the design values.

2.3.4 Discussion regarding safety formats

General for all the safety formats above is that they do not always account properly for the model uncertainty, especially for difficult to model failure modes, Schlune (2011). The probabilistic method is the most accurate, but it is not feasible in most practical application due to the vast amount of uncertainties to be included in the analyses. The partial factor method is, as stated earlier, not advised for NLFEA due to the low material strengths used. The global resistance factor method is an extension of the partial factor method where the mean values are obtained from the characteristic values. The ECOV method uses both the mean and characteristic material strengths in the analyses. But for both methods, the concrete strengths are determined by testing specially cured samples. The mean strengths of in situ concrete can be lower and have larger variability than the tested samples, but this is disregarded. The reliability level of the structure can as a consequence of this be lower than intended, Schlune (2011).

2.4 Reliability analysis of structures

The assessment of the reliability of a structure is not easily conducted. It is a vast topic spanning from defining “failure” of a structure to occur to making sophisticated computer simulations and evaluating the results. Further, there may be several failure modes on sectional level, which in some combinations will lead to structural failure. This section treats several ways of evaluating the integral expression for failure probability previously presented in equation (2.12).

Analytical evaluation of the integral describing probability of failure is generally not possible in practical applications. Conventional techniques for numerical integration are possible to use, but their applicability in practical situation is limited, Melchers (1999). Round off errors and the so called “curse of dimensionality” are the main limitations of numerical integration measures. The latter means the rapid increase in computational demands when the number of dimensions in the integration space increases. The practical limit is often taken as 5 dimensions, and that is when simplified regions are used to confine the integration space, Davis *et. al.* (1975).

Other methods have been developed for integration in many dimensions which also accommodates any type of distributions for the random input variables. These numerical solution strategies for evaluating the probability integral are commonly known as Monte Carlo simulations or just simulations, Melchers (1999). Section 2.4.1 aims to give a general overview of the Monte Carlo simulation techniques.

Another approach can be taken when evaluating the convolution integral in equation (2.10). Instead of using simulations, the integrand can be simplified. The so called First Order Reliability Method (FORM) and Second Order Reliability Method (SORM) use this methodology in order to assess the probability of failure. An overview of these methods will be given in Section 2.4.2.

Furthermore, an implicit limit state function, obtained from e.g. FEA, can be approximated by fitting a so called response surface to a set of evaluations of the implicit function. This results in a closed form, differentiable expression which can be used for both Monte Carlo simulations and FORM/SORM. The concept of the procedure is presented in Section 2.4.3 below.

2.4.1 Monte Carlo simulations

The Monte Carlo techniques involve sampling values of the basic variables in order to conduct many simulated experiments. The input variables for the limit state function are randomly (or rather pseudo randomly) collected from their probabilistic distributions. Every realization of the random variables is checked against the limit state and the probability of failure can be calculated as:

$$p_f \approx \frac{n(G(x_i) \leq 0)}{N} \quad (2.25)$$

where $n(G(x_i) \leq 0)$ is the number of virtual experiments (or trials) where the limit state is violated and N is the total number of trials. The number of virtual experiments conducted governs the accuracy of the estimation of p_f and is logically dependent on the evaluated function. It has been suggested that around 10 000 - 20 000 simulations are needed to reach a 95% confidence limit, Melchers (1999).

2.4.1.1 Sampling of basic variables

The basic variables for evaluating the limit state function can be sampled in different ways. The most adequate and simplest way to sample the basic variables is simply to generate them from their distributions, with the sampling center located at the origin in the standard Gaussian space (i.e. u -space). This type of sampling is known as crude Monte Carlo sampling, and is very time consuming and computing expensive. This is because in reliability analyses the tail of the limit state functions is studied, i.e. very small probabilities of failure are of interest. A vast amount of realizations of the basic variables and corresponding evaluations of the limit state function are required to have enough data for a good representation in the tail region, Olsson *et. al.* (2003).

Importance sampling is often used in order to reduce the number of simulations needed to obtain the desired result. One way to do this is to position the sampling center at the design point on the failure surface instead of the origin in the u -space. The design point is often found using a search algorithm for the Gaussian space where gradients are used to locate the design point. This requires the basic variable to be

transformable to said space, and also for the failure surface to be differentiable. This is not always the case. The design point can also be found from updating the sampling center based on previous samplings, a procedure that is generally applicable but may be less effective.

When the design point is the sampling center, approximately half the realizations will yield failure. The probability of failure in case of importance sampling can be calculated as the sum of the weight factors for the realizations causing failure divided by the total number of realizations, Olsson *et. al.* (2003). That is in mathematical terms:

$$p_f = \frac{1}{N} \sum_{i=1}^N (W(\tilde{\mathbf{v}}_i) | (g(\tilde{\mathbf{v}}_i) < 0)) \quad (2.26)$$

where N is the number of realizations, $\tilde{\mathbf{v}}_i$ is the realization of the importance sampling distribution, $g(\tilde{\mathbf{v}}_i) < 0$ is the failure criterion and $W(\tilde{\mathbf{v}}_i)$ is the weight factor corresponding to the importance sampling. The weight factor can be calculated as:

$$W(\tilde{\mathbf{v}}_i) = \frac{\phi_{\mathbf{u}}(\tilde{\mathbf{v}}_i)}{h_{\mathbf{v}}(\tilde{\mathbf{v}}_i)} \quad (2.27)$$

where $\phi_{\mathbf{u}}(\tilde{\mathbf{v}}_i)$ is the joint probability density function of the set \mathbf{u} of the stochastic variables in the u -space and $h_{\mathbf{v}}(\tilde{\mathbf{v}}_i)$ is called the importance sampling probability density function. Many distribution types can be used for the importance sampling pdf, the simplest is a multi-dimensional Gaussian distribution with unit standard deviation, Olsson *et. al.* (2003). However, this might not be the most effective sampling function as the optimal choice is a function that minimizes the variance of p_f , Melchers (1999).

For a structural system with several limit state functions the importance sampling function should preferably have several modes, each assigned a certain weight coefficient. The weight coefficients are used to rank the sampling function modes by importance depending on the importance of the corresponding limit state.

2.4.1.2 Latin hypercube importance sampling

The Latin hypercube sampling method is a sampling plan which can be employed for Monte Carlo simulations, Olsson *et. al.* (2003). First, the method will be presented in its simplest form, and then its application to importance sampling will be explained. It should be mentioned that there are several alterations and versions of Latin hypercube sampling. The precise measures of these are beyond the scope of this thesis, where instead an overview and explanation of the concept is provided.

The basic sampling plan is represented by a matrix which is constructed as:

$$\mathbf{S} = \frac{1}{N} (\mathbf{P} - \mathbf{R}) \quad (2.28)$$

where N is the number of realizations, \mathbf{P} is a matrix of size $N \times K$ where K is the number of stochastic variables. Each of the columns in the \mathbf{P} matrix contains a random permutation of the numbers 1,2, ... N . The permutation matrix \mathbf{P} is typically modified to avoid spurious correlation of sampling plan, a procedure involving the covariance matrix and Cholesky decomposition. The matrix \mathbf{R} is of the same size, $N \times K$, but each element consists of an independent random value from the uniform (0,1) distribution.

In order to make this clearer, a basic example for a sampling of two basic variables and five realizations is shown in Figure 2.4 below. The simple example is from Olsson *et. al.* (2003).

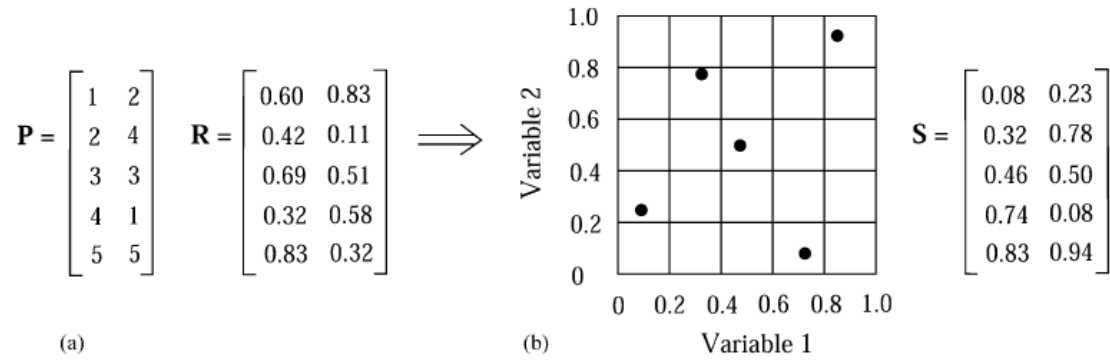


Figure 2.4 Basic LHS sampling plan for two basic variables and five realizations, from Olsson *et. al.* (2003)

The sampling plan, described by \mathbf{S} , is transformed into standard Gaussians variables to obtain realizations in the u -space centered at the origin. This is done as:

$$\hat{u}_{ij} = \Phi^{-1}(s_{ij}) \quad (2.29)$$

It should be noted that other distributions can be used for the importance sampling distribution. In case of other distributions, the sampling plan \mathbf{S} is mapped using the pertinent inverse *cdf*. In this case however, the vector $\hat{\mathbf{u}}_i = [\hat{u}_{i1} \ \hat{u}_{i2} \ \dots \ \hat{u}_{ij}]$ is centered at the origin of the u -space and moved to the design point by adding the design point position vector, \mathbf{m} , for each realization. That is:

$$\tilde{\mathbf{u}}_i = \hat{\mathbf{u}}_i + \mathbf{m} \quad (2.30)$$

where $\tilde{\mathbf{u}}_i$ is the sample centered at the design point. The probability of failure can now be calculated according to equation (2.26) but the weight factor is now given as:

$$W(\tilde{\mathbf{u}}_i) = \frac{\phi_u(\tilde{\mathbf{u}}_i)}{\phi_u(\hat{\mathbf{u}}_i)} \quad (2.31)$$

where ϕ_u is the standard Gaussian *pdf* of K -dimensions, centered at the origin of the u -space.

2.4.2 First and second order reliability method (FORM/SORM)

The first order reliability method is based on the first order second moment methodology. The reliability index is calculated as the length of the vector between the approximation of the limit state surface and the origin in the normalized space, Zhao & Ono (1999). The basic variables in the limit state function are represented by their first and second moments only. That is, their expected value and standard deviation. Possible skew and flatness of the random variables are ignored and they can be represented by standard normal distributions. Random variables with other distributions can be transformed into standard normal variables, using more or less involved techniques depending on the type of random variable. A deeper discussion

on the transformations will not be held here, but can be found in Melchers (1999). The basic calculations behind the second moment concept are presented below.

If the basic variables are transformed into standard normal distributions from other distribution types, the term failure probability should be used with caution. Following the notation in Melchers (1999), it is instead called the nominal probability of failure, p_{fN} . Considering the simple limit state $Z = R - S$ where both R and S are represented by normal distributions, the nominal probability of failure can be written as:

$$p_{fN} = \Phi(-\beta) \text{ and } \beta = \frac{\mu_Z}{\sigma_Z} \quad (2.32)$$

where Φ is the standard normal distribution and β is the reliability index. In case of several basic random variables the limit state function can be approximated as:

$$G(\mathbf{X}) = Z(\mathbf{X}) = a_0 + a_1X_1 + a_2X_2 + \dots + a_nX_n \quad (2.33)$$

where $Z(\mathbf{X})$ is normally distributed and the reliability index can be calculated using equation (2.32).

In most cases the limit state function $G(\mathbf{x}) = 0$ is nonlinear, but it can be linearized in order to more easily obtain the mean and standard deviation. It is usually performed by a first order Taylor series expansion of $G(\mathbf{x}) = 0$ around a certain point. This gives rise to the name “first order reliability method”. The point is preferably chosen as the point of maximum likelihood of the limit state function, which is where failure is most likely to occur.

The so called Hasofer–Lind transformation is often used for transforming the random variables to standard normal form with mean value zero and unit variance, i.e. $N(0,1)$. It is done by the performing the simple operation:

$$Y_i = \frac{X_i - \mu_{X_i}}{\sigma_{X_i}} \quad (2.34)$$

The limit state function must also be transformed accordingly and is expressed on standardized normal form as $g(\mathbf{y}) = 0$, Melchers (1999). In an n -dimensional standard normal space, when $g(\mathbf{y}) = 0$, the reliability index can be calculated as:

$$\beta = \min(\sum_{i=1}^n y_i^2)^{1/2} \quad (2.35)$$

The point, \mathbf{y} , satisfying the above expression is known as the design point for the FORM method. It is typically found using an iterative procedure (i.e. in case of nonlinear limit state function).

In cases when the limit state function is regarded too nonlinear for a linear approximation surface to be adequate, a second order polynomial can be used as approximation for the failure surface.

The results from a finite element analysis do not yield an explicit expression for the failure surface, thus the FORM/SORM methods cannot be implemented directly. But there are measures to apply the methods to FEA results; one involves a so called response surface. It is presented in the following section.

2.4.3 Response surface

In many practical applications, such as finite element analysis, the limit state is given implicitly. The limit state surface is not explicitly described by a set of equations, instead the boundary between the safe and failure domain must be revealed by several numerical analyses with different input values. The input values can either be random or sampled according to some scheme, Melchers (1999).

Even though the limit state surface is only given implicitly, a suitable function can be fitted to a set of results obtained from analyses performed with different deterministic input values for the basic variables. The fitted closed form function is differentiable and now represents a tractable approximation of the failure surface, i.e. the response surface. It should be determined with greater accuracy close to the design point, with lower accuracy accepted elsewhere, in order to yield a reasonable estimation of the probability of structural failure.

The concept of constructing a response surface is presented below based on Bucher & Bourgund (1990) and Melchers (1999). The implicit limit state function of the structure is given as $G(\mathbf{X})$ and it can be evaluated for discrete values of $\mathbf{X} = \mathbf{x}$. Consider a set of points in the \mathbf{x} -space denoted $\bar{\mathbf{x}}$ and evaluate $G(\bar{\mathbf{x}})$. A response surface, $\bar{G}(\mathbf{x})$, can be determined as the best fit of an n -degree polynomial in respect to $G(\bar{\mathbf{x}})$. A second order polynomial is typically used for the response surface and it can be mathematically described as:

$$\bar{G}(\mathbf{X}) = A + \mathbf{X}^T \mathbf{B} + \mathbf{X}^T \mathbf{C} \mathbf{X} \quad (2.36)$$

where A , \mathbf{B} and \mathbf{C} are regression coefficients on scalar, vector and a matrix form obtained from conducting numerical analyses with input parameters chosen according to some strategy. The determination of the coefficients based on evaluation of the implicit limit state can be described as by Rajashekhar & Ellingwood (1993):

$$G(\mathbf{x}) = \mathbf{D}\mathbf{d} + \mathbf{e} \quad (2.37)$$

where \mathbf{D} contains constants together with linear, quadratic and cross combinations of x_j . The matrix \mathbf{d} contains the regression coefficients and \mathbf{e} is the error vector, containing both lack of fit errors and experimental errors. The error vector is assumed to have zero mean value and therefore vanishes when assessing the expected value of \mathbf{d} . The expected value of the regression coefficients can be determined as, Rajashekhar & Ellingwood (1993):

$$E(\mathbf{d}) = (\mathbf{D}^T \mathbf{D})^{-1} \mathbf{D}^T G(\mathbf{x}) \quad (2.38)$$

The experimental design strategy should reflect that it is, as previously stated most important to have an accurate approximation close to the design point in order to get a fair assessment of the probability of failure. An iterative procedure suggested by Bucher & Bourgund (1990) is presented below.

As the design point is not known, the mean values of the basic variables can be used in a first set of numerical experiments and a first iteration design point can be determined. New input values for the basic variables can be determined based on the location of the design point, and the iterative procedure can be repeated until the design point and thus the response surface have stabilized. When the cross combinations of x are neglected, the expression for the polynomial can be put into mathematical term as:

$$\bar{g}(\mathbf{x}) = a + \sum_{i=1}^n b_i x_i + \sum_{i=1}^n c_i x_i^2 \quad (2.39)$$

were a , b_i and c_i are the regression coefficients to be determined. The suggested way of obtaining the coefficients involves linear interpolation between the axes of the basic variables. It is suggested that the values are chosen initially as the mean values along with values incorporating the standard deviation of the variable. That is, $x_i = \bar{x}_i$ and $x_i = \bar{x}_i \pm f_i \sigma_i$ where f_i is a factor ($f_i = 3$ is suggested as starting value) and σ_i is the standard deviation. When the value of the implicit limit state function is evaluated $2n + 1$ times for the x_i values, the coefficients can be determined through solving the linear equation system. A starting value of the design point can be established from $\bar{g}(\mathbf{x}) = 0$, assuming that \mathbf{X} consists of uncorrelated Gaussian random variables. Using it as input in the expression below, a new center of approximation point, \mathbf{x}_M , can be determined.

$$\mathbf{x}_{M_{i+1}} = \mathbf{x}_{M_i} + (\mathbf{x}_{M_{i-1}} - \mathbf{x}_{M_i}) \frac{g(\mathbf{x}_{M_i})}{g(\mathbf{x}_{M_i}) - g(\mathbf{x}_{M_{i-1}})} \quad (2.40)$$

where the new center of interpolation is determined through linear interpolation. The procedure of constructing the response surface according to equation (2.39) is repeated. This procedure can be repeated until sufficiently stable \mathbf{x}_M is achieved. The number of iterations required depends on the shape of the actual limit state surface. An illustration of the procedure can be seen in Figure 2.5 below.

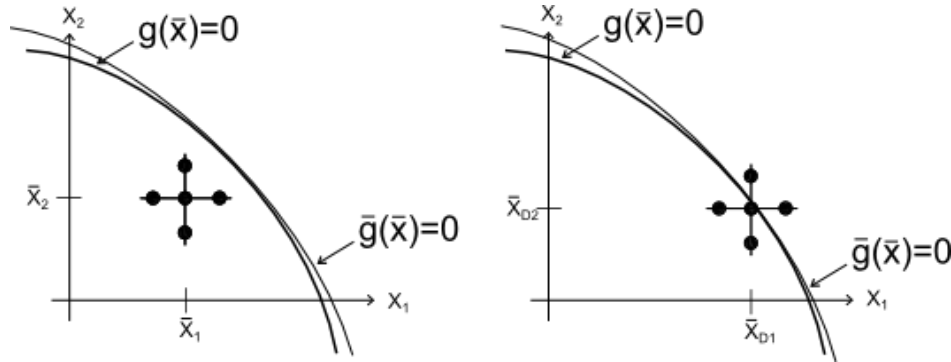


Figure 2.5 Depiction of the procedure suggested by Bucher et. al. (1990)

In some cases it is not appropriate to neglect the mixed x -terms, since the approximation then would be too gross. In that case, mixed terms can be included in the expression for the response surface as:

$$\bar{g}(\mathbf{x}) = a + \sum_{i=1}^n b_i x_i + \sum_{i=1}^n c_i x_i^2 + \sum_{i \neq j} \sum d_{ij} x_i x_j \quad (2.41)$$

where the last summation term incorporates the cross combinations of x needed for sufficient accuracy, Bucher & Bourgund (1990).

The response surfaces are closed form, differentiable functions of the basic variables. They can therefore be used to conduct FORM and SORM evaluations on results gained from finite element analyses.

2.4.4 Procedure suggested in Model Code 2010

The procedure for conducting a nonlinear probabilistic analysis, in order to obtain the design resistance, is briefly presented below. First a resistance function is developed and described by a numerical model. The model should enable deterministic analysis based on a set of input parameters and it should be based on a nonlinear finite element method. Then the basic input variables for the resistance function are randomized from their probabilistic properties. Two common approaches are to either randomize the basic input parameters between samples or to randomize them within each sample. The sample here means the structure to be analyzed. The analysis of the resistance can now be performed. A common way to conduct this probabilistic analysis is by means of the Latin Hypercube Sampling method (LHS), based on Monte Carlo sampling. This analysis yields the resistance of the structure, described by probabilistic parameters such as the distribution type along with its mean value and standard deviation. The design value corresponding to the target reliability index or probability of failure can be obtained directly from the resistance distribution function.

3 Case study – comparison of safety formats

This chapter presents the case study performed in order to compare results obtained from the different safety formats in the Model Code 2010, fib (2013), which were presented in Section 2.3.

3.1 Solution strategy for NLFEA

A nonlinear finite element model can be set up in many different ways. For example the structural idealization, the type of elements used and the mesh division are decisions made by the analyst. Also the analysis can be performed in different ways, for example different iterative solution strategies can be used and the analysis can be either force or displacement controlled. The model assumptions should be verified by checking that the model can produce accurate results. Typically a linear elastic analysis has been performed prior to the nonlinear. The resulting stress fields from the LFEA can be used as a comparison in the first step. They will of course differ markedly in many cases, but can be useful as a first comparison. To assess how well the nonlinear analysis represents the actual behavior of the structure, a benchmark study can be performed. This is basically a comparison between the NLFEA results and data from a physical experiment.

3.1.1 Portal frame experiment

The benchmarking of the NLFEA in this project is made against the data from an experiment on a portal frame, Seraj & Kotsovos *et. al.* (1995 & 1999).

The frame had a height of 1.800 m high and was 2.868 m wide in outer dimensions. The reinforcement design of the frame was based on a linear elastic analysis performed with a vertical load at midspan of the beam member with a magnitude of 24 kN along with a horizontal load of 20 kN on the upper-left corner. The elastic analysis was performed based on centerline dimensions. The resulting shear and moment diagrams are presented in Figure 3.1 below.

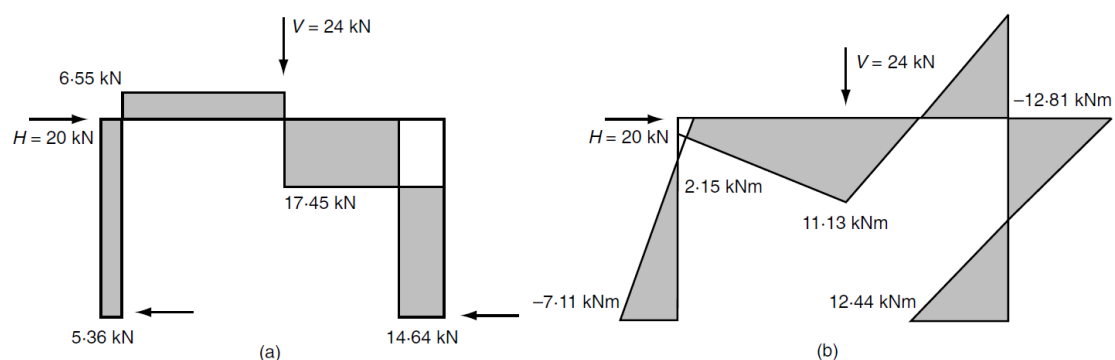


Figure 3.1 Elastic analysis of the studied frame, loaded vertically and horizontally. (a) and (b) are shear and moment diagrams, respectively from Kotsovos & Pavlovic (1999)

The frame was designed using the compressive force path method suggested by Kotsovos & Pavlovic (1999). The frame was cast using a concrete mix with cube

strength of 45 MPa and the strength was estimated to 48 MPa on test day Seraj *et. al.* (1995). It is the test day value that is most representative for tested structures typically and thus it will be used in this NLFEA analysis. The other concrete properties were estimated from the mean strength according to the Model Code 2010 fib (2013). The main steel reinforcement was all of diameter $\phi = 10 \text{ mm}$ and had yield strength $f_{yk} = 560 \text{ MPa}$ and ultimate strength $f_{uk} = 680 \text{ MPa}$. All the material properties for concrete and reinforcement steel used in the model are presented in Table 3.1 and Table 3.2 below.

Table 3.1 *Material properties of concrete used in the FE-model, where $f_{cm,cube}$ is the concrete mean cube strength, f_{cm} is the mean cylinder strength and f_{ctm} is the mean tensile strength. $E_{c,i}$ and $E_{c,r}$ are the initial and reduced elasticity moduli, G_f and G_c are the fracture energy in tension and compression respectively and ν is the Poisson's ratio*

	$f_{cm,cube}$ [MPa]	f_{cm} [MPa]	f_{ctm} [MPa]	$E_{c,i}$ [GPa]	$E_{c,r}$ [GPa]	G_f [N/m]	G_c [N/m]	ν [-]
Concrete	48	38	2.896	33.551	29.738	140.5	$250G_f$	0.15

Table 3.2 *Material properties and dimensions of the reinforcement used in the FE-model, where E is the elasticity modulus, f_y and f_u are the yield and ultimate strength. ϕ and A_s are the reinforcement diameter and area respectively and ϵ_y and ϵ_u are the yield and ultimate strain*

	E [GPa]	f_y [MPa]	f_u [MPa]	ϕ [mm]	A_s [mm ²]	ϵ_y [-]	ϵ_u [-]
Main reinforcement	200	560	680	10	78,54	0.0028	0.1166
Shear reinforcement	200	460	510	1.5	1.77	0.0023	0.1175

The dimensions of the frame along with the reinforcement information are presented in Figure 3.2. Joint and loading regions are indicated A-E in the same figure.

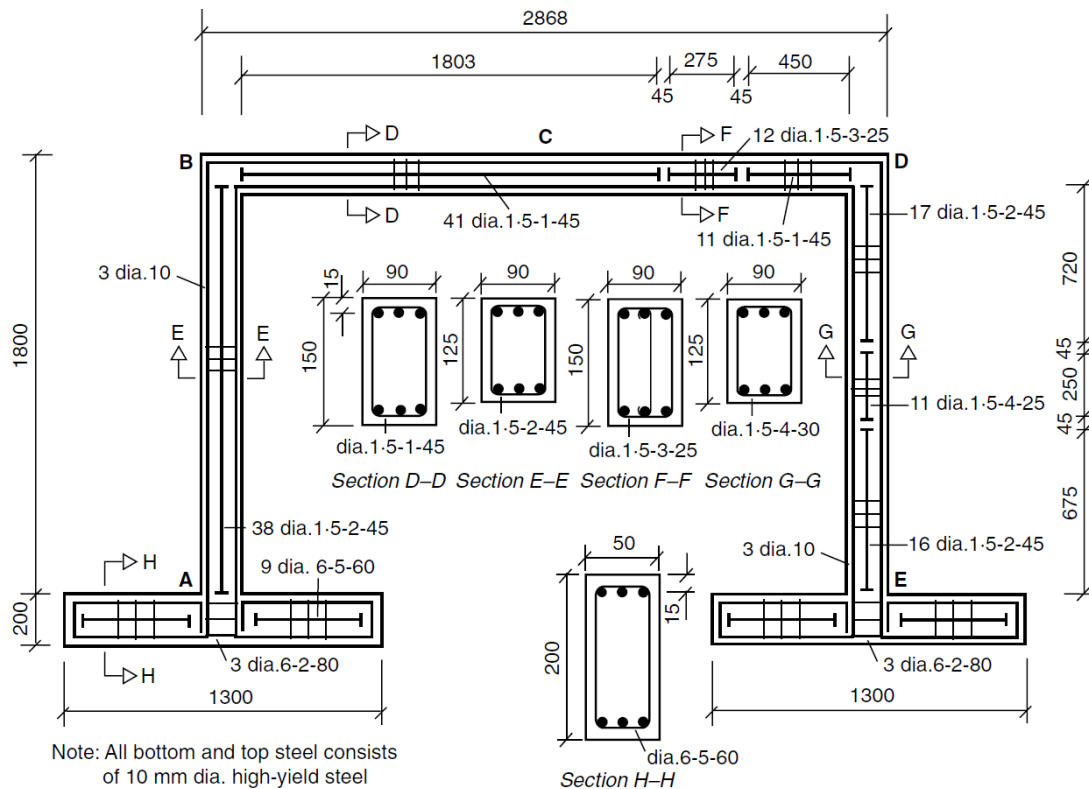


Figure 3.2 Dimensions (in mm) and reinforcement layout of the portal frame from Kotsovos & Pavlovic (1999)

The footings of the portal frame were fixed to the floor by means of post tensioning. When testing the structural capacity of the frame, first the vertical load was applied at point C and incrementally increased to 23.69 kN. Without further increasing the vertical load, the lateral load was applied at point B in increments until failure occurred at 19.95 kN. Even though the aim was to keep the vertical load constant it increased during application of the horizontal loading due to swaying of the frame since the vertical load was applied by a tension jack. The actual vertical load at the time of failure was estimated to 33.68 kN based on strain measurements in the reinforcement steel and the assumption that the moment in the beam at point C is proportional to the vertical loading. This gives a ratio of $\frac{\Delta F_V}{\Delta F_H} \approx 0.5$ between the horizontal load and the additional vertical load due to the sway effect. The results from the experiment are compared with those obtained from a NLFEA in Section 3.1.4.1.

3.1.2 Collapse analysis of frame

A kinematic collapse analysis of the frame was conducted serving as an upper estimate of the load carrying capacity of the concrete frame. The capacity is used for comparison with the result from the NLFEA and the experimental values. The analysis was made based on the plastic moment capacity of the members of the frame and the possible mechanisms that can form. The procedure described by Cook & Young (1999) was followed and calculations can be found in appendix I. The

comparison between the collapse loads and the NLFEA results can be found in Section 3.1.4.2.

3.1.3 Setup of the NLFE-model

The FE-software DIANA v.9.4.4 developed by TNO DIANA (2014) was used for the analyses. The finite element model was set up using 20 node volume elements with quadratic interpolation for the concrete and embedded truss elements for the reinforcement. The mesh was chosen relatively coarse with 3 elements over the height of the frame members and 2 elements over the width. The structure was modelled as fixed against translations in all three dimension at the ends of the column footings (i.e. at A and E). The nodes on the $x - z$ plane (see Figure 3.3 for coordinate system) located in the center of the frame depth are fixed in the y direction. Since there is no load in this direction, it should not have any physical effect. However, it was done in order to decrease the possibility of spurious deformations thus achieving better convergence. The two loads were both applied as pressure loads in the pertinent directions. The surfaces over which the loads are distributed were 90x90 mm for the vertical load and 90x150 mm for the horizontal load. Note that the loading plates were not modelled and that the loads were applied directly to the concrete. The mesh along with the loads (in purple) and the boundary conditions (in red) can be seen in Figure 3.3 below.

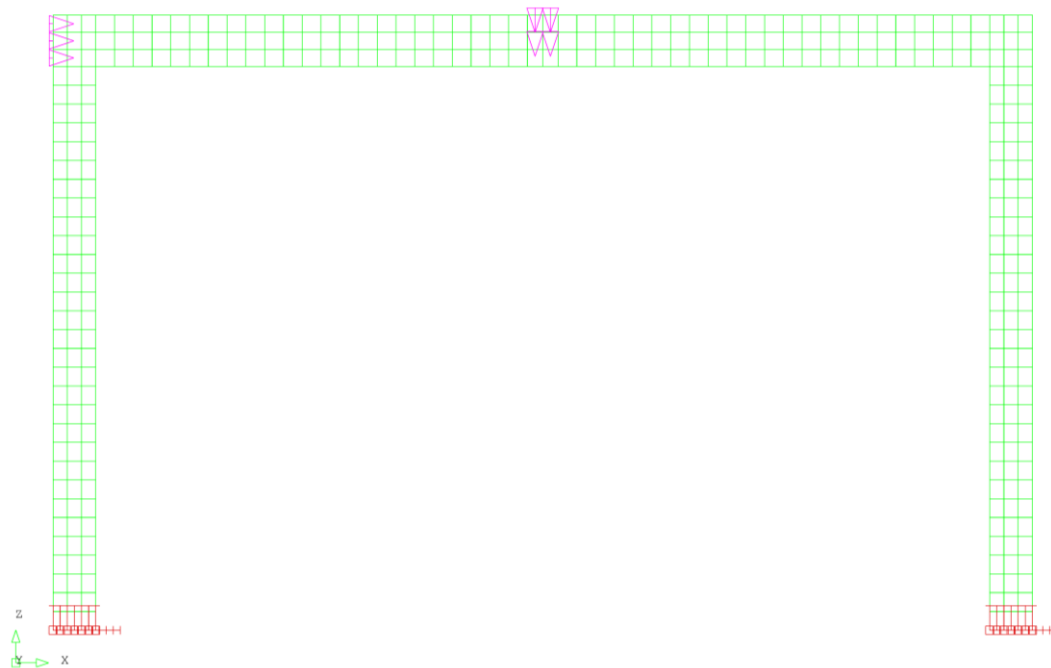


Figure 3.3 FE - mesh with loads and boundary conditions

A linear elastic analysis was first made, comparing the results with the linear elastic analysis presented in the paper by Seraj *et. al.* (1995). The results were also compared with those obtained from a simple frame analysis made in MATLAB using the toolbox CALFEM from Lund University (2004). The bending moments in the frame along with shear and normal forces were checked and the values from Seraj *et. al.*'s paper agreed well with the values from both the MATLAB and FE-model.

The reinforcement bars were now added to the FE-model. Information about the placement of the bars is found in Figure 3.2. The corner reinforcement was not clearly specified in the information about the experiment. Anchorage of the reinforcement bars and ductility requirements are the main concerns in practice which is why special detailing typically is required in the corner regions. However, since embedded reinforcement bars with no slip between reinforcement and concrete are used in the FE-model these practical issues are overcome even with simple theoretical reinforcement placement in the corners.

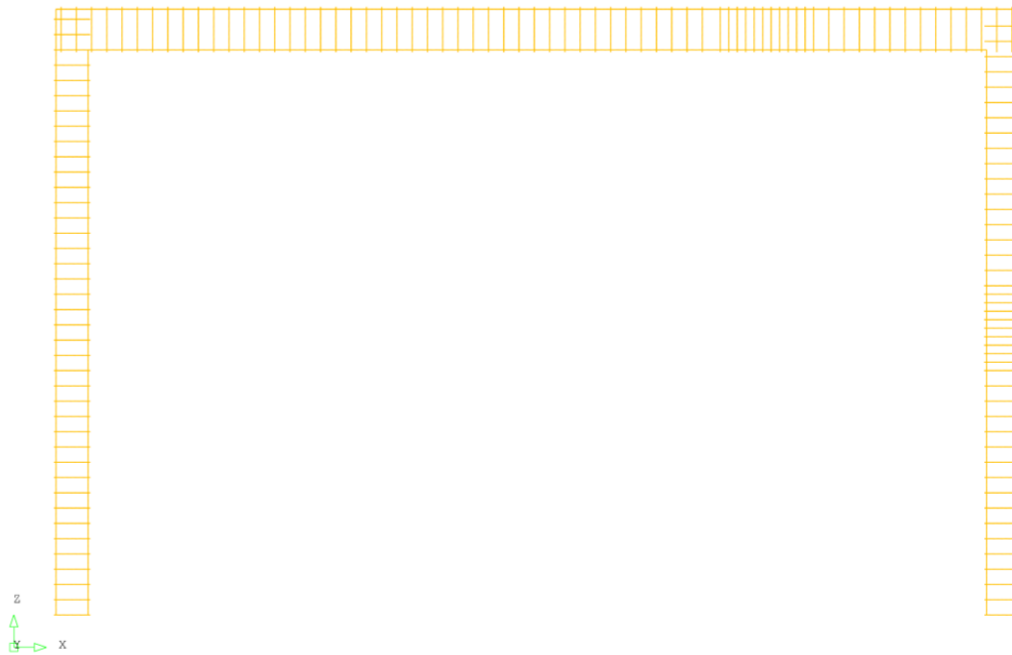


Figure 3.4 Main and shear reinforcement

When conducting nonlinear finite element analyses it is suitable to start linear elastically and introduce nonlinearities progressively. If several nonlinearities are introduced at the same time it is difficult to find any sources of errors. It is highly probable that several such errors will have to be resolved before the NLFEA works properly.

The nonlinear material model for the concrete follows the guidelines provided by the Dutch ministry of infrastructure, Rijkswaterstaat (2012) and a bilinear elastic-plastic model including strain hardening was chosen for the reinforcement. More information about the material models is presented later in this chapter in Section 3.1.5.

The first nonlinearity to be introduced to the model was the material model of the concrete, still keeping the reinforcement behavior elastic and disregarding geometrical nonlinearities. Once the NLFEA was able to run without diverging for the case of only nonlinear behavior in the concrete, plasticity in the reinforcement was introduced. Lastly, geometrical nonlinearities were included in the model in a similar procedure.

When the NLFEA has produced convergent results, the work of interpreting the response of the structure begins. Each of the load steps was checked with respect to a couple of aspects, which are briefly presented here. The concrete stress fields were checked in order to make sure the structure carries the load in a physically reasonable

way. Also the reinforcement stresses were checked along with the crack pattern in the concrete. Further the propagation of the cracks were checked, e.g. that the modelled structure cracks first at the locations of highest elastic moments. For the unconverged load steps at the end of the analysis it was found useful to plot the residual forces in the nodes. This allows insight in the problem regions of the structure, i.e. the regions preventing convergence of the solution.

After the analysis had been assessed and reasonable behavior of the structure had been determined, MATLAB was used in order to post-process the output from the analysis. For each load step a large amount of information was stored in a database. The analyst can chose what data to store based on the aim of the analysis. The data that were extracted from the output file and post-processed in MATLAB were support reactions, displacements and reinforcement stresses. This information was used to construct force-displacement and reinforcement strain plots to compare to the results from the experiment presented in Section 3.1.1.

3.1.4 Benchmarking results

The ability of the nonlinear FEM to represent the behavior of the concrete frame is presented in this section. The results from NLFEA using different model setups are compared to the plastic capacity of the frame calculated in Section 3.1.2 and also to the results from the physical experiment presented in Section 3.1.1 above. The model setups differ regarding the coarseness of the mesh and the load increment size.

3.1.4.1 Comparison with experiment

A working NLFEA has been set up according to the procedure presented in Section 3.1.3 above. As there are many possible working parameter settings for the analysis and they do not all yield good results, a comparison between the experimental results and the NLFEA results for different model setups is presented in this section. Comparative force-deflection plots are presented for the best of the studied model setups with regards to the accuracy of the predicted capacity.

For NLFEA of concrete structures, as mentioned earlier, it is not as simple as increasing the mesh resolution to obtain more accurate results. This since the accuracy of the analyses is dependent on how well the material model for concrete represents the actual behavior. Furthermore, the analysis time is of course greatly dependent on the number of integration points and thus the number of elements. So it is preferred to use as few elements as possible, provided that the model performs well.

The incremental increase in loading is also of interest. Large increments reduce the number of calculations since the final load is reached in fewer steps, but can cause the analysis to diverge. Therefore an increment size that agrees with the experimental results but that still is computationally economic is sought.

A comparative study between different number of elements over the thickness (E.O.T.) as well as load increment size is presented in Table 3.3 below. The initial vertical load ($F_V = 23.7 \text{ kN}$) was applied in 5% increments for all cases, i.e. 5% of the target load in each increment. Then the horizontal load F_H was applied in either 5% or 2% increments. The additional vertical load due to the sway effect of the frame, $\Delta F_V = 0.5\Delta F_H$ as described earlier, was added simultaneously. The resisting force was calculated by summarizing the support reactions. When failure occurred the

resisting forces from the last converged load step were used to construct the table below.

Table 3.3 Comparison between different E.O.T. and load step increments

	F_{EXP}	$F_{NLFEA} (F_{NLFEA}/F_{EXP})$					
		2 E.O.T.		3 E.O.T.		4 E.O.T.	
Load step		5%	2%	5%	2%	5%	2%
$F_{V,max}$	33.7	34.9	37.2	33.2	34.8	32.1	31.9
$F_{H,max}$	20.0	23.0 (116%)	27.3 (137%)	19.0 (95%)	22.4 (112%)	17.0 (85%)	16.4 (82%)
$F_{NLFEA,tot}$	-	57.9 (108%)	64.5 (120%)	52.2 (96%)	57.2 (107%)	49.1 (92%)	48.3 (90%)

As can be seen in Table 3.3, the analysis setup with 3 E.O.T. and 5% load increments yields results closest to the experimental values. With this setup the difference between the analysis and the experimental results is 5% for the horizontal load and 4% for the total load.

The analysis results from the 3 E.O.T. and 5% load increments are presented in more detail below. The data has been post processed in MATLAB and the same software has been used to construct the plots.

The top subplot of Figure 3.5 shows the vertical deflection at midspan of the top beam subjected to the first added vertical load. The bottom subplot shows the horizontal deflection in the top right corner for the horizontal load. Note that the two loads are treated separately in this figure. The results from the NLFEA imply a higher stiffness than what the experimental results show for the vertical load. For the horizontal load however, the NLFEA shows similar stiffness as the experiment. The frame in the practical experiment deflects much more horizontally than the NLFEA frame but carries only marginally more load.

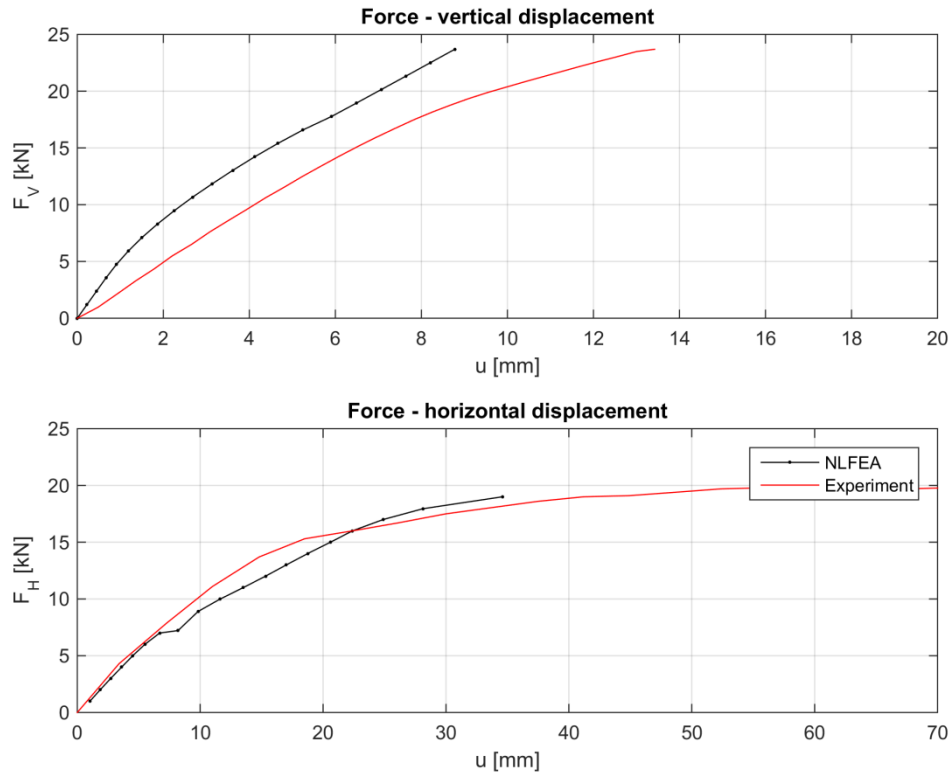


Figure 3.5 Force-displacement relations: (above) vertically at midspan of the top beam and (below) horizontally at upper right corner

The strain in the reinforcement steel at midspan of the top beam is presented in Figure 3.6 below. In this plot, the total load is used and it can be noted that the application of the horizontal load starts at 24 kN. The NLFEA results are regarded to agree reasonably well with the experimental values.

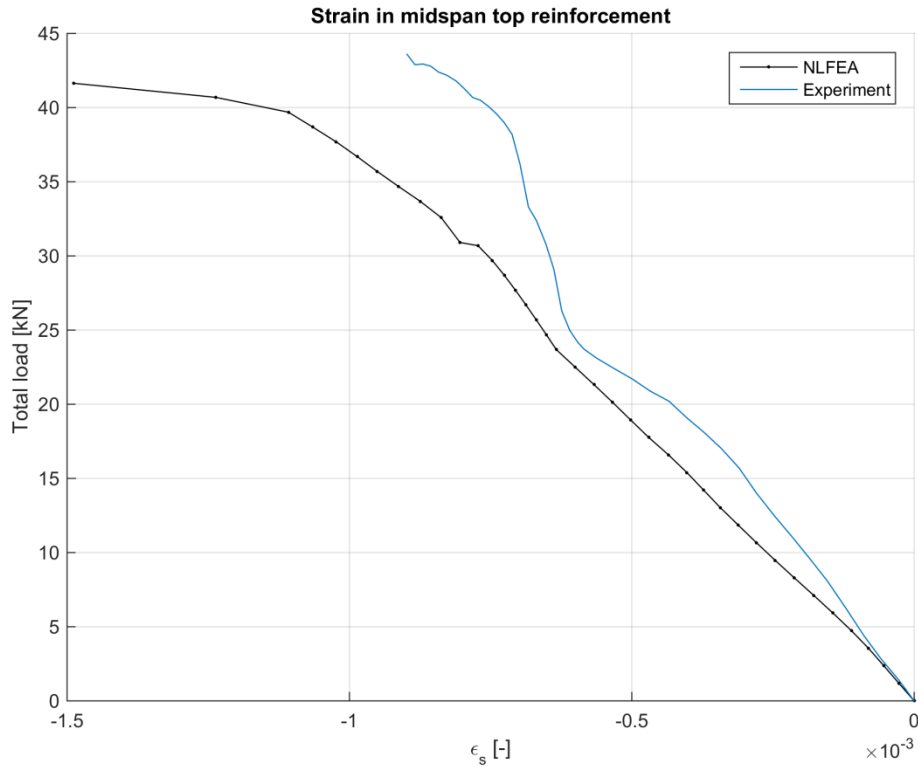


Figure 3.6 Strain in midspan top reinforcement

A similar plot is shown in Figure 3.7 below, but here the strain in the bottom reinforcement is presented. The results agree very well until the horizontal load is applied and the experimental strain in the reinforcement stays roughly constant between 24 and 36 kN. The strain in the experiment is then increased rapidly and the end value agrees well with the NLFEA. This behavior originates from the sway effect of the experimental frame, which is not accurately represented by assuming a linear increase of the vertical load in the NLFEA. Even though the strain in the midspan reinforcement is not perfectly represented by the NLFEA during the entire load history due to this simplification the end value is close to the experimental value and the result is deemed satisfying. The yield strain of the reinforcement steel is 2.8 ‰ and it is clearly seen in aforementioned figure.

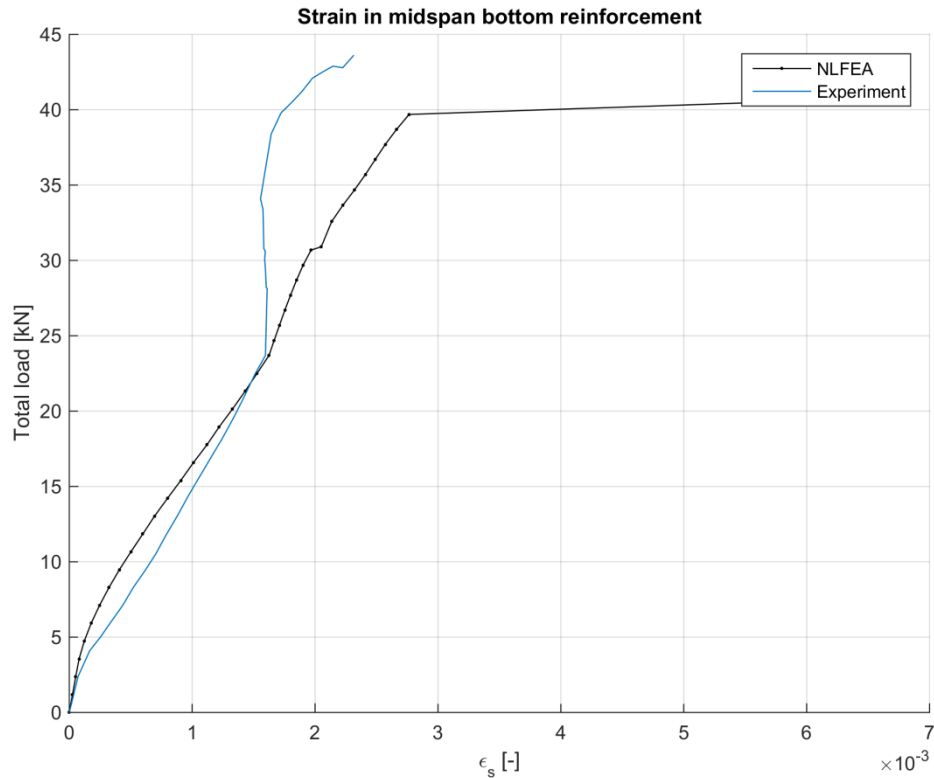


Figure 3.7 Strain in midspan bottom reinforcement

The strain in the reinforcement located at the right hand side column support is presented in Figure 3.8 below. Here the horizontal load is particularly of interest, and therefore the vertical load is omitted. However, the effect of the vertical load can be seen as the nonzero strain value when the horizontal load is zero. The results agree well except for when the horizontal load approaches the maximum value, where the experiment shows a much more ductile behavior.

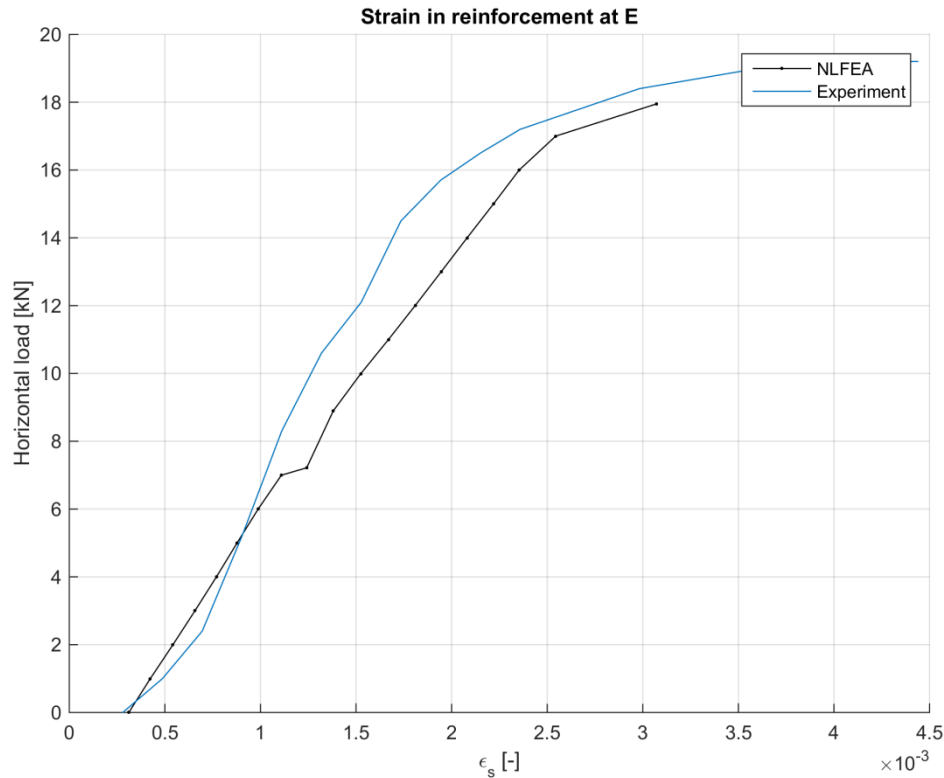


Figure 3.8 Strain in the reinforcement at the lower right support. Bulleted line represents NLFEA and blue line experiment

The failure mechanism was the same in the NLFEA as in the experiment; flexural failure occurred at the supports as well as the top right corner. The results from the comparison are considered satisfying even if the deflection differs quite a bit. It is not unusual for a NLFEA to show a stiffer behavior than reality. Further it is also found uncommon for a NLFEA to accurately yield both the ultimate capacity and the stiffness in the same analysis. A possible explanation for this is that correct stiffness representation requires a more accurate analysis which is more sensitive, and therefore more likely to experience converge problems at load levels close to the ultimate experimental capacity. This might therefore rather be a product of numerical difficulties than an inability of the model to represent both the ultimate strength and stiffness at the same time.

3.1.4.2 Comparison with plastic capacity

The collapse loads was calculated based on theory of plasticity as described in Section 3.1.2 above. The results were used for comparison against the results from the NLFEA for the three considered load cases, that is only horizontal, only vertical and a combination of both. They are represented by mechanism 1, 2 and 3 respectively. The collapse loads of the NLFEA were investigated by simply loading the frame horizontally, vertically and with a combination of both and thereby obtain a maximum loading. It should be noted that the collapse load calculated by means of hand calculations only considers failure in bending, which may not always be the case. However, the results from the analyses were studied and the failure was determined to

be due to bending, not shear, for all mechanisms. An overview of the comparison can be seen in Table 3.4 below.

Table 3.4 Comparative table between collapse load from hand calculations and NLFEA using DIANA

	Mechanism 1	Mechanism 2	Mechanism 3	
	P_H [kN]	P_V [kN]	P_V [kN]	P_H [kN]
Plasticity analysis	30,8	43,5	23,7	23,5
NLFEA	30,8	39,2	23,7	15,0
Difference	0%	-10%	0%	-36%

The results from the NLFEA agree well with the plastic capacity calculated using collapse analysis for mechanism 1 and 2. For those mechanisms only one of the loads contributes to the external work. The difference is larger for mechanism 3 where both loads contribute to the external work. This kinematic collapse analysis provides an upper bound solution and thus lower NLFEA results are expected, which is also the case.

3.1.4.3 Model uncertainty

There is always a factor of model uncertainty present when an idealized model is used. This causes the results obtained by the model to differ from reality to a certain extent. A statically indeterminate structure is more difficult to model and therefore the model uncertainty can be higher. The maximum capacities from the NLFEA presented above differ about 5-10% compared to the experimental data and the collapse analysis and it is regarded reasonable. Furthermore, the capacities predicted by the NLFEA are lower than the upper bound estimates, which is crucial.

3.1.5 Chosen solution strategy

The chosen solution strategy is based on the benchmarking results and is presented in this section. The information about the properties chosen is found from the DIANA User's Manual published by TNO DIANA (2012).

The choices regarding the material models for concrete and reinforcement steel are presented in Table 3.5 below. Many choices are based on a trial and error basis but for some properties preset values are used. Those properties are indicated with ϕ .

Table 3.5 Information about constitutive properties implemented in the solution strategy, properties where preset values are used are marked with^ϕ

Property	Choice in DIANA	Comment
Fixed crack model ^ϕ	Totcrk fixed	Physically appealing crack model, stress strain relationship is evaluated in a coordinate system which is fixed upon cracking.
Tension softening ^ϕ	Exponential	Concrete softens exponentially once the tensile capacity is reached based on fracture energy and crack bandwidth.
Crushing behavior of concrete ^ϕ	Parabolic	Parabolic diagram based on fracture energy and crack bandwidth.
Lateral influence of cracking ^ϕ	VC1993	Perpendicular tensile strains reduce the concrete compressive strength according to Vecchio & Collins (1993)
Influence of lateral confinement ^ϕ	Vecchi	Confinement increase the concrete compressive strength according to Selby & Vecchio (1997)
Shear retention	Constant	Constant shear retention curve after cracking, retention factor is chosen to 0.1 for computational stability reasons
Poisson's ratio reduction	Damage	Poisson's ratio reduced after cracking
Plasticity model for reinforcement steel	Hardening	Von Mises plasticity model with tensile hardening

The choices regarding the compatibility on element level, e.g. element types and numerical integration scheme are presented in Table 3.6 below.

Table 3.6 Information about compatibility properties implemented in the solution strategy, properties where preset values are used are marked with[‡]

Property	Choice in DIANA	Comment
Element type, concrete [‡]	CHX60	20-node isoparametric solid brick element with quadratic interpolation between nodes
Element type, reinforcement [‡]	Standard embedded truss elements	Perfect bond between reinforcement and concrete, justified by large scale analysis and anchorage assumptions, strains computed from displacement fields of mother (concrete) elements
Integration method	3x3x3 Gauss points	Full integration was found to yield better convergence
Geometrically nonlinear	Total Lagrange	Uses undeformed geometry as reference for strains and stresses

The choices regarding equilibrium on a structural level are presented in Table 3.7 below.

Table 3.7 Information about equilibrium properties implemented in the solution strategy

Property	Choice in DIANA	Comment
Load increments	5% of target total load for both vertical load and horizontal load	The values found to be adequate from the benchmarking analysis
Iteration method	Modified and regular Newton – Raphson, max. 100 iterations	A well-known iteration procedure, regular NR used when divergence occurred for modified NR
Convergence criteria	Relative energy variation 0.1%, relative out of balance force 1%	Relatively strict convergence criteria

3.2 Design using LFEA ANSYS/MultiCon

In order to follow the approach suggested by Engen (2014) a frame with realistic dimensions was designed using LFEA with partial safety factors on the materials. In this procedure, the structure is designed based on nonlinear sectional resistance, but using the linear elastic distribution of cross-sectional forces and moments in the structure for the given load case. The linear elastic stress field is one out of many possible stress distributions in equilibrium, and it is considered conservative to design for it if sufficient stress redistribution capacity is provided. A concrete of class C45/55 is used along with B500 reinforcement. The design of the structure is conducted using Multiconsult's in-house post processor MultiCon, Brekke *et. al.* (1994), and in compliance with the provisions given in Eurocode.

3.2.1 Frame properties and loading

First the dimensions of the frame are chosen. In order to put the larger frame in a context it is considered to act as support for a bridge in a location where an ordinary column support is not possible. The supporting girder for the bridge is therefore prolonged a horizontal distance before the vertical columns connect it to the ground. It is, as the benchmarked example, subjected to an initial vertical load followed by a horizontal load. The vertical load can be thought of as the dead load from the supported bridge, and the horizontal load can be seen as markedly simplified earthquake loading. It should be stressed that this is merely a way of putting the structure in a context and that the structure is not designed to sustain the loads from neither an actual bridge nor an earthquake.

The geometry of the frame is chosen to have ratios between the member dimensions consistent with those of the benchmarked case. The width and height of the frame is 10 and 6 m respectively. The top girder has a height of 1 m while the columns have a thickness of 0.8 m. All members of the frame have a common width of 0.5 m. The labelling of the structural parts together with the dimensions can be seen Figure 3.9.

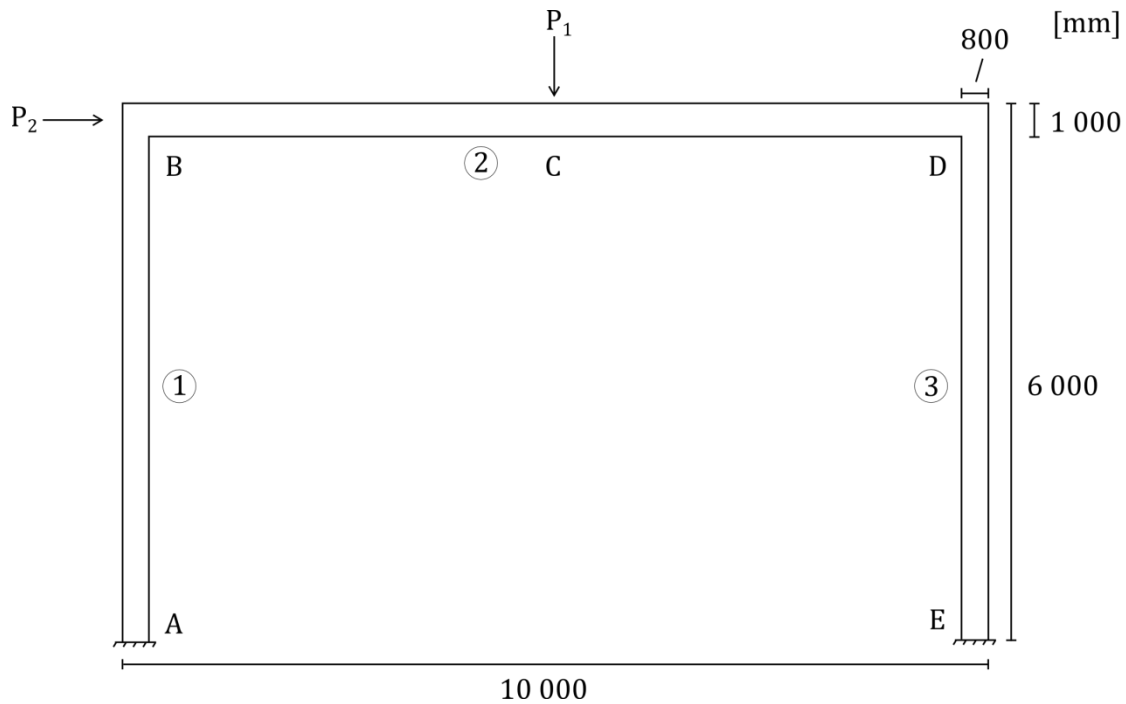


Figure 3.9 Dimensions and labeling of the frame designed using LFEA and MultiCon

The vertical load on the frame is $P_1 = 800 \text{ kN}$ and the horizontal load is $P_2 = 675 \text{ kN}$, keeping the ratio between the loads as in the benchmarked example.

3.2.2 Modelling in ANSYS

The model for the linear FE-analysis is set up in ANSYS 14.5 developed by ANSYS (2014) using solid 3D-elements with 8 nodes and enhanced strain formulation. The latter meaning a certain number of inaccessible internal degrees of freedom are introduced to prevent shear locking for bending dominated problems. Further, zero mass surface elements were placed on the outer surfaces of the body in order to accommodate easy load application. The loads are applied as pressures on the surface elements, over an area of $(0.5 \times 0.5) \text{ m}^2$ for the vertical load and $(1.0 \times 0.5) \text{ m}^2$ for the horizontal load. The pressures are chosen such that the resulting forces equal unit loads of 1 kN each.

When unit loads were used in the LFEA, they are scaled up in the postprocessor in order to represent the desired loads. An advantage with this procedure, made possible by linear superpositioning, is that there is no need to run additional finite element analyses if the loads are changed. They can simply be changed in the postprocessor. For such a simple case as this, the time required for a linear analysis is very short. But for a large analysis with millions of D.O.F.'s and vast amount of loads the time required to conduct even a linear analysis can be substantial.

3.2.3 Design using in-house postprocessor MultiCon

The frame is designed for the ultimate limit state using the provisions stated in the Eurocode 0 and 2, CEN (2008) & (2005) respectively.

The geometry of the structure and the results from the LFEA are imported into the postprocessor. Each finite element is represented by a set of two sectional coordinates. A plot of the imported structure can be seen in Figure 3.10 below.

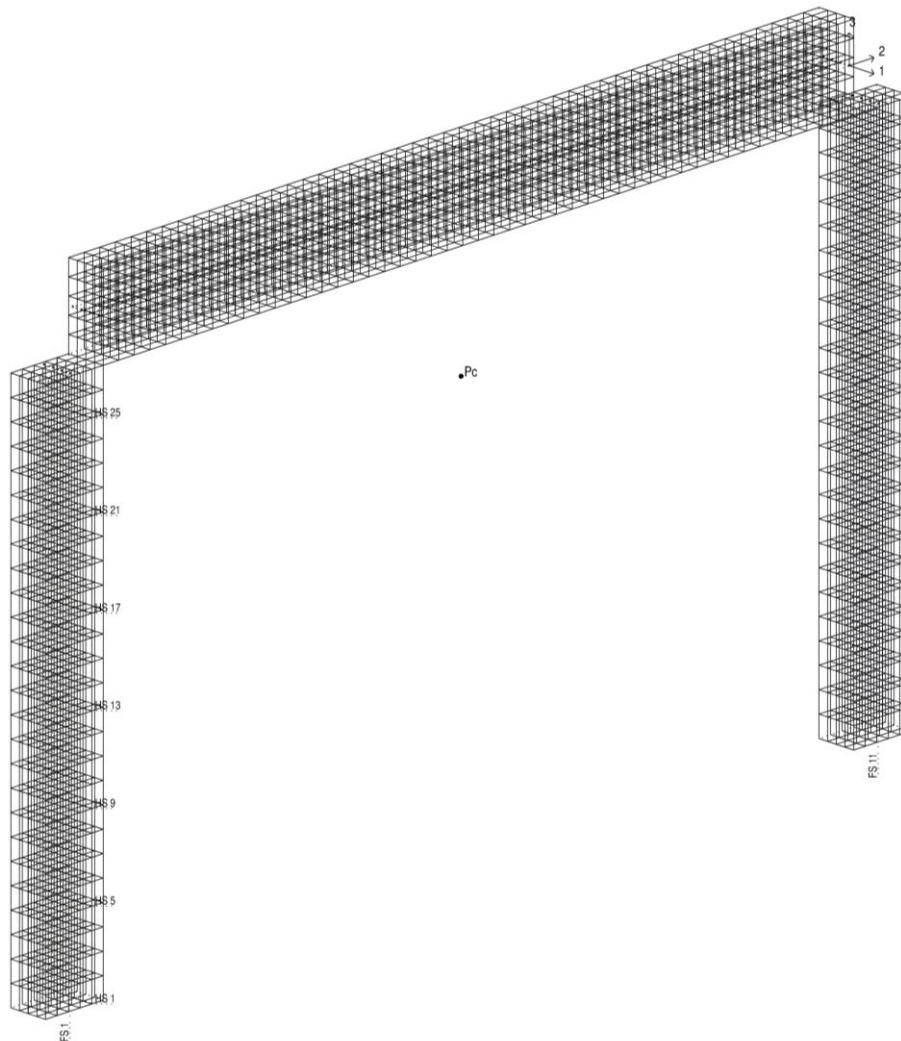


Figure 3.10 Geometry in MultiCon

The unit loads are scaled up to equal the aforementioned loads of 800 kN and 675 kN in the vertical and horizontal directions respectively. The vertical load is considered permanent while the horizontal load is considered a variable load. The design load combinations are given as shown in Table 3.8 below. The expressions become more complex when several permanent and variable loads are included, but those expressions are not needed for this case and thus not presented in the table. For this simple set of only two loads, it is clear that equation (6.10) in Eurocode 0 will govern the critical design load.

Table 3.8 ULS load combinations according to Eurocode 0 (EC0), CEN (2008) for the cases when the load contribution is unfavorable

Equation in EC0	Permanent load	Variable load
(6.10)	$\gamma_G G = 1,35G$	$\gamma_Q Q = 1,5Q$
(6.10a)	$\gamma_G G = 1,35G$	$\gamma_Q \psi Q = 1,5 \cdot 0,7Q$
(6.10b)	$\xi \gamma_G G = 0,85 \cdot 1,35G$	$\gamma_Q Q = 1,5Q$

The stresses in the finite elements' integration points resulting from the design load combination are integrated to cross-sectional forces in the postprocessor. Moments are calculated together with normal and shear forces based on linear elastic theory.

A number of construction code dependent parameters need to be specified before the sectional design module of the postprocessor can be used. These are for example material strengths, minimum reinforcement amounts and concrete cover. The postprocessor designs the reinforcement on a sectional level for the design moments and sectional forces previously calculated. This is done by dividing the section into several layers, with a force resultant in each layer. Moments, normal and shear forces are then calculated in an iterative process to represent the nonlinear material behavior in the cross sectional resistance calculations. Note the difference between NLFEA, where structural behavior on global level is simulated. The required bending and shear reinforcement amounts are output from the postprocessor, as well as utilization ratios for the reinforcement and concrete. The input parameters for the design are presented in Table 3.9 below.

Table 3.9 Cover and reinforcement input parameters for postprocessor MultiCon

Parameter	Value	Comment
Concrete cover	50 mm	Conservatively chosen
Longitudinal bar diameters	$\phi 16, \phi 20, \phi 25, \phi 28, \phi 32$	$8\phi 16$ satisfies minimum requirement
Transversal bar diameters	$\phi 10, \phi 12, \phi 14, \phi 16, \phi 20, \phi 25$	
Minimum clear distance between bars	32 mm	Dep. on bar diameter, conservatively chosen
Minimum long. reinforcement amount	1421 mm^2 (beam) 1200 mm^2 (columns)	
Minimum shear reinforcement amount	$600 \text{ mm}^2/\text{m}$ (beam) $\phi_{\min} = 8 \text{ mm}$ (columns)	Minimum area for beam and diameter for column
Maximum stirrup spacing	900 & 600 mm (beam) 400 mm (columns)	Longitudinally and transversally for beam (width is 500 mm so latter automatically fulfilled)

An overview of the longitudinal reinforcement of the designed frame can be seen in Figure 3.11 below. It should be noted that the reinforcement in the corners is not representative of a construction that were to be built. Special reinforcement detailing is typically used in the corners to ensure proper anchorage. The choice of using embedded reinforcement in the NLFEA is based on the assumption of no anchorage slip and it is deemed adequate for the purpose of ULS capacity checking. The reinforcement is placed symmetrically in the frame, mirrored around a vertical line through the midspan of the beam section.

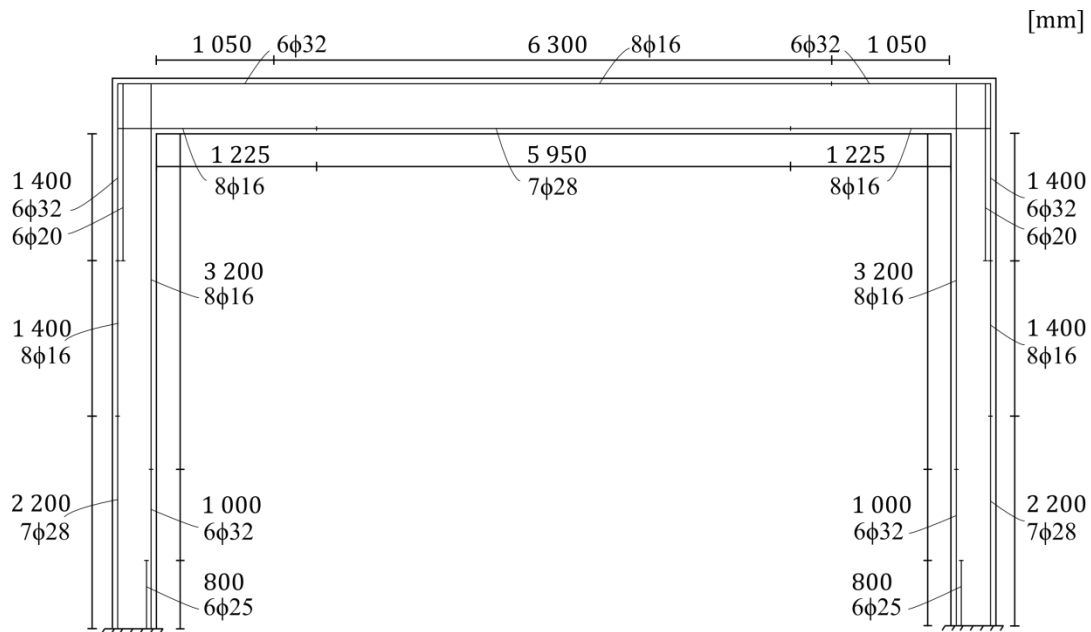


Figure 3.11 Longitudinal reinforcement overview

The longitudinal bars are placed so that the concrete cover to the outermost reinforcement, i.e. the hooped stirrups, is 50 mm. Furthermore it should be noted that in some locations the reinforcement is placed in two layers. The clear distance between the layers is 50 mm.

The stirrup placing in the frame is depicted in Figure 3.12 below.

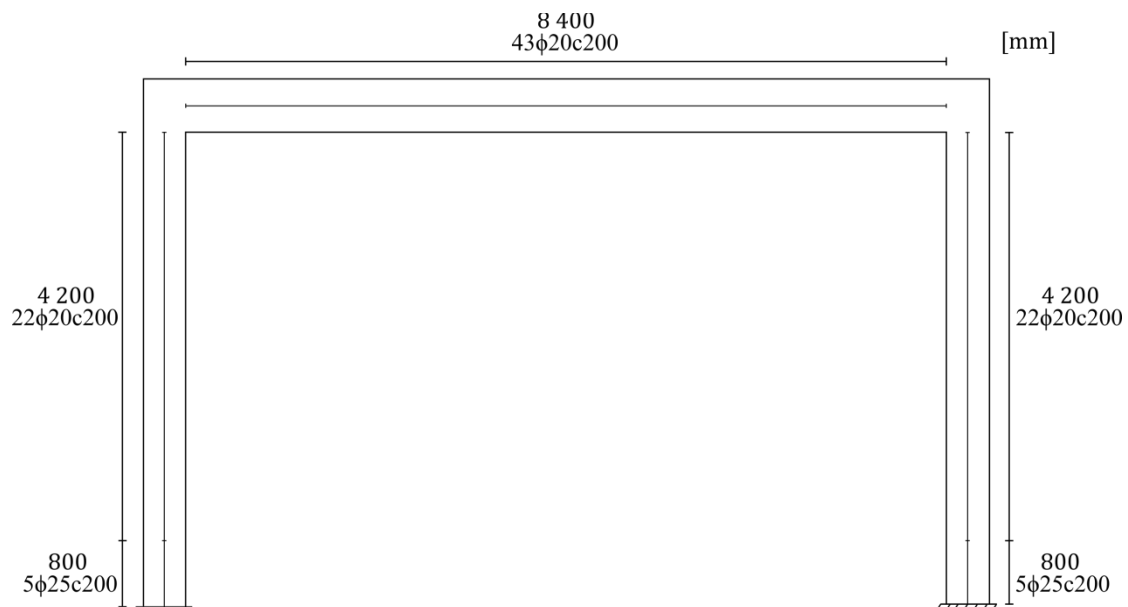


Figure 3.12 Shear reinforcement overview

The reinforcement in the designed frame as it is modelled in DIANA is depicted in Figure 3.13.



Figure 3.13 Designed reinforcement plot from DIANA

3.3 Safety assessment of designed frame using different safety formats

Safety evaluations of the designed frame using the different, previously presented, safety formats for NLFEA are presented in this section. This is made to compare the results from the safety formats. The frame is modelled in DIANA using the key properties, such as mesh division and load increments, as were found suitable in Section 3.1.4. Then the ultimate design resistance is evaluated using the three main safety formats in the Model Code 2010, fib (2013). That is the deterministic format (partial safety factor method) and the two semi-probabilistic formats (GRFm and ECOV). They are all described in detail in Section 2.3.

3.3.1 Modelling consideration in DIANA

A preprocessor was developed in MATLAB to set up the input file for the NLFE-model DIANA. The choice of developing a preprocessor instead of writing the code directly was justified by acknowledging the many repetitive features of the model (reinforcement bars and stirrups) and valuing the possibility to swiftly change the geometry and reinforcement.

The reinforcement is placed solely based on the output from MultiCon thus neglecting constructability considerations. The reinforcement placing varies over the length of the columns and the beam as the reinforcement diameters change. The placement keeps the distance from the concrete surface to the outermost reinforcement equal to the concrete cover of 50 mm. The characteristic diameters of the reinforcement bars are used to describe the reinforcement bars place in the concrete members, in compliance with the MultiCon design. The characteristic bar diameter includes the ribs on the bars and it thus the relevant measure for when placing the reinforcement.

For the capacity calculations however, it is logical to use the nominal diameters of the reinforcement as the ribs only provide bond to the concrete.

3.3.2 Checking the DIANA model

Once the FE-model of the frame designed in ANSYS/MultiCon had been set up, a first elastic check was conducted by comparing the moments and displacements with those obtained from simple frame analyses. The agreement was found to be within a few percent, which is regarded satisfying. Identical results are hindered by uncertainties due to result extraction from the FE-analysis, where bending moments cannot be extracted directly for solid elements but have to be calculated from Gauss point stresses in the studied sections. Furthermore, the reinforcement placed in the FE-model but not included in the simple frame analysis, will affect the stiffness properties of the members and cause differences in elastic behavior between the methods.

The plastic capacity was checked by hand calculations for the case of a vertical load. The check was done in a different manner for this case compared to the benchmarked frame, this since the reinforcement layout in the designed frame gives rise to hinges forming at other locations. A static approach was found to yield more reasonable results than a kinematic approach for this case. The collapse load was approached from below using a static approach by choosing a moment distribution in equilibrium. For the case of only a vertical load applied at midspan of the top beam, the first mechanism will form due to plastic hinges at three sections of the frame. One of the hinges forms just below the loading point and the other two form in each column. The hinges in the columns are located a distance down from the top where the reinforcement amount changes to a lesser amount than above. An overview of the frame and the hinge formation can be seen in Figure 3.14 below.

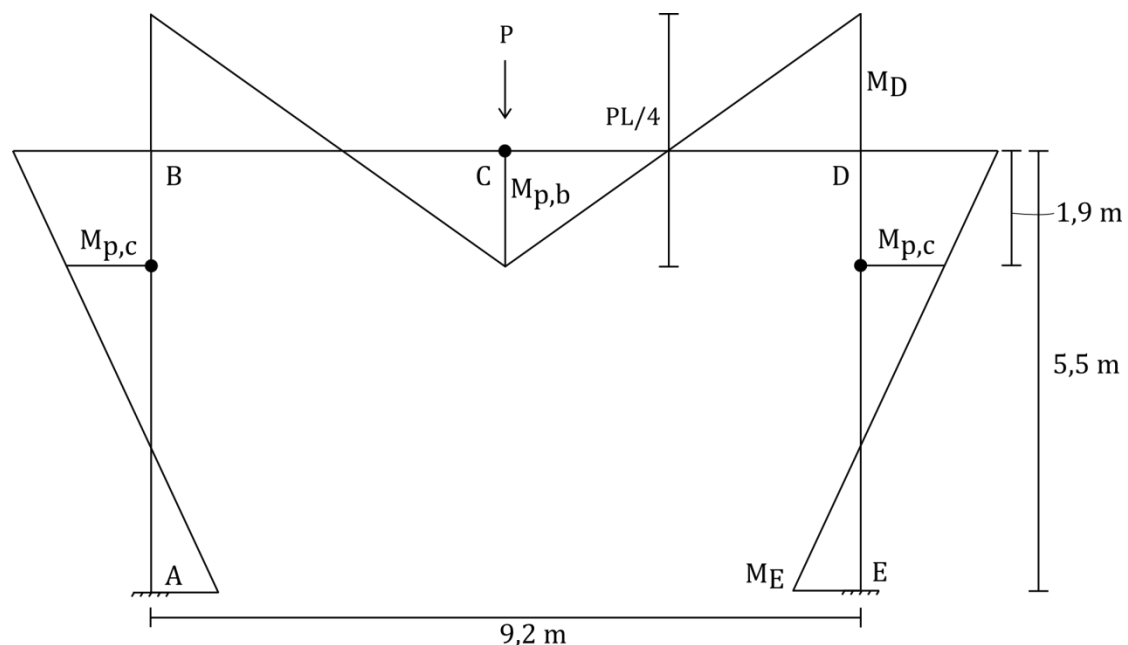


Figure 3.14 Overview of the moment distribution and plastic hinge formation where $M_{p,b}$ and $M_{p,c}$ are the plastic moment capacities in the beam and columns sections respectively

Yielding will first take place at the mid span of the top beam for the given sectional resistances, thus a plastic hinge attaining constant moment will be formed there. Thereafter the load is increased and the moment is assumed to elsewhere increase linear elastically. The difference between the mid span moment and the corner moments is $PL/4$ due to equilibrium consideration and the ratio between the corner moments and the support moment is also constant and found from elastic analysis. This enables the moment along the columns to be described using linear functions dependent only on the load and the location of the studied section. With the moment capacity and location of the plastic hinges in the columns known, the load required to form the three hinges can be solved for.

The lower bound solution found from the static approach above is rather conservative. This since the two corner sections of the frame support each other when the plastic hinges have been formed. To collapse the frame, either the corners need to be bent to a smaller angle than 90 degrees and/or the columns need to deflect outwards at the hinges. This additional resistance is not accounted for in the lower bound solution above, so the expected value of the load from NLFEA is well above the results obtained here. This agrees with the result from NLFEA where the maximum vertical load is roughly 50% higher than the lower bound load calculated above.

3.3.3 Loading and behavior of frame

The load application plan for the frame is to first apply one of the loads in increments. This phase is called load sequence 1. A load sequence consists of 20 increments each applying of 5% of the load in question. Thereafter the other characteristic load is applied, called load sequence 2. Once both characteristic loads have been applied they are magnified simultaneously until reaching their design values at the end of load sequence 3. If the structure is able to carry more load than the design loads, the vertical and horizontal loads are scaled up until failure occurs. The main load history consists of first applying the vertical load followed by the horizontal load. An alternative load history is also studied in which the horizontal load is applied first followed by the vertical load. This load history is referred to as the inverted load history. An illustration of the loading process can be found in Figure 3.15 below. It should be noted that many load histories can be considered, e.g. Pimentel *et. al.* (2014) suggests a linear increase of the loads using a common load factor from the beginning of the loading.

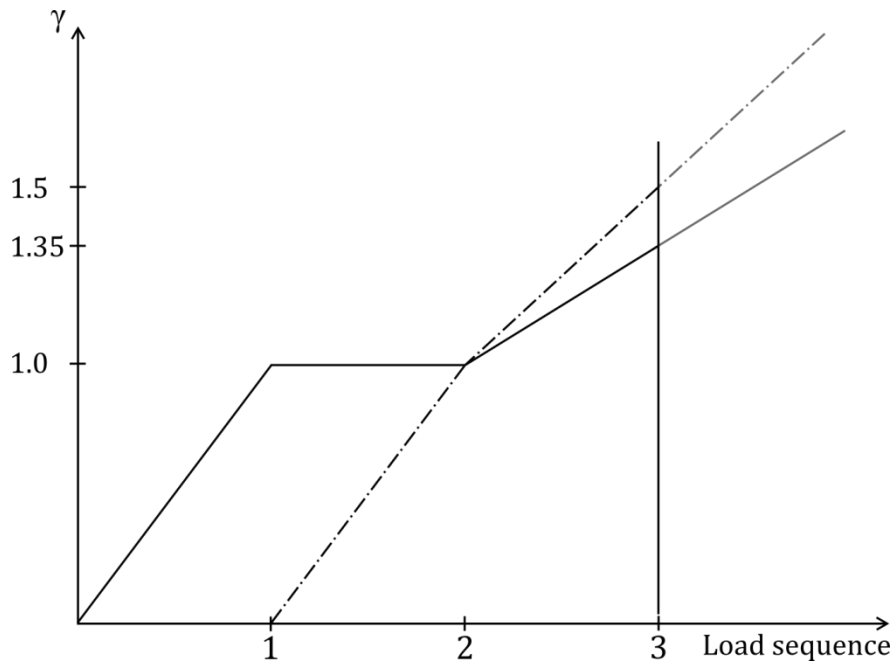


Figure 3.15 Illustration of the loading sequences, the solid line and bulleted line represents the first and second load respectively

Computational problems arose in parts of the frame which were cracked in tension and later compressed during the load history. Unreasonable divergence occurred after large residuals forces were found in the problem regions. It was found that changing the iteration method, from modified to regular Newton-Raphson method before the cracked parts were subjected to compression, relieved the problem. The new iteration method was used for the remaining load increments.

3.3.3.1 Structural behavior of the frame for main load history

The structural behavior of the frame subjected to the main load history is presented in this section. Load sequence information can be found in Table 3.10 below.

Table 3.10 Loading sequence information for main load history

Loading sequence	Load	Increment size	No. of increments	Iteration method in DIANA	Max. no. of iterations
1	Vertical	5%	20	Modified NR, first tangent “tangent”	100
2a	Horizontal	5%	5	Modified NR, first tangent “tangent”	100
2b	Horizontal	5%	15	Regular NR, first tangent “linear”	100
3	Vertical and horizontal	5%	Max. possible	Regular NR, first tangent “linear”	100

For all the different safety formats the behavior of the frame until it reaches failure is similar. The first cracks appear in the beam just below the vertical load during load sequence 1. At the end of load sequence 1 the vertical characteristic load has been applied and cracks have formed in the outer corner regions and on the insides of the column in their supported end. This is depicted in Figure 3.16 below.

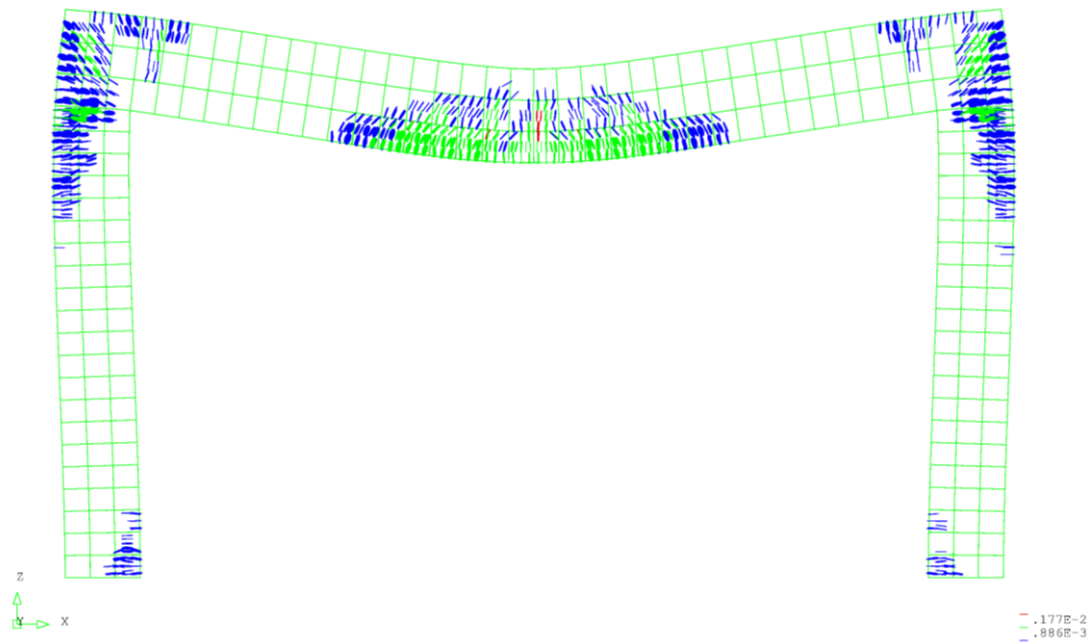


Figure 3.16 Deformed shape and crack pattern at the end of load sequence 1, with the vertical load applied to its characteristic value

When the horizontal load is being applied in sequence 2, cracks form below the existing ones in the outer side of both columns. For the left column these start from the foundation while they for the right column propagate downward from the corner. Also the interior side cracks develop in the lower portion of the right column. Furthermore, since the right corner is displaced to the right, cracks form in the upper right part of the beam and the outer upper right column. Additional cracks form on the left of the existing cracks on the bottom side of the beam at midspan. To illustrate the cracking more clearly, a plot from the end of load sequence 2 is presented in Figure 3.17 below.

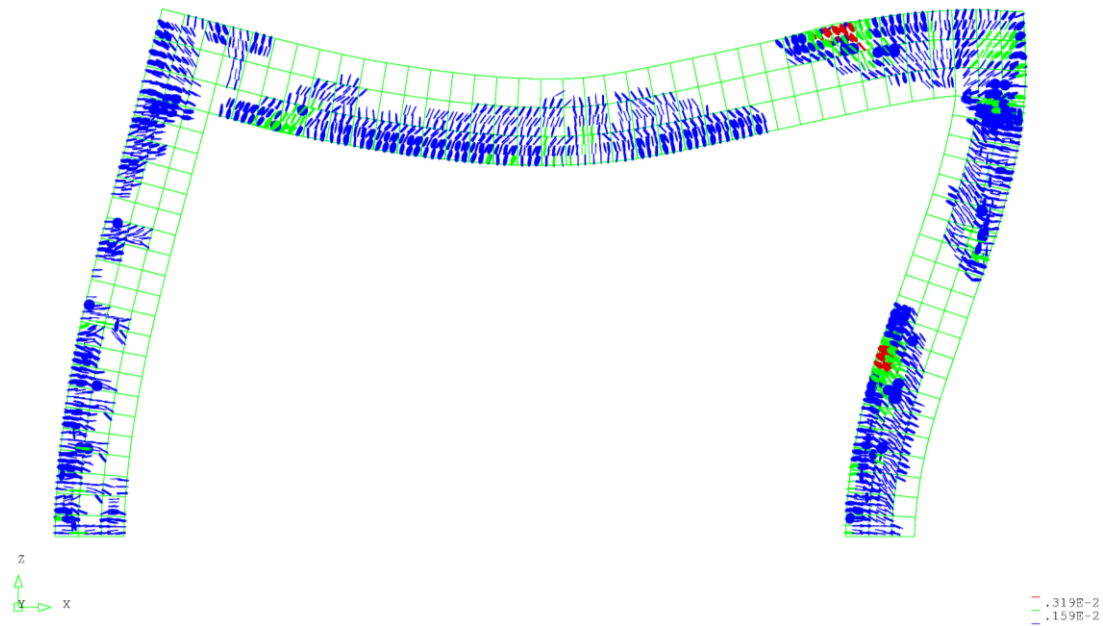


Figure 3.17 Deformed shape and crack pattern at the end of load sequence 2, with both the vertical and horizontal load applied to their characteristic values (vertical load first)

The same tendency of the crack formation was present until failure. It occurs for load levels between 94-137% for the main load history, depending on the material strength parameters used. The ultimate strength of neither the main nor the shear reinforcement was reached at the end of the analysis when the numerical integration diverged. The main reinforcement was however yielding in several places including the bottom left and right columns, top right column and midspan and left side portion of the beam. Yielding in stirrups only occur approximately one third way up in the right column. The stresses in the main reinforcement for the last converged load step in sequence 3 is depicted Figure 3.18 below.

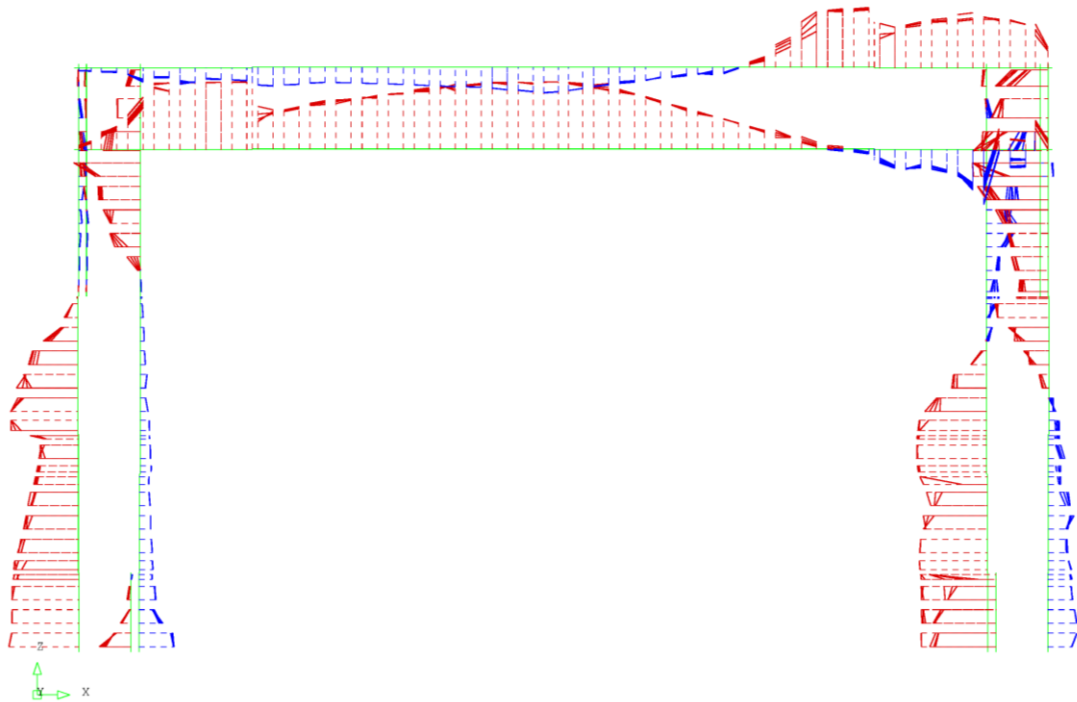


Figure 3.18 Reinforcement stresses at last converged load step, blue and red indicate compressive and tensile stresses respectively

The concrete compressive stresses are very high in the interior side of the upper right corner of the frame due to the geometry which causes a stress concentration. Also the outer lower portion of the right column is subjected to high compressive stresses. It should be noted that stresses well above the uniaxial compressive strength are present in some parts of the structure. It is however reasonable due to the confinement of the concrete.

In order to verify that the divergence originates from an actual compression failure of the concrete, the stress strain relation for the most stressed element was studied. The element was located on the interior side of the right column, adjacent to the corner. The stress values are extracted from a Gauss point close to the concrete surface since these are subjected to less confinement than the interior points and will thus fail first. Failure of concrete in one Gauss point does not automatically yield structural failure, but when sufficiently many integration points have failed the analysis cannot find equilibrium and the structure collapses. The stress-strain curve from the studied Gauss point in the aforementioned concrete element is presented in Figure 3.19 below. The parabolic shape of the concrete stress strain curve is a bit distorted. This is considered to be due to the cracking behavior of the concrete which influences the Gauss point stresses from which the principal stress is calculated. In order to make the depiction more clear the load increments after failure occurred in the studied Gauss point are excluded.

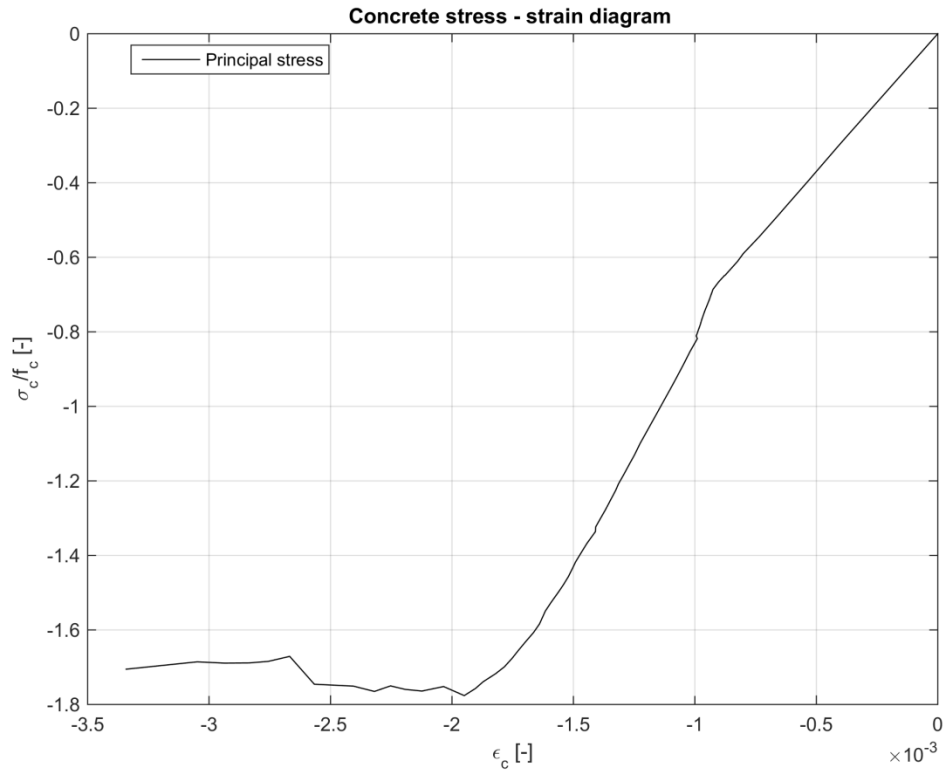


Figure 3.19 Stress-strain diagram for concrete element in interior part of upper right corner for the load increment until just before failure

In conclusion, the ultimate capacity was reached after the reinforcement yielded at several locations but the structural failure was caused by concrete in the top right corner failing in compression.

3.3.3.2 Structural behavior of the frame for inverse load history

The structural behavior of the frame subjected to the inverse load history is presented in this section. Load sequence information is presented in Table 3.11 below.

Table 3.11 Loading sequence information for inverse load history

Loading sequence	Load	Increment size	No. of increments	Iteration method in DIANA	Max. no. of iterations
1	Horizontal	5%	20	Modified NR, first tangent “tangent”	100
2	Vertical	5%	20	Regular NR, first tangent “linear”	100
3	Vertical and horizontal	5%	Max. possible	Regular NR, first tangent “linear”	100

The crack pattern at the end of the horizontal load application is presented in Figure 3.20 below. The upper left corner is subjected to an opening deformation and the upper right corner is subjected to a closing deformation. Also the column supports resist the horizontal load. This is clearly reflected in the crack pattern.

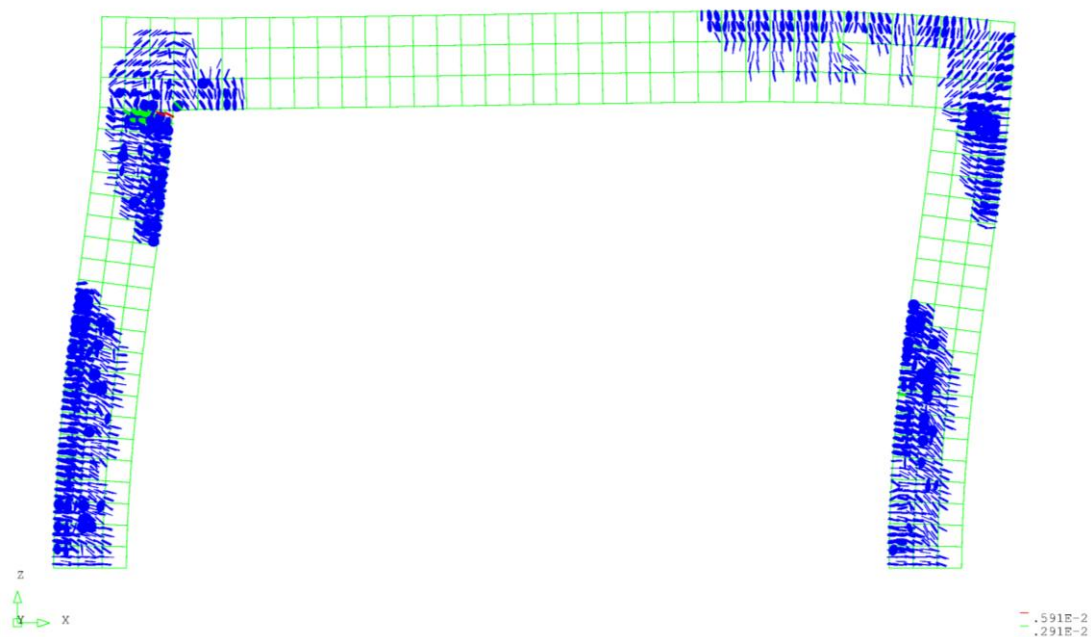


Figure 3.20 Deformed shape and crack pattern at the end of load sequence 1, with the horizontal load applied to its characteristic value

The deformed shape and crack pattern after application of the vertical load are presented in Figure 3.21 below. Note the difference in structural behavior due to the load history, cf. Figure 3.17. In contrast to the case of the main load history, the outside left corner do not crack when subjected to both characteristic loads when the

horizontal load is applied first. Logically the interior side of the upper left is not cracked for the main load history but for the inverse load history.

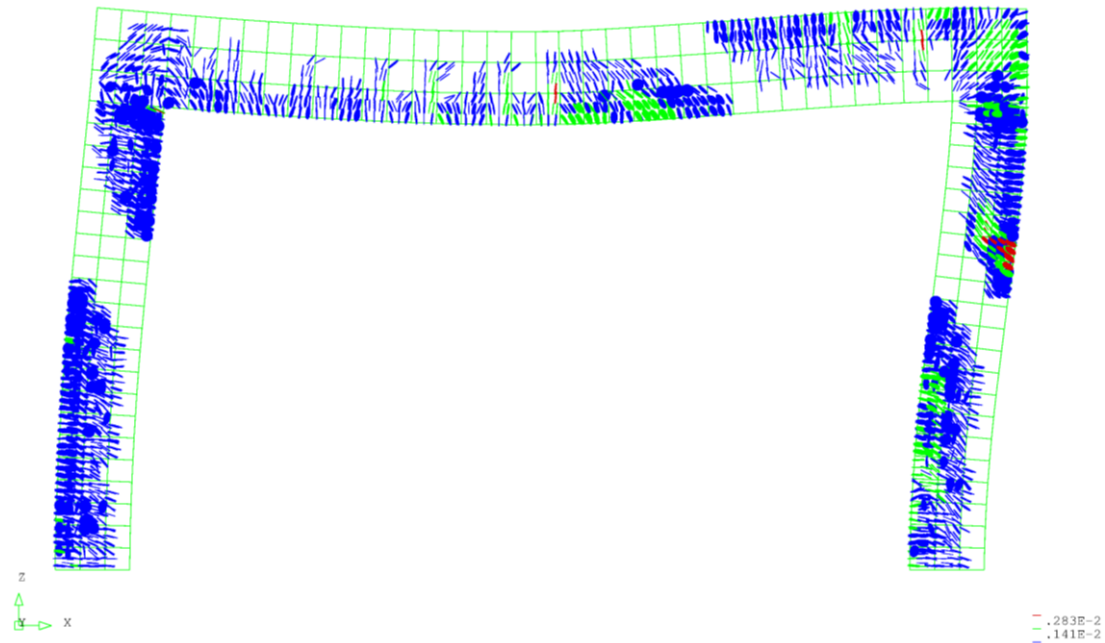


Figure 3.21 Deformed shape and crack pattern at the end of load sequence 2, with both the vertical and horizontal load applied to their characteristic values (horizontal load first)

3.3.3.3 Method of estimation of a coefficient of variance of resistance (ECOV)

For the ECOV safety format two separate NLFEA are performed, using the mean and the characteristic material strength properties, respectively. The material strength parameters for concrete are calculated according to the Model Code 2010, fib (2013). The formulas for these material strength parameters are based on the mean compressive strength. The characteristic values are obtained using the characteristic compressive strength as a fictional mean value of the compressive strength in the calculations. This gives the characteristic levels of the material properties such as tensile strength and fracture energy. It is not clearly stated in the Model Code 2010 how to obtain the characteristic values and other ways of determining them could also be considered. For the reinforcement steel a Young's modulus of 200 GPa is used for both cases. This is a choice made by the author and reflects that the elasticity of steel is little dependent on the yield and ultimate strength. The reinforcement steel strength properties are found from Norwegian Standard NS3573. The input parameters for the analyses are presented in Table 3.12 below.

Table 3.12 Table of mean and characteristic material strength parameters used for ECOV analyses

Steel					
Mean values			Characteristic values		
E_{sm}	200 000	MPa	E_{sk}	200 000	MPa
f_{ym}	533	MPa	f_{yk}	500	MPa
f_{um}	628	MPa	f_{uk}	600	MPa
ϵ_{um}	0.1171	[-]	ϵ_{uk}	0.1170	[-]
Concrete					
Mean values			Characteristic values		
E_{cm}	37 486	MPa	E_{ck}	35 496	MPa
f_{cm}	53.0	MPa	f_{ck}	45.0	MPa
f_{ctm}	3.80	MPa	f_{ctk}	3.33	MPa
G_{fm}	149.2	N/m	G_{fk}	144.8	N/m
G_{cm}	37 294	N/m	G_{ck}	36 211	N/m

Generally the two analyses give a similar response for both sets of parameters. In the uncracked stage it is almost identical. As the load increased a somewhat stiffer behavior can be seen in the frame analyzed using the mean values. The ultimate capacity of said frame is also higher than that of the frame analyzed using the characteristic strength parameters. The results from the analyses for the main load history are presented in Figure 3.22 and Figure 3.23 below. The first figure shows the vertical force versus the vertical displacements at midspan while the second shows the horizontal force and horizontal displacement at the right corner. Load sequences 2 and 1 respectively have been left out in the plots for clarity.

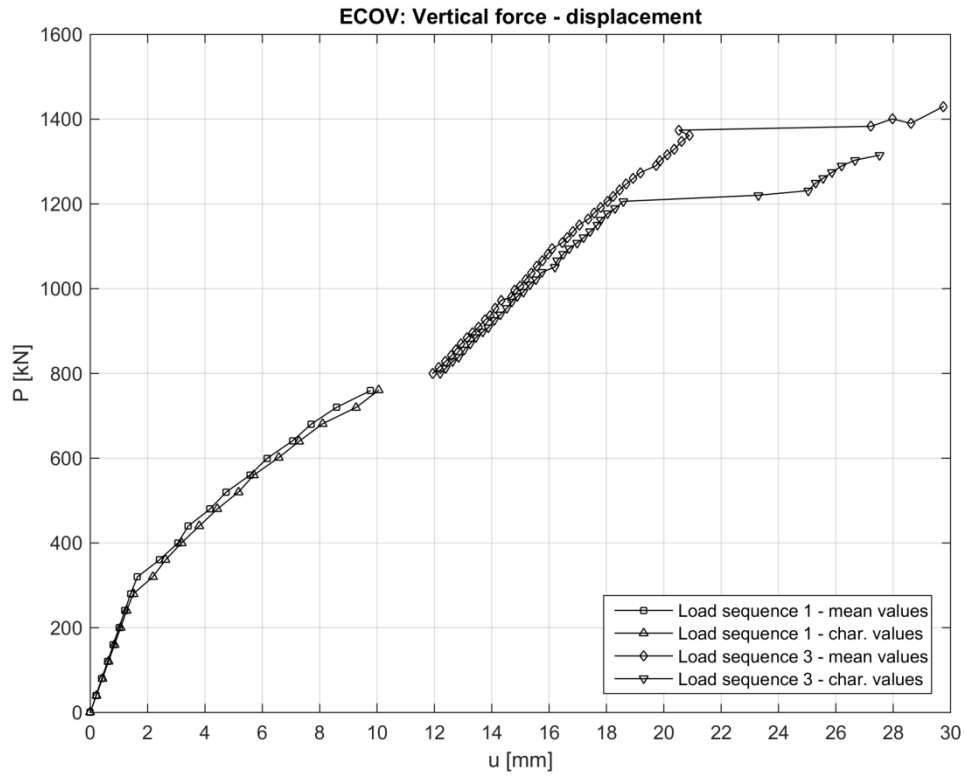


Figure 3.22 Vertical force vs vertical deflection for ECOV analyses for the main load history

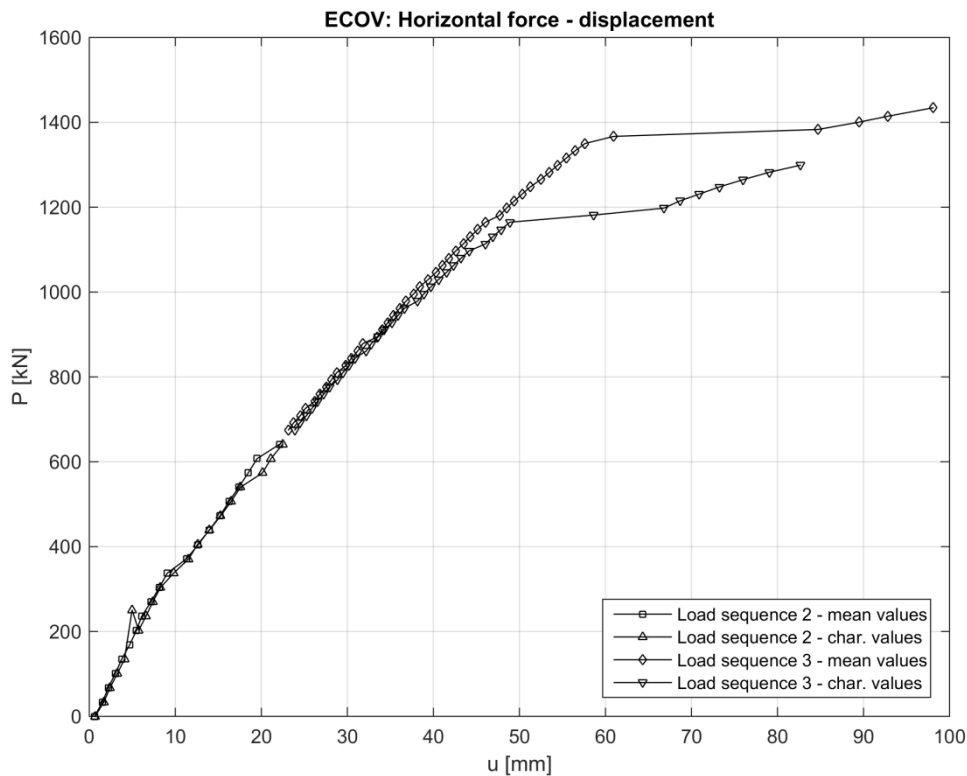


Figure 3.23 Horizontal force vs horizontal deflection for ECOV analyses for the main load history

3.3.3.4 Global resistance factor method (GRFm)

In the global resistance factor method one single analysis is performed using the mean values of the material strength parameters. Information concerning how these should be determined has been presented previously in Section 2.3.2.1. The input parameters for the analysis are presented in Table 3.13 below.

Table 3.13 Mean material strength parameters used for GRFm analyses

Steel		
E_{sm}	220 000	MPa
f_{ym}	550	MPa
f_{um}	660	MPa
ϵ_{um}	0.1170	[-]
Concrete		
E_{cm}	30 171	MPa
f_{cm}	31.5	MPa
f_{ctm}	2.83	MPa
G_{fm}	123.1	N/m
G_{cm}	30 779	N/m

The vertical force versus vertical displacement at midspan for the NLFEA based on the mean values from the global resistance factor method is shown in Figure 3.24 below. The results are again from a frame subjected to the main load history. Load sequence 2 is omitted for clarity since the horizontal load applied in said sequence only marginally affects the vertical displacement at midspan.

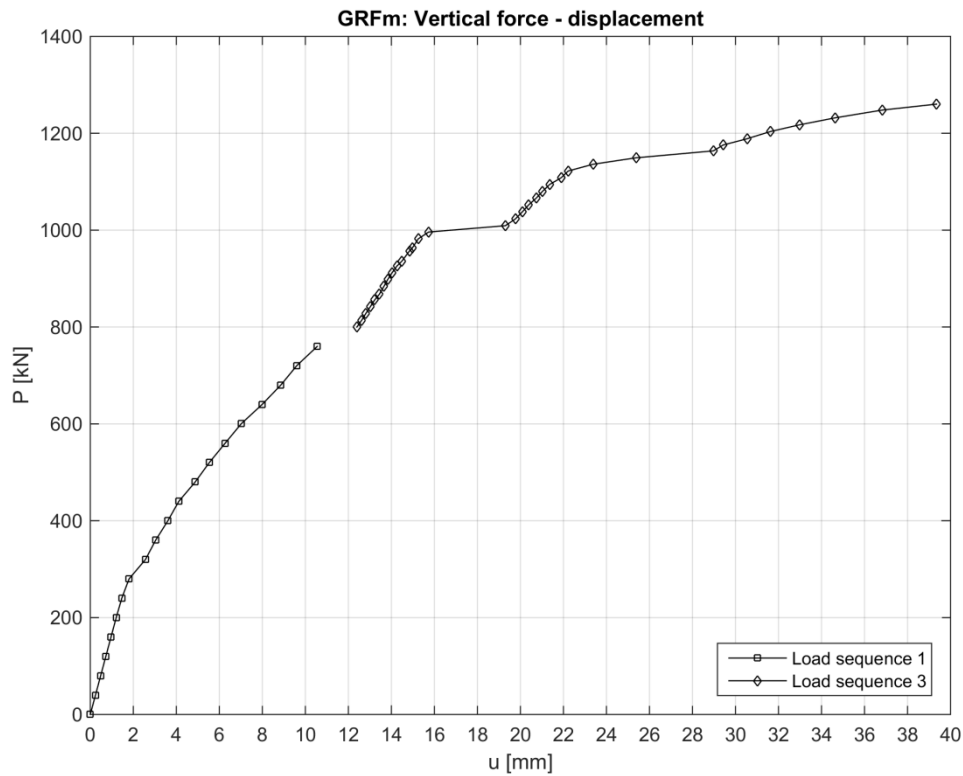


Figure 3.24 Vertical force vs vertical deflection for GRFm analysis for the main load history

The horizontal force versus the horizontal displacement from the considered analysis is presented in Figure 3.25 below.

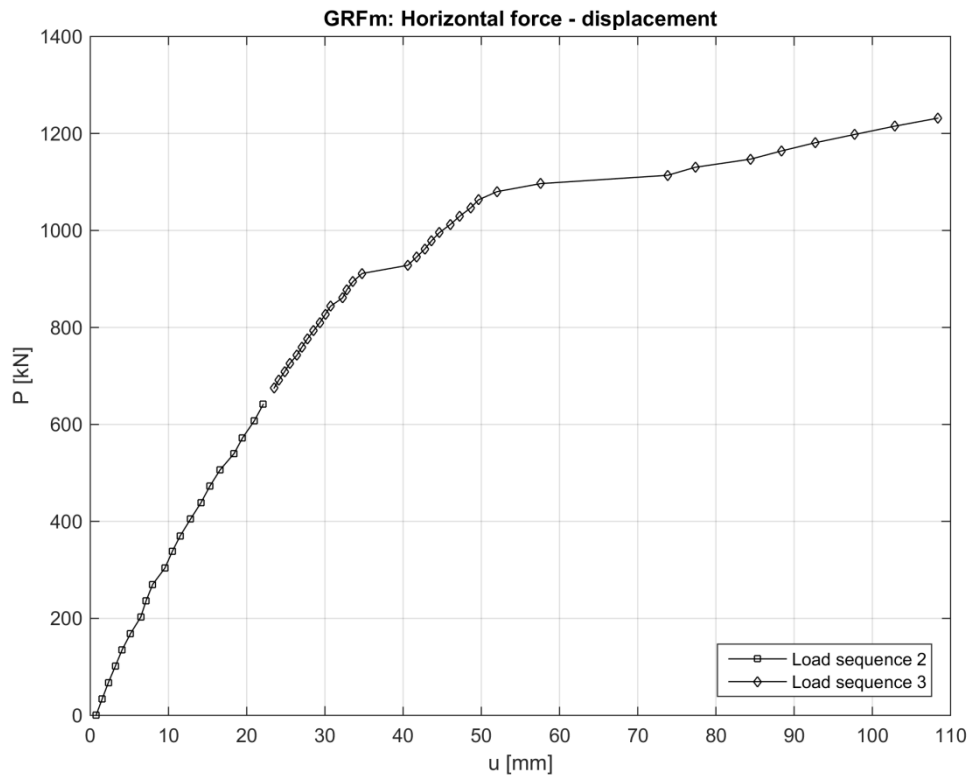


Figure 3.25 Horizontal force vs horizontal deflection for GRFm analysis for the main load history

3.3.3.5 Partial safety factor method (PSF)

The partial safety factor method uses the design values of the strength parameters as input for the NLFEA. It should be noted that the model uncertainty is typically incorporated in the partial coefficient for the materials and is therefore reflected in the design values. The input parameters for the analysis are presented in Table 3.14 below.

Table 3.14 Design material strength parameters used for PSF analysis

Steel		
E_{sd}	173 913	MPa
f_{yd}	435	MPa
f_{ud}	522	MPa
ε_{ud}	0.1170	[-]
Concrete		
E_{cd}	23 664	MPa
f_{cd}	30.0	MPa
f_{ctd}	2.22	MPa
G_{fd}	96.6	N/m
G_{cd}	24 141	N/m

In Figure 3.26 below, the vertical force at midspan is plotted against the vertical displacement at the same location. Again load sequence 2 is omitted for clarity.

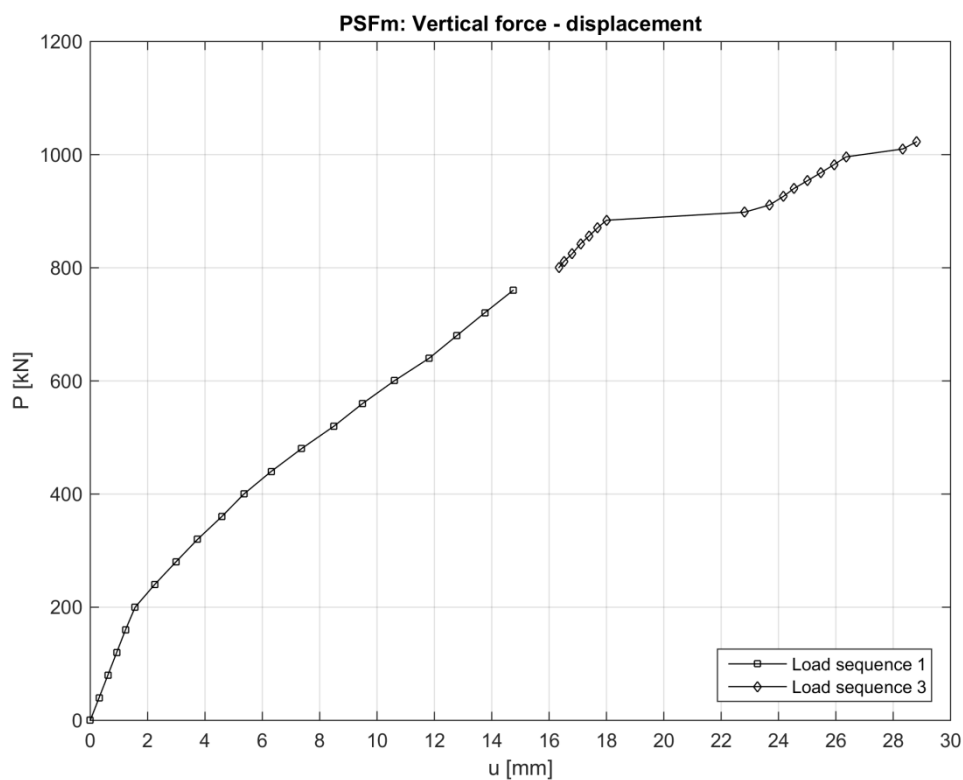


Figure 3.26 Vertical force vs vertical deflection for PSF analysis for the main load history

The horizontal force plotted versus the horizontal displacement at the right corner of the frame can be seen in Figure 3.27 below. The load corresponding to a displacement of 6 mm is deviating markedly from the otherwise linear behavior. It is assumed to be caused by a numerical error.

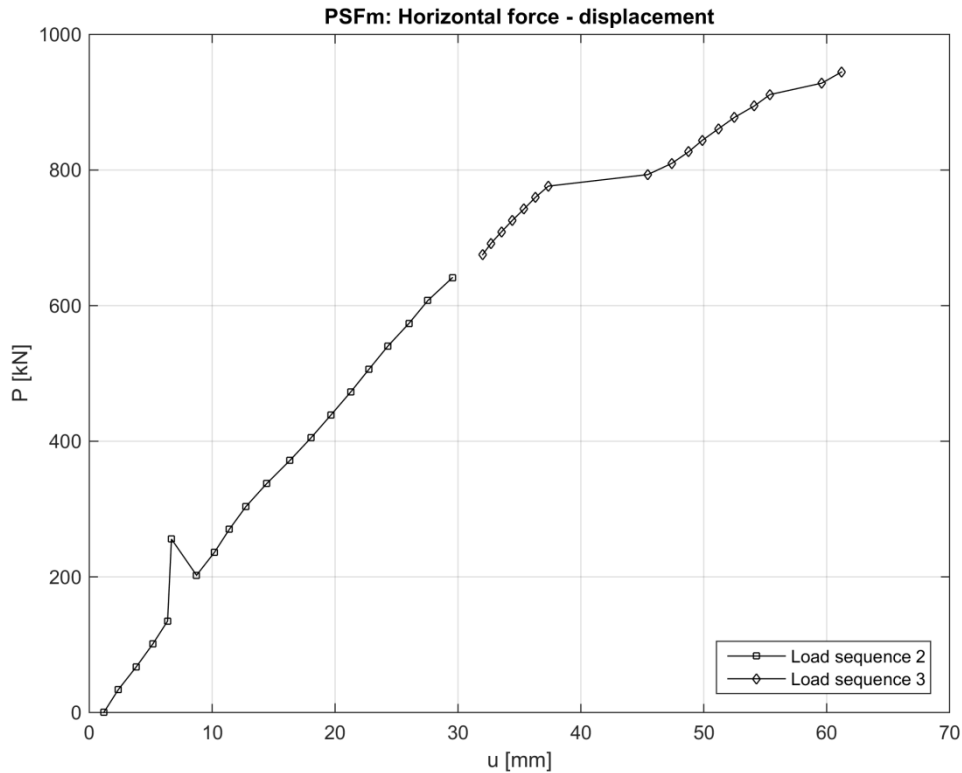


Figure 3.27 Horizontal force vs horizontal displacement for PSF analysis for the main load history

3.3.3.6 Comparison between the main and inverted load history

Plots of the last load sequences are used to compare the frame response for the two studied load histories. It is made for a frame analyzed with mean strength parameters from the ECOV analysis. As can be seen in Figure 3.28, depicting the vertical force – displacement, the frame shows similar stiffness both cases. The vertical displacement at the beginning of load sequence 3 is however larger for the main load history case where the vertical characteristic load is applied first. This is reasonable since the inverse case cause the beam to deflect upwards due to the rigidity of the right corner. For both load histories the frame show ductile behavior when the failure is imminent.

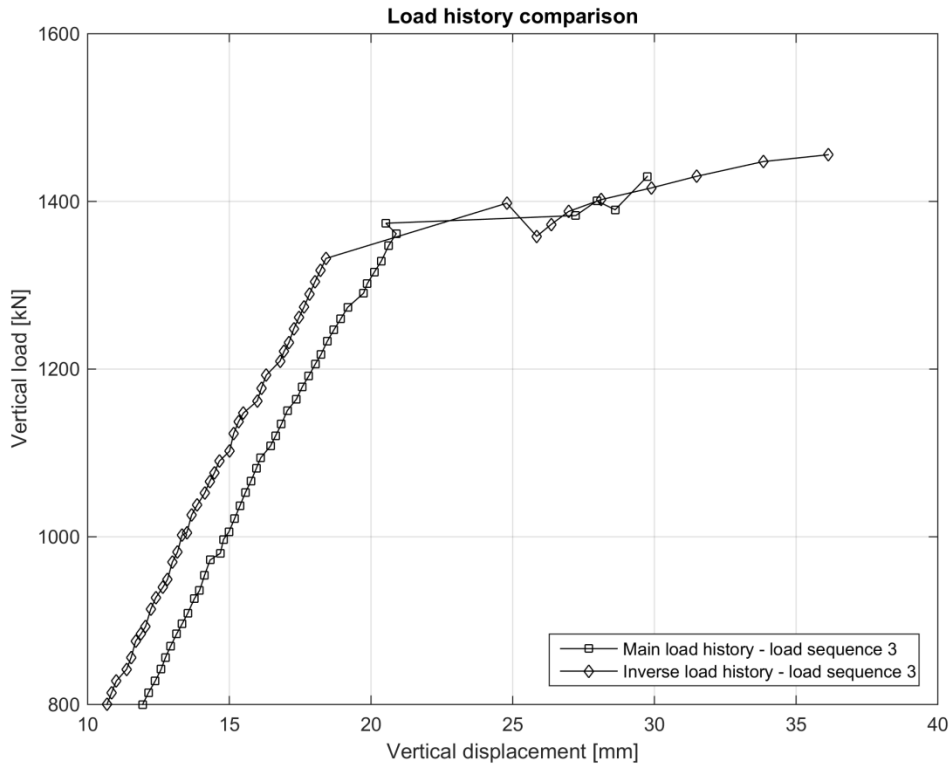


Figure 3.28 Load history comparison for the vertical load in load sequence 3

In case of the horizontal load-deflection relation, as presented in Figure 3.29 below, the frame shows almost identical results for both load histories. The inverse load case has a little larger horizontal displacement at the start of load sequence 3, but has initially larger stiffness so that the displacement is the same at a displacement of around 40 mm. The stiffness is thereafter decreased for the frame subjected to the inverse load history and when the ultimate capacity is reached the displacement is again larger. The frame with mean strength properties is able to carry marginally larger vertical and horizontal loads in the case with the inverse load history. This is not the case with the frame analyzed with the characteristic strength properties.

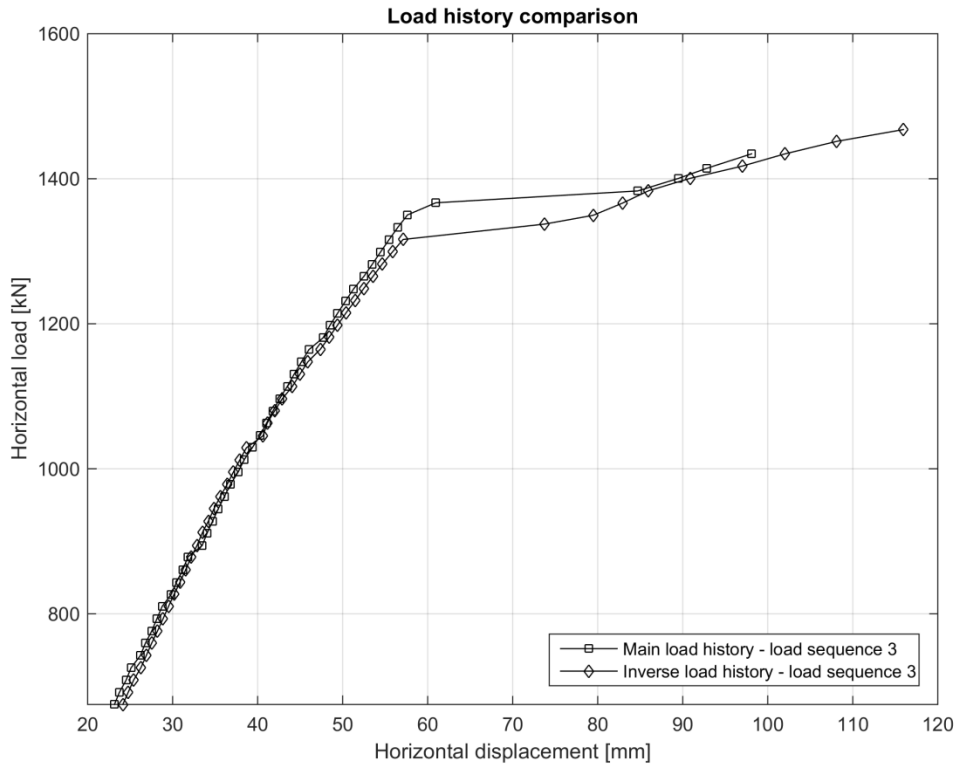


Figure 3.29 Load history comparison for the horizontal load in load sequence 3

3.3.4 Comparison between safety formats

In this section the design resistances of the structure corresponding to a probability of failure of 0.1% are presented for the three safety formats and the two different load histories. The calculations follow the procedure presented in Section 2.3.

A choice has to be made regarding what measure to use to define the structural resistance. Since one of the loads is considered permanent while the other is variable and they act in orthogonal directions the choice is not trivial to make. Here it was chosen to use the total load applied to the structure as the measure of resistance. Because the ratio between the permanent and variable load was kept constant in the loading process, scaled by their corresponding load factor, the total load was found to be the most reasonable choice.

The design resistances for the safety formats corresponding to the main load history, where the vertical load is applied first are presented in Table 3.15 below. The frame was designed for a total load of 2093 kN.

Table 3.15 Design resistances calculated according to the three studied safety formats for the main load history

	R_m [kN]	R_k [kN]	V_R	γ_R	γ_{Rd}	R_d [kN]
ECOV	2864	2614	0.055	1.18	1.06	2284
GRFm	2492	-	-	1.2	1.06	1959
PSFm	-	-	-	-	-	1967

The design resistances for the case of the inverted load history where the horizontal load is applied first are presented in Table 3.16 below. Note that the design resistance according to the ECOV format is decreased for this load history. This is because the analysis based on the characteristic values had a lower capacity, which increased the coefficient of variation and thus the design resistance. An interesting observation is that, between the main and inverse load history, R_m increases while R_k decreases. The results could be explained by the inverse load history being more dependent on the concrete strength than the main load history, together with the larger percental difference between mean and characteristic values for concrete compared to the steel.

Table 3.16 Design resistances calculated according to the three studied safety formats for the inverted load history

	R_m [kN]	R_k [kN]	V_R	γ_R	γ_{Rd}	R_d [kN]
ECOV	2923	2402	0.119	1.437	1.06	1920
GRFm	2491	-	-	1.2	1.06	1959
PSFm	-	-	-	-	-	1939

It should be clearly noted that the total design loads presented above are only valid for similar loading conditions and load histories. For other constellations of loads and different load histories new analyses has to be made and design resistances calculated.

3.4 Response surface and reliability assessment

The implementation of the response surface methodology presented in Section 2.4.3 together with application of FORM/SORM as presented in Section 2.4.2 is accounted for below. The results are also presented.

3.4.1 Construction of the response surface

The procedure for response surface construction proposed by Zhao & Qiu (2013) is principally followed in this project. The aim is to first find a control point which

serves as a starting position when finding the initial center point located on the limit state surface. This point is in the center of the set used to fit the response surface. Finding the center point is an iterative procedure with a convergence criterion put on $G(\mathbf{X}) \approx 0$. Once the center point is found several analyses are run for the basic variables located near said point. The implicit limit state function (LSF) is given as the total load carrying capacity from NLFEA minus the design loads:

$$G(\mathbf{X}) = R_{tot}(\mathbf{X}) - (1,35F_V + 1,5F_H) = R_{tot}(\mathbf{X}) - R_d \quad (3.1)$$

The basic variables are chosen as few as possible due to the time consuming process of evaluating the function in equation 3.1 by means of NLFEA. The basic variables included are the compressive strength of concrete and the yield strength of the reinforcement steel. From these values the other material parameters are estimated using Model Code 2010 fib (2013) for concrete and the relationship between yield and ultimate strength of reinforcement steel is given by NS 3576-3 Norwegian Standard (2012). The coefficients of variation for concrete and reinforcement steel are taken as 0.20 and 0.10 respectively, as described by Schlune *et. al.* (2012) and Pimentel *et. al.* (2014). For both the main and the inverse load history a response surface is constructed for each of the design loads according to the safety formats, yielding a total of eight surfaces.

The basic variables and the corresponding evaluations of the implicit limit state function is the initial set of data points. A response surface is fitted based on these data points. A second order polynomial including cross terms are used for the fitting which is performed using the least square method in MATLAB.

Since a response surface is described by a closed form equation, the first order reliability method can be used to calculate the Hasofer-Lind safety index β and the design point. For this a MATLAB script is used, constructed by Kostandyan *et. al.* (2013). The design point is located where the combination of the basic variables will most likely lead to failure. More evaluations of the LSF from equation 3.1 are run for values around the design point in order to increase the accuracy in the area. The FORM and also SORM are used to determine the final design point, the safety indices and the corresponding probabilities of failure.

3.4.2 Results from response surface analysis

A total of eight different response surfaces were constructed using the design resistances given by the safety formats. The response surface for the design resistance obtained with ECOV for the main load history is depicted together with data points in Figure 3.30 below. Note that more data points were used but they are hidden behind the surface.

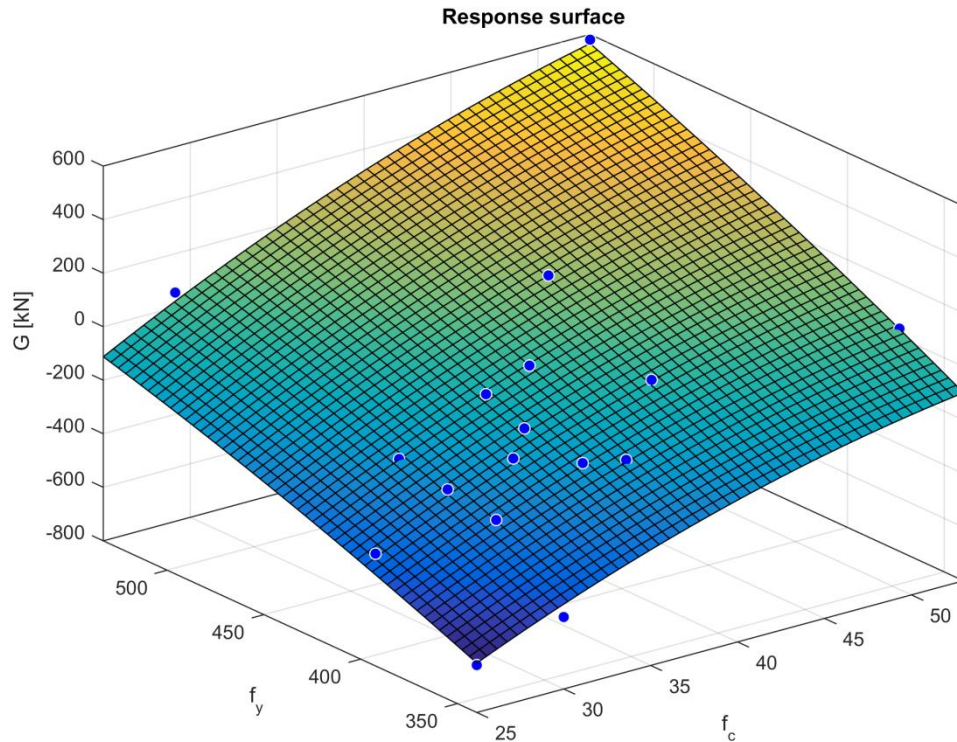


Figure 3.30 Response surface for the design resistance obtained with ECOV for the main load history

The most interesting part of the surface is the contour line where $\bar{g}(\mathbf{X}) = 0$ since it divides the space between the safe and the failure region. A contour plot of the response surface corresponding to the previously mentioned case is depicted in Figure 3.31 below. The design point obtained by FORM is also included.

For the main load history the design point, where failure is most probable to occur, is located where both the concrete and the reinforcement have lower strength than their mean values.

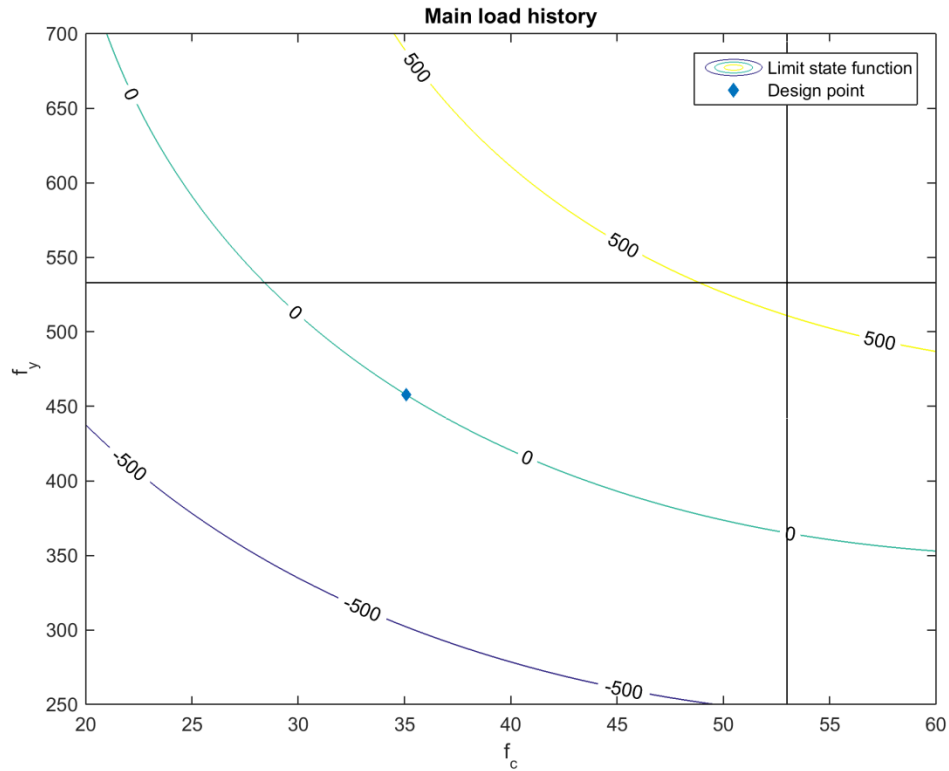


Figure 3.31 Contour plot for the design resistance obtained using ECOV for the main load history

A similar plot but for the inverse load history is depicted in Figure 3.32 below. For this case the design point is located where the steel has a higher capacity than the mean value but the concrete has a substantially decreased value compared to the mean.

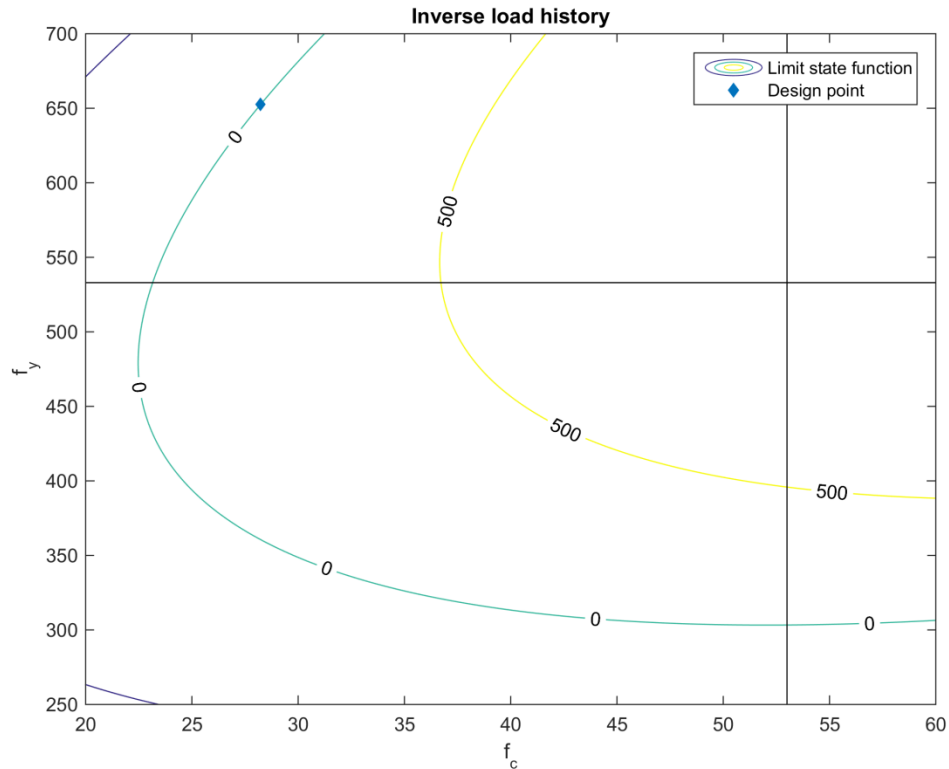


Figure 3.32 Contour plot for the design resistance obtained using ECOV for the inverse load history

The resulting safety indices and corresponding failure probabilities obtained by FORM and SORM for the safety formats are presented in Table 3.17 below. Furthermore, the load used in the linear elastic design is also presented. The intended safety index for the safety formats is $\beta = 0.8 \cdot 3.8 = 3.04$ as described in Section 2.3. This corresponds to a probability of failure of 10^{-3} .

For the main load history the ECOV safety format implies a design resistance that is too high which leads to a lower safety index than intended. The other safety formats are well on the safe side. The difference between the FORM and SORM safety indices is small for all cases, which is expected due to an uncomplicated failure surface.

Table 3.17 Safety indices and probabilities of failure for main load history based on the safety formats' and linear elastic design loads

	$\beta_{\text{FORM}}(p_f)$	$\beta_{\text{SORM}}(p_f)$
ECOV	2.47 ($6.71 \cdot 10^{-3}$)	2.45 ($7.09 \cdot 10^{-3}$)
GRFm	4.06 ($2.45 \cdot 10^{-5}$)	4.06 ($2.48 \cdot 10^{-5}$)
PSF	4.02 ($2.92 \cdot 10^{-5}$)	4.02 ($2.97 \cdot 10^{-5}$)
LFEA	3.39 ($3.50 \cdot 10^{-4}$)	3.38 ($3.62 \cdot 10^{-4}$)

The safety indices and failure probabilities for the inverse load history are presented in Table 3.18 below. All the safety formats in Model Code 2010, fib (2013) produce design load that is above the target safety index for this load history. All the design loads except ECOV yield a smaller safety index when the frame is first loaded horizontally.

Table 3.18 Safety indices and probabilities of failure for inverse load history based on the safety formats' and linear elastic design loads

	$\beta_{\text{FORM}}(p_f)$	$\beta_{\text{SORM}}(p_f)$
ECOV	3.72 ($1.01 \cdot 10^{-4}$)	3.67 ($1.24 \cdot 10^{-4}$)
GRFm	3.60 ($1.61 \cdot 10^{-4}$)	3.53 ($2.04 \cdot 10^{-4}$)
PSF	3.66 ($1.27 \cdot 10^{-4}$)	3.60 ($1.58 \cdot 10^{-4}$)
LFEA	3.14 ($8.51 \cdot 10^{-4}$)	3.02 ($1.27 \cdot 10^{-3}$)

4 Discussion

As stated in the introduction it is of great importance to be able to make accurate assessments of reinforced concrete structures. This enables making new structures more efficient and thereby reducing the material cost and environmental impact. Moreover, assessment of the increasing number of existing structures approaching the end of their service lives is another important field; determining if they are still safe for use and/or if their service life can be prolonged by restrictions or rehabilitation. It is clear that also this analysis application has environmental and monetary benefits. A central question is therefore if the safety formats for nonlinear analysis in present design codes correctly assess the probability of failure.

The matter of determining the ultimate capacity from the analyses is not trivial. It depends largely on the convergence criteria used for the equilibrium iterations. For all the analyses presented in this thesis a relatively strict convergence criterion was used as accounted for in Section 3.1.5. For consistence the ultimate capacity of the frame was always determined as the resistance for the last converged load step, without regard to possible close-to-converged subsequent steps before divergence. One could argue that the structure has not failed until divergence occurs in the iterations, since it is in fact close to equilibrium even if the out of balance energy and forces exceed the convergence criterion. The unconverged load steps may not be realistic with respect to how the structure would respond on sectional level and perhaps include spurious deformations etc., even if global equilibrium almost is fulfilled.

Therefore it remains unclear if the global equilibrium could be fulfilled with a physically feasible response on a sectional level; hence these load increments are excluded.

Very limited information is provided in Model Code 2010 (fib 2013) regarding how the structural resistance should be defined when used in the safety formats. It is logically dependent on the structure's present loading situation, but the resistance is also influenced by previous load situations. The frame considered in this project has a simple load situation, but nevertheless questions arise what measure to use for the safety formats. In this project the total load carrying capacity was used irrespective of the directions of the separate loads, keeping the same ratio between the permanent and variable load. Many other cases could also be used. For example as in the benchmarking example in Section 3.1.1, where the maximum horizontal load for a given vertical load was used. If cyclic loading and other time dependent aspects are included in the analyses the question of how to define the structural resistance is not so straight forward.

The loading history was also found to be important judging by the performed NLFEA. In general the loading capacity was somewhat lower for the inverse load history compared to the main. Applying the horizontal load first causes the frame to deflect laterally. When the vertical load is then applied, as well as when both loads are scaled up thereafter, the frame behaves differently than for the main load history. The loads are carried in a way that further increases the concrete stress in the interior side of the upper right corner of the frame. This exemplifies the importance of considering the load history in nonlinear analyses. For a case where both the structure and loading situation is more complex this is a topic requiring careful considerations. Preferably the load history should include all loads that the structure has been subjected to during its life, including the construction phase. Moreover it is important that the loads are applied in the correct order. For example, consider a post-tensioned concrete beam

which is to be analyzed to determine the maximum midspan point load that can be applied. The NLFEA should include the loads originating from removal of the formwork and application of the prestressing as well as other time dependent effects before the vertical point load is introduced in the analysis.

Since it is desired to increase the use of nonlinear analyses in engineering applications there should be more descriptive guidelines. These should treat aspects such as how to define the design resistance as well as acceptable simplifications of the structural model and loading history.

In the safety assessment that was performed, the response surface was fitted using a second order polynomial. The failure mode was compression failure in the concrete in the upper right corner for all the analyses close to the design point. Thus the ultimate capacity was much dependent on the concrete strength. A higher order polynomial failure surface was considered unnecessary due to the simple ultimate limit behavior. For a second order polynomial surface, SORM should be able to represent the probability of failure adequately since it approached the surface with a second order Taylor expansion around the design point. Therefore it was considered unnecessary to use Monte Carlo simulations with importance sampling as considered earlier in the project. Only two basic variables were included for the safety assessment, i.e. concrete compressive strength and steel yield strength. The other material parameters were calculated based on these values and provided as input in the analyses. This is similar to assuming full correlation between the strength properties. In reality the strength parameters are correlated, for example the compressive and tensile strength, but not 100%. But for this relatively simple safety assessment it is considered adequate to make this simplification. Furthermore, it was considered to treat the frame dimensions, reinforcement placing and load application points as random variables following some distributions. This was however excluded due to the vast amount of time required to generate the many new required models. It should also be pointed out that the number of analyses needed to be run increase exponentially with the number of basic variables included in the study. It would nevertheless be very interesting to see what impact it would have on the safety to treat the aforementioned parameters as random.

It was found that the failure probabilities for the frame were very much dependent on the type of distribution the basic variables follow. The normal distribution is often a good choice if the quality control during manufacturing is sufficient to ensure a low coefficient of variation, otherwise the lognormal distribution is a better choice according to Ghosh (1991). Since the frame designed in this thesis is not built in reality, this is of little help when choosing a distribution. Further, it could be argued that the concrete compressive strength should follow a normal distribution since the other concrete properties are approximated based on said strength. However a comparison was made between a normal and a lognormal distribution for the concrete properties, with 0.15 and 0.2 as the coefficient of variation respectively, and the difference was found to be small. This suggests that the use of lognormal material strength properties as used in the thesis is an adequate choice. The reason for comparing the results using normal and lognormal distributions for different coefficients of variation is that a normal distribution is typically used when the level of certainty is higher, as described above.

The design resistance obtained using ECOV did not reach the intended safety index for the main load history, i.e. when the vertical load is applied first. The design resistance was found to be significantly higher for this safety format and said load

history than for the other safety formats. This was mostly due to a low coefficient of variation. It was obtained due to a small difference in capacity between analyses using mean and characteristic material strength parameters, leading to a low factor of safety resulting in a high design load. All safety formats except for ECOV reached a lower safety index for the inverse load history compared to the main. This points out, as stated earlier, that the load history is very important in nonlinear analyses.

5 Conclusions and suggestions for further work

Even though nonlinear finite element analyses (NLFEA) has been performed in research settings for many years it is yet to be used extensively in engineering practice. This due to several reasons, for example the inability to superimpose loads leading to vast computational time but also the lack of safety formats surely leading to the intended safety level as well as sufficient guidance.

The author suggests that the safety formats in Model Code 2010, fib (2013) are evaluated for more complex structures. The ECOV safety format was found not to meet the intended safety level for one of the studied load histories. It points out the importance of load history considerations when it comes to NLFEA. Therefore it would be of interest to assess the safety level of the safety formats applied to e.g. a shell structure subjected to a broad variety of loading conditions. Different types of failure modes should be included and preferably also their effect on the modelling uncertainty. Other safety formats that more objectively include the failure mode and modelling uncertainty are perhaps needed, since the generality of a safety format might lead to excessive conservatism in some cases.

Furthermore a framework of engineering guidelines for NLFEA is desired. These should treat all aspects important to conduct accurate NLFEA. Questions have been raised during this thesis regarding how to treat the load history but also how to define the design resistance. If the guidelines should be accessible for engineers to use in practice, it is of great importance but also a great challenge, to present simplifications that can be made in the models and analyses. It requires substantial research to prove which simplifications that can be done conservatively without degrading the accuracy to such an extent that the purpose of NLFEA is extinguished.

6 References

- ANSYS Mechanical 14.5 (2014): ANSYS inc., Canonsburg, USA. Available from: <<http://www.ansys.com/Products/Simulation+Technology/Structural+Analysis/ANSYS+Mechanical>>
- Brekke, D.-E., Åldstedt, E., Grosch, H. (1994): Design of Offshore Concrete Structures Based on Postprocessing of Results from Finite Element Analysis (FEA): Methods, Limitations and Accuracy, *Proceedings of the Fourth International Offshore and Polar Engineering Conference*. April 1994.
- Bucher, C.G., Bourgund, U. (1990): A fast and efficient response surface approach for structural reliability problems, *Structural Safety*, vol 7, no. 1, pp. 57-66
- CEN (2005): *EN 1992-2 Eurocode 2: Design of concrete structures - Part 2: Concrete bridges - Design and detailing rules*, Brussels.
- CEN (2008): *EN 1990 Eurocode 0: Basis of structural design*, Brussels.
- Cervenka, V. (2013): Reliability-based non-linear analysis according to fib Model Code 2010, *Structural Concrete*, vol 14, no. 1, pp. 19-28.
- Cook, R.D, Malkus, D.S., Plesha, M.E., Witt, J.W. (2001): *Concepts and Applications of Finite Element Analysis, 4th edition*, John Wiley & Sons ,Hoboken, New Jersey.
- Cook, R.D., Young, W.C. (1999): *Advanced Mechanics of Materials*, Prentice Hall, Upper Saddle River, New Jersey.
- Davis, P. J., Rabinowitz, P. (1975): *Method of Numerical Integration*, Academic Press, Waltham, Massachusetts.
- Engen, M. (2014): Workshop on solutions strategy for NLFEA, Oslo, October, 2014.
- Engen, M., Hendriks M.A.N., Øverli, J.A., Åldstedt E. (2014): Application of NLFEA in the Design of Large Concrete Structures, *Proceedings of the XXII Nordic Concrete Research Symposium*, Reykjavik, Iceland.
- fib (2013): Chapter 7 - Design , *fib Model Code for Concrete Structures 2010*, Ernst & Sohn GmbH & Co, Hoboken, New Jersey.
- Ghosh, S.N. (1991): *Cement and Concrete Science & Technology*, ABI Books, Nehru Place, New Dehli.
- JCSS (2001): *Part 1 - Basis of Design*, Probabilistic Model Code, Delft, The Netherlands.
- Kostandyan, E.E., Sørensen, J.D. (2013): Reliability Assessment of IGBT Modules Modeled as Systems with Correlated Components, *Proceedings on the 2013 Annual Reliability and Maintainability Symposium (RAMS 2013)*, pp. 1-6.
- Kotsovos, M.D., Pavlovic, M.N. (1999): *Ultimate limit-state design of concrete structures: a new approach*, Thomas Telford, University of Michigan.
- Lund University (2004): CALFEM MATLAB-Toolbox, Division of Structural Mechanics, Lund, Sweden. Available from: <<http://www.byggmek.lth.se/calfem>>
- Melchers, R.E. (1999): *Structural Reliability Analysis and Prediction*, John Wiley & Sons, Hoboken, New Jersey .

- Hinton, E. (1992): *NAFEMS Introduction to Nonlinear Finite Element Analysis*, National Agency for Finite Element Methods & Standards, Hamilton, Great Britain.
- Norwegian Standard (2012): *NS3576-3: Steels for reinforcement of concrete - Dimensions and properties- Part 3*, Standard Norge, Lilleaker, Oslo.
- Olsson, A., Sandberg, G. Dahlbom, O. (2003): On Latin hypercube sampling for structural reliability analysis, *Structural Safety*, no. 25, pp. 47-68.
- Pimentel, M., Bruhwiler, E., Figueiras, J. (2014): Safety examination of existing concrete structures using the global resistance safety factor concept, *Engineering Structures*, vol 70, pp. 130-143.
- Rajashekhar, M.R., Ellingwood, B.R. (1993): A new look at the response surface approach for reliability analysis, *Structural Safety*, vol 12, no. 3, pp. 205-220.
- Rijkswaterstaat (2012): Guidelines for Nonlinear Finite Element Analysis of Concrete Structures, *Rijkswaterstaat Technisch Document (RTD)*, The Netherlands.
- Schlune, H. (2011): *Safety Evaluation of Concrete Structures with Nonlinear Analysis*, Ph.D. Thesis, Department of Structural Engineering, Chalmers University of Technology, Publication no 3232. Gothenburg, Sweden.
- Schlune, H., Plos, M., Gylltoft, K. (2011): Safety formats for nonlinear analysis tested on concrete beams subjected to shear forces and bending moments , *Engineering Structures* , vol 33, no. 8, pp. 2350-2356.
- Schlune, H., Plos, M., Gylltoft, K. (2012): Safety formats for non-linear analysis of concrete structures, *Magazine of Concrete Research*, vol 64, pp. 563-574.
- Selby, R.G., Vecchio, F.J. (1997): A constitutive model for analysis of reinforced concrete solids, *Canadian Journal of Civil. Engineering*, vol 24, no. 3, pp. 460-470.
- Seraj, S., Kotsovos, M., Pavlovic, M. (1995): Application of the compressive-force path concept in the design of reinforced concrete indeterminate structures: A pilot study, *Structural Engineering and Mechanics*, vol 3, no. 5, pp. 475-495.
- TNO DIANA (2012): *DIANA User's Manual release 9.4.4*, TNO DIANA BV, Delft, The Netherlands.
- TNO DIANA (2014): *DIANA FEM-software release 9.4.4*, TNO DIANA BV, Delft, The Netherlands. Available at: < <http://tnodiana.com/content/DIANA>>
- Vecchio, F., Collins, M. (1993): Compression Response of Cracked Reinforced Concrete, *Journal of Structural Engineering*, vol 119, no. 12, pp. 3590-3610.
- Zhao, Y.-G., Ono, T. (1999): A general procedure for first/second-order reliability method (FORM/SORM), *Structural Safety*, no. 21, pp. 95-112.
- Zhao, W., Qiu, Z. (2013), An efficient response surface method and its application to structural reliability and reliability-based optimization, *Finite Elements in Analysis and Design*, vol 67, pp. 34-42.

7 Appendices

A. Kinematic collapse analysis of benchmarked frame

Mechanism 1

In Figure 1 below, the notation of the loads, dimensions and member numbers can be seen. The moment capacities of the members are usually independent of the mechanism forming. The moment capacities are 13.27 kNm for members 1 and 3 and 16.57 kNm for member 2. Since the capacity is lower for member 1 and 3 than for member 2, yielding at point B and D corresponds to yielding of the first mentioned members.

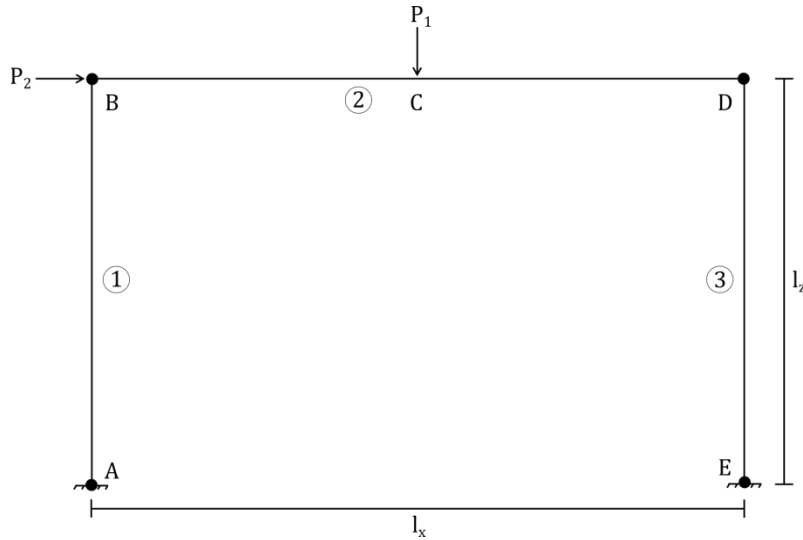


Figure 1 Locations of plastic hinges for mechanism 1 presented as bullets

Only the load P_2 performs any work in this mechanism, and the collapse load can be calculated as:

$$P_2 = \frac{4 \cdot M_1}{l_z} = 30.77 \text{ kN}$$

Mechanism 2

The plastic hinges for this mechanism are at B, C and D as can be seen in Figure 2.

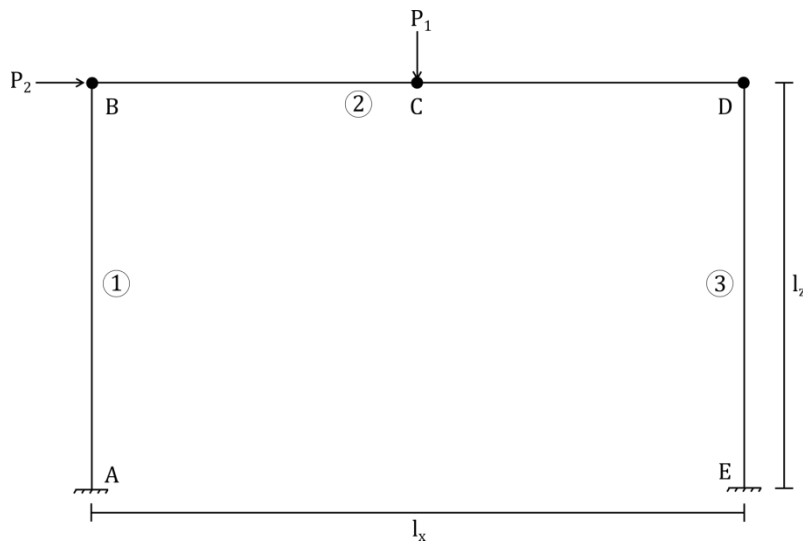


Figure 2 Locations of plastic hinges for mechanism 2 presented as bullets

Only the load P_1 performs any work, and the collapse load can be calculated as:

$$P_1 = \frac{(2 \cdot M_1 + 2 \cdot M_2) \cdot 2}{l_x} = 43.52 \text{ kN}$$

Mechanism 3

Plastic hinges form at A, C and D for mechanism 3, which can be seen in Figure 3. Both of the loads perform work in this collapse mechanism, therefore it is necessary to determine a pair of loads that cause failure. Since the vertical load in the practical experiment is originally 23.69 kN, this value is chosen for P_1 .

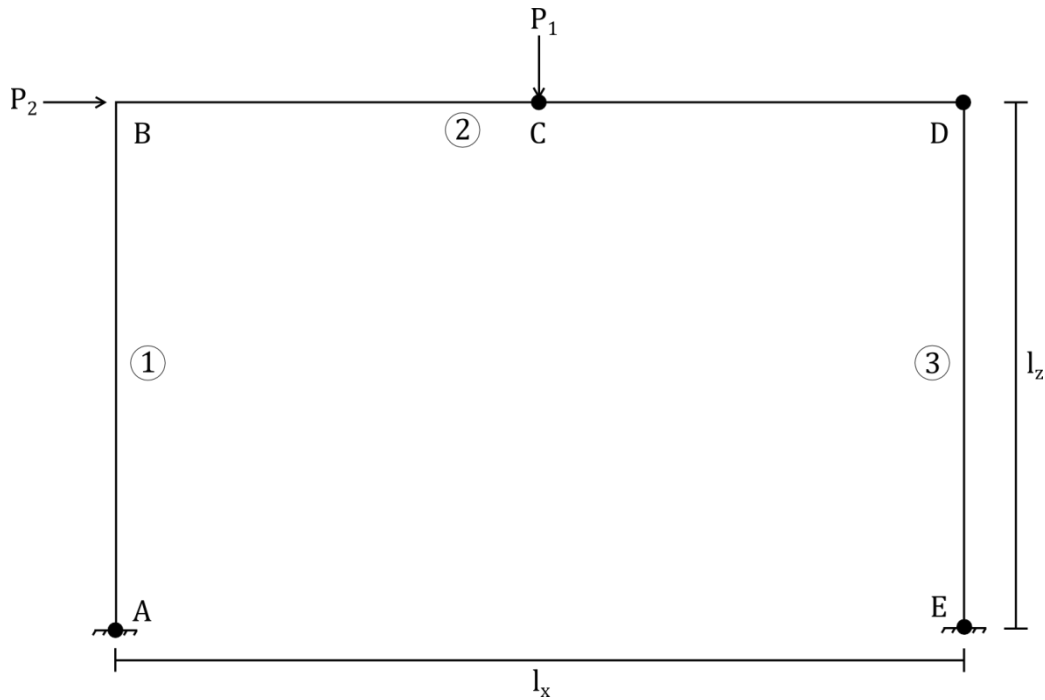
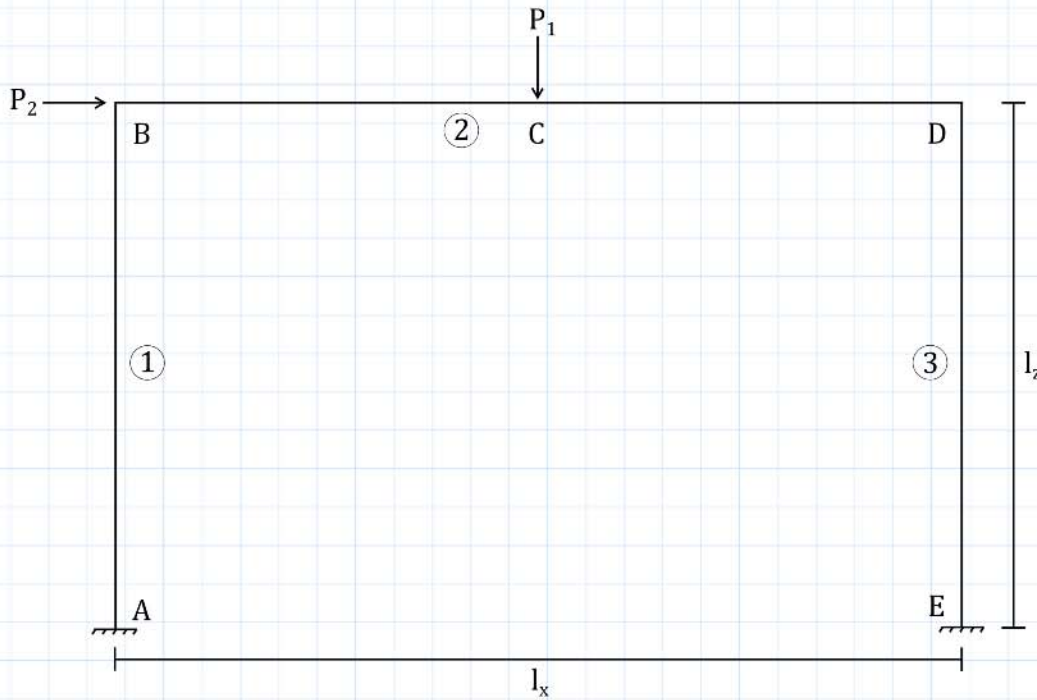


Figure 3 Locations of plastic hinges for mechanism 3 are presented as bullets

The load P_2 causing failure given that $P_1 = 23.69 \text{ kN}$ can be calculated as:

$$P_2 = \frac{2 \cdot M_1 + 2 \cdot M_2 - P_1 \cdot \frac{l_x}{2}}{l_z} = 15.76 \text{ kN}$$

LOAD CARRYING CAPACITY OF VERTICALLY AND HORIZONTALLY LOADED FRAME



Frame properties:

$$l_x := (2868 - 125) \text{ mm} = (2.743 \cdot 10^3) \text{ mm} \quad \text{"width, centerline value"}$$

$$l_z := \left(1800 - \frac{150}{2}\right) \text{ mm} = (1.725 \cdot 10^3) \text{ mm} \quad \text{"height, centerline value"}$$

$$P_1 := 23.69 \text{ kN} \quad \text{"vertical load, not causing any yield"}$$

Material parameters:

$$f_{cm} := 38 \text{ MPa} \quad E_{cm} := 29738 \text{ MPa} \quad \varepsilon_{c1} := 2.3 \cdot 10^{-3} \quad \text{"Model Code 2010"}$$

$$f_{ym} := 560 \text{ MPa} \quad E_s := 200000 \text{ MPa} \quad \varepsilon_y := \frac{f_{ym}}{E_s} = 0.003$$

$$\phi := 10 \text{ mm} \quad \alpha := \frac{E_s}{E_{cm}} = 6.725$$

Cross section parameters:

Cross section member 1 and 3:

$$w_1 := 90 \text{ mm} \quad h_1 := 125 \text{ mm} \quad cc_1 := 15 \text{ mm} \quad d_{1.top} := cc_1 \quad d_{1.bottom} := h_1 - cc_1 = 110 \text{ mm}$$

Cross section member 2:

$$w_2 := 90 \text{ mm} \quad h_2 := 150 \text{ mm} \quad cc_2 := 15 \text{ mm} \quad d_{2.top} := cc_2 \quad d_{2.bottom} := h_2 - cc_2 = 135 \text{ mm}$$

$$\pi \cdot (10 \text{ mm})^2$$

$$\pi \cdot (10 \text{ mm})^2$$

$$A_{s.top} := 3 \cdot \frac{\pi \cdot (10 \text{ mm})}{4} \quad A_{s.bot} := 3 \cdot \frac{\pi \cdot (10 \text{ mm})}{4}$$

Plastic moment capacity of cross sections:
 “Assume concrete failure limits the capacity”

Plastic moment capacity of member 1 and 3:

$$x := 25.085 \text{ mm} \quad \text{Iterated compression block height to obtain force equilibrium in cross section}$$

$$\varepsilon_{s1.bottom} := (d_{1.bottom} - x) \frac{0.0035}{x} = 0.012 \quad f_{s1.bottom} := \min(E_s \cdot \varepsilon_{s1.bottom}, 560 \text{ MPa})$$

$$\varepsilon_{s1.top} := (d_{1.top} - x) \frac{0.0035}{x} = -0.001 \quad f_{s1.top} := E_s \cdot \varepsilon_{s1.top} = -281.423 \text{ MPa}$$

$$C_{c1} := 0.85 \cdot f_{cm} \cdot w_1 \cdot 0.9 \cdot x = 65.63 \text{ kN}$$

$$C_{s1} := A_{s.top} \cdot f_{s1.top} = -66.309 \text{ kN}$$

$$T_1 := A_{s.bot} \cdot f_{s1.bottom} = 131.947 \text{ kN} \quad C_{c1} - C_{s1} = 131.939 \text{ kN}$$

Moment around concrete compressive force resultant

$$M_1 := A_{s.bot} \cdot f_{s1.bottom} \cdot (d_{1.bottom} - 0.45 \cdot x) + A_{s.top} \cdot f_{s1.top} \cdot (0.45 \cdot x - d_{1.top}) = 13.271 \text{ kN} \cdot \text{m}$$

Plastic moment capacity of member 2:

$$x := 25.085 \text{ mm} \quad \text{Iterated compression block height to obtain force equilibrium in cross section}$$

$$\varepsilon_{s2.bottom} := (d_{2.bottom} - x) \frac{0.0035}{x} = 0.015 \quad f_{s2.bottom} := \min(E_s \cdot \varepsilon_{s2.bottom}, 560 \text{ MPa})$$

$$\varepsilon_{s2.top} := (d_{2.top} - x) \frac{0.0035}{x} = -0.001 \quad f_{s2.top} := E_s \cdot \varepsilon_{s2.top} = -281.423 \text{ MPa}$$

$$C_{c2} := 0.85 \cdot f_{cm} \cdot w_2 \cdot 0.9 \cdot x = 65.63 \text{ kN}$$

$$C_{s2} := A_{s.top} \cdot f_{s2.top} = -66.309 \text{ kN}$$

$$T_2 := A_{s.bot} \cdot f_{s2.bottom} = 131.947 \text{ kN} \quad C_{c2} - C_{s2} = 131.939 \text{ kN}$$

Moment around concrete compressive force resultant

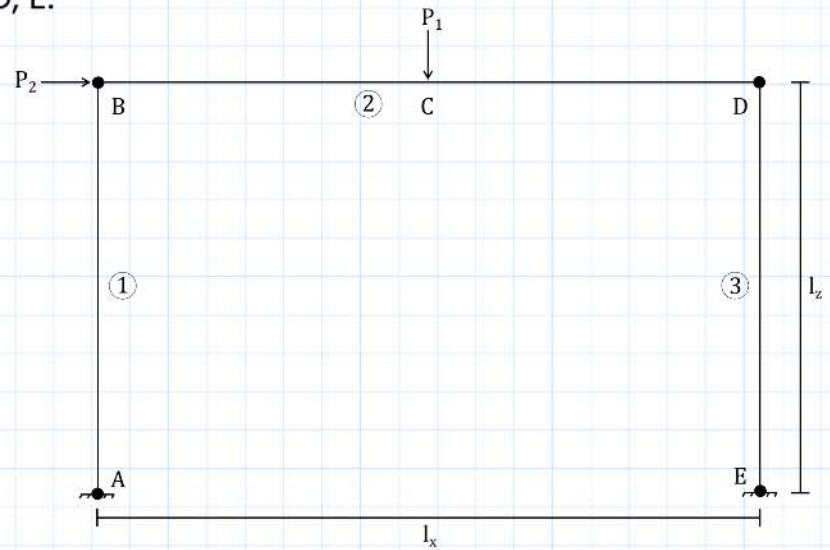
$$M_2 := A_{s.bot} \cdot f_{s2.bottom} \cdot (d_{2.bottom} - 0.45 \cdot x) + A_{s.top} \cdot f_{s2.top} \cdot (0.45 \cdot x - d_{2.top}) = 16.57 \text{ kN} \cdot \text{m}$$

Plastic capacity according to collapse theory, e.g. Adv mech of materials (Cook & Young)

Mechanism 1, hinges at A, B, D, E:

$$P_2 \cdot (l_y \cdot \theta) - M_1 \cdot (\theta + \theta + \theta + \theta)$$

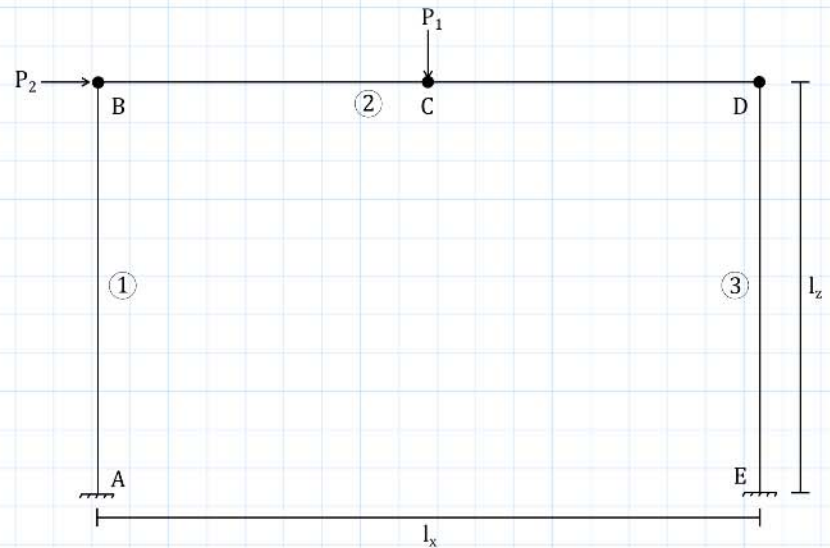
$$P_2 := \frac{M_1 \cdot 4}{l_z} = 30.773 \text{ kN}$$



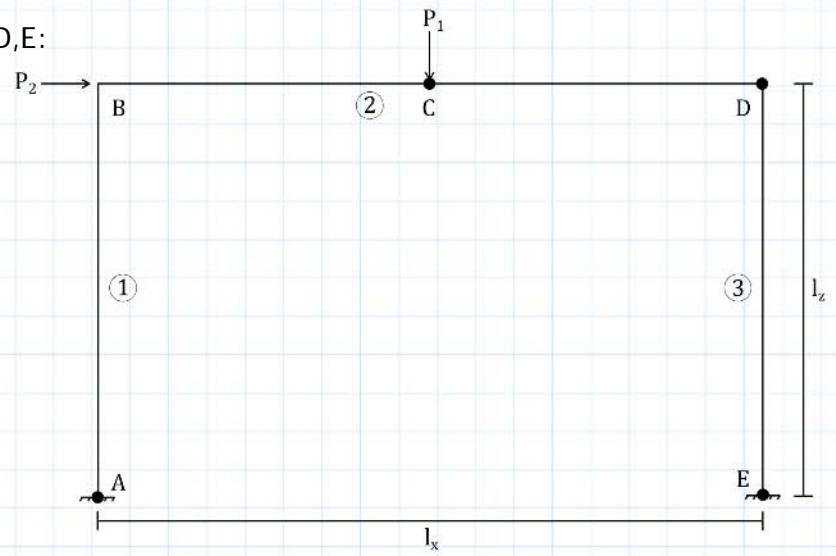
Mechanism 2, hinges at B, C, D:

$$P_{1.check} \cdot \left(\frac{l_x}{2} \cdot \theta \right) - M_1 \cdot (\theta + \theta) - M_2 (2 \cdot \theta)$$

$$P_{1.check} := \frac{(M_1 \cdot 2 + M_2 \cdot 2) \cdot 2}{l_x} = 43.515 \text{ kN}$$



Mechanism 3, hinges at A, C, D, E:



$$P_1 \cdot \left(\frac{l_x}{2} \cdot \theta \right) + P_2 \cdot l_z \cdot \theta - M_1 \cdot (\theta + \theta + \theta) - M_2 (2 \cdot \theta)$$

$$P_2 := \frac{M_1 \cdot 3 + M_2 \cdot 2 - P_1 \cdot \frac{l_x}{2}}{l_z} = 23.455 \text{ kN}$$

B. Static collapse analysis of designed frame

LOAD CARRYING CAPACITY OF VERTICALLY LOADED FRAME

Frame properties:

$$l := 10000 \text{ mm} - 800 \text{ mm} = (9.2 \cdot 10^3) \text{ mm} \quad \text{Approximated beam span length, mid column}$$

$$cc := 50 \text{ mm} \quad \text{Concrete cover}$$

Material parameters:

$$f_{cm} := 53 \text{ MPa} \quad E_{cm} := 37486 \text{ MPa} \quad \varepsilon_{c1} := 2.3 \cdot 10^{-3} \quad \text{Model Code 2010}$$

$$f_{ym} := 533 \text{ MPa} \quad E_s := 220000 \text{ MPa} \quad \varepsilon_y := \frac{f_{ym}}{E_s} = 0.002$$

$$\alpha := \frac{E_s}{E_{cm}} = 5.869$$

Reinforcement bars:

$$\begin{aligned} \phi_{10} &:= 10 \text{ mm} & \phi_{10.k} &:= 12 \text{ mm} \\ \phi_{12} &:= 12 \text{ mm} & \phi_{12.k} &:= 14 \text{ mm} \\ \phi_{14} &:= 14 \text{ mm} & \phi_{14.k} &:= 16 \text{ mm} \\ \phi_{16} &:= 16 \text{ mm} & \phi_{16.k} &:= 18 \text{ mm} \\ \phi_{20} &:= 20 \text{ mm} & \phi_{20.k} &:= 24 \text{ mm} \\ \phi_{28} &:= 28 \text{ mm} & \phi_{28.k} &:= 32 \text{ mm} \\ \phi_{32} &:= 32 \text{ mm} & \phi_{32.k} &:= 36 \text{ mm} \end{aligned}$$

Cross section parameters:

Cross section 1 and 3:

$$w_1 := 500 \text{ mm} \quad h_1 := 800 \text{ mm}$$

$$cc_{1c} := cc + \phi_{20.k} + \frac{\phi_{16.k}}{2} = 83 \text{ mm} \quad cc_{1t} := cc + \phi_{20.k} + \frac{\phi_{16.k}}{2} = 83 \text{ mm}$$

$$d'_1 := cc_{1c} = 83 \text{ mm} \quad d_1 := h_1 - cc_{1t} = 717 \text{ mm}$$

$$A_{s.1c} := 8 \cdot \frac{\pi \cdot (\phi_{16})^2}{4} = (1.608 \cdot 10^3) \text{ mm}^2 \quad A_{s.1t} := 8 \cdot \frac{\pi \cdot (\phi_{16})^2}{4} = (1.608 \cdot 10^3) \text{ mm}^2$$

Cross section 2:

$$w_2 := 500 \text{ mm} \quad h_2 := 1000 \text{ mm}$$

$$cc_{2c} := cc + \phi_{20.k} + \frac{\phi_{16.k}}{2} = 83 \text{ mm} \quad cc_{2t} := cc + \phi_{20.k} + \frac{\phi_{28.k}}{2} = 90 \text{ mm}$$

$$d'_2 := cc_{2c} = 83 \text{ mm} \quad d_2 := h_2 - cc_{2t} = 910 \text{ mm}$$

$$A_{s.2c} := 8 \cdot \frac{\pi \cdot (\phi_{16})^2}{4} = (1.608 \cdot 10^3) \text{ mm}^2 \quad A_{s.2t} := 7 \cdot \frac{\pi \cdot (\phi_{28})^2}{4} = (4.31 \cdot 10^3) \text{ mm}^2$$

Plastic moment capacity of cross sections:
 “Assume concrete failure limits the capacity”

Plastic moment capacity of member 1 and 3:

$$x_1 := 61.3 \text{ mm}$$

Iterated compression block height to
 obtain force equilibrium in cross section

$$\varepsilon_{s1c} := \frac{(x_1 - d'_1)}{x_1} \cdot 0.0035 = -0.001$$

Compression reinforcement
 strain/stress

$$f_{s1c} := \min(E_s \cdot \varepsilon_{s1c}, 500 \text{ MPa}) = -272.577 \text{ MPa}$$

$$\varepsilon_{s1t} := \frac{d_1}{x_1} \cdot 0.0035 = 0.041$$

Tensile reinforcement strain/
 stress

$$f_{s1t} := \min(\text{abs}(E_s \cdot \varepsilon_{s1t}), 500 \text{ MPa}) = 500 \text{ MPa}$$

$$C_{c1} := 0.85 \cdot f_{cm} \cdot w_1 \cdot 0.9 \cdot x_1 = (1.243 \cdot 10^3) \text{ kN}$$

$$C_{s1} := A_{s1c} \cdot f_{s1c} = -438.44 \text{ kN}$$

$$T_1 := A_{s1t} \cdot f_{s1t} = 804.248 \text{ kN}$$

$$C_{c1} + C_{s1} - T_1 = 0.017 \text{ kN}$$

Moment around concrete compressive force resultant

$$M_1 := T_1 \cdot (d_1 - 0.45 \cdot x_1) + C_{s1} \cdot (0.45 \cdot x_1 - d'_1) = 578.757 \text{ kN} \cdot \text{m}$$

Plastic moment capacity of member 2:

$$x_2 := 97.32 \text{ mm}$$

Iterated compression block height to
 obtain force equilibrium in cross section

$$\varepsilon_{s2c} := \frac{(x_2 - d'_2)}{x_2} \cdot 0.0035 = 5.15 \cdot 10^{-4}$$

Compression reinforcement
 strain/stress

$$f_{s2c} := \min(E_s \cdot \varepsilon_{s2c}, 500 \text{ MPa}) = 113.3 \text{ MPa}$$

$$\varepsilon_{s2t} := \frac{d_2}{x_2} \cdot 0.0035 = 0.033$$

Tensile reinforcement strain/
 stress

$$f_{s2t} := \min(\text{abs}(E_s \cdot \varepsilon_{s2t}), 500 \text{ MPa}) = 500 \text{ MPa}$$

$$C_{c2} := 0.85 \cdot f_{cm} \cdot w_2 \cdot 0.9 \cdot x_2 = (1.973 \cdot 10^3) \text{ kN}$$

$$C_{s2} := A_{s,2c} \cdot f_{s2c} = 182.243 \text{ kN}$$

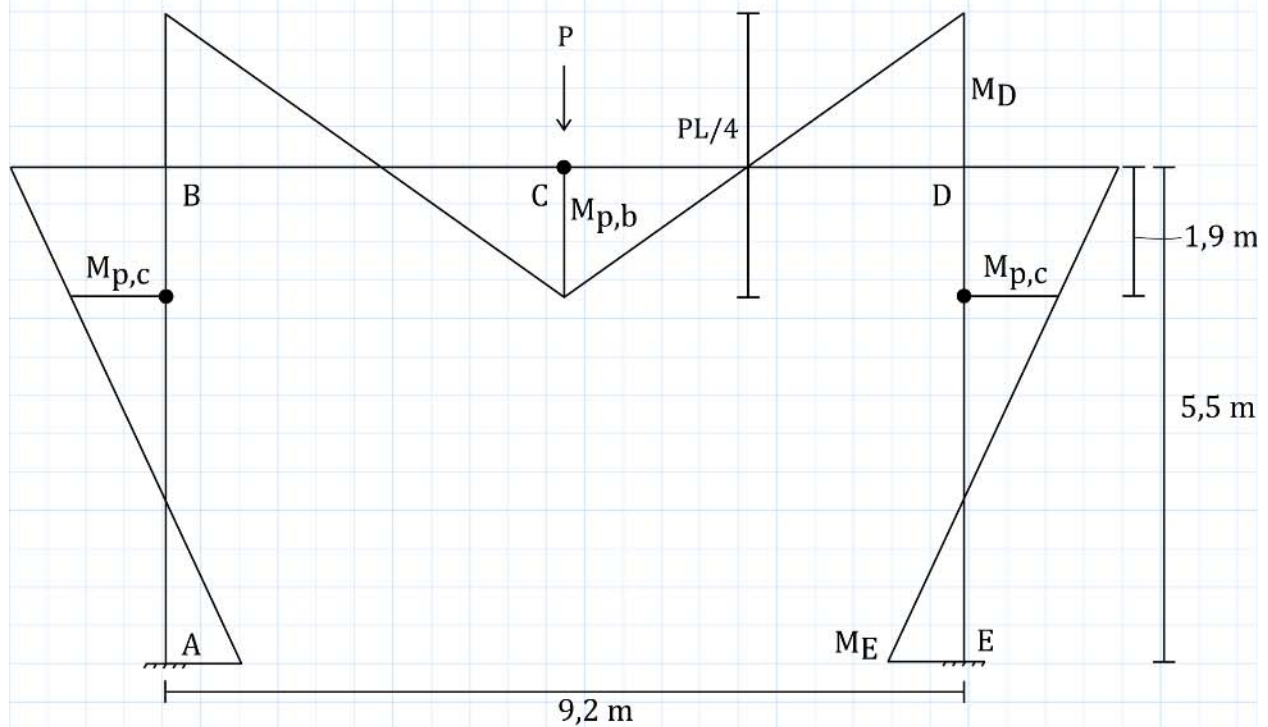
$$T_2 := A_{s,2t} \cdot f_{s2t} = (2.155 \cdot 10^3) \text{ kN}$$

$$C_{c2} + C_{s2} - T_2 = 0.03 \text{ kN}$$

Moment around concrete compressive force resultant

$$M_2 := T_2 \cdot (d_2 - 0.45 \cdot x_2) + C_{s2} \cdot (0.45 \cdot x_2 - d'_2) = (1.86 \cdot 10^3) \text{ kN} \cdot \text{m}$$

Static analysis, assuming linear elastic moment distribution between hinges. Gives lower bound solution, equilibrium satisfied. Based on "Handboken Bygg, Allmänna grunder".



Relation between midspan moment and corner moment

$$M_C + M_D \quad \text{equals} \quad \frac{P \cdot l_x}{4}$$

Plastic moment at midspan of beam

$$M_C := M_2$$

Relation between corner moment and bottom column moment

$$P := 1328.95 \text{ kN} \quad l_x := 9.2 \text{ m} \quad l_y := 5.5 \text{ m} \quad x_h := 1.9 \text{ m}$$

$$M_D := \frac{P \cdot l_x}{4} - M_C \quad m := M_D$$

$$M_E := -\frac{M_D}{2.02} \quad \text{Taken from linear elastic frame calculations, valid for these geometry, load and stiffness properties}$$

$$k := \frac{M_E - M_D}{l_y} \quad k \cdot x_h + m = 578.755 \text{ kN} \cdot \text{m} \quad \text{Moment in critical section, where reinforcement amount changes}$$

$$M_1 = 578.757 \text{ kN} \cdot \text{m} \quad \text{Plastic capacity of column in bending}$$